



Investigation of Ice Interactions on Drilling Rigs in Shallow Water

Project work handed in as “Studienarbeit“

Author:

B. S. Alexander Dummer | Matriculation no.: 8201014

Date: 30.03.2013

Advisor:

Prof. Dr.-Ing. habil. Mathias Paschen

University of Rostock

Chair of Ocean Engineering

Albert-Einstein-Str. 2

18059 Rostock

Acknowledgement

At first I want to thank Professor Paschen for giving me the opportunity to treat this topic at the University of Rostock, his supervision and support.

Furthermore I would like to acknowledge Professor Sangesland from the Norwegian University of Science and Technology (NTNU) for providing me with this task and his support during the work.

I also would like to thank Professor Høyland for his encouraging helpfulness, support, informative and well-rounded courses at NTNU. These lead to arouse my major interests in working with ice technology.

Finally I want to thank my parents for supporting me while studying the semester in Norway and thereby enable me to do this work.

Abstract

The following work provides an introduction and investigation about the influence of sea ice on structures in cold regions. Thereby the focus lies on drilling rigs for shallow water conditions from 40 to 60 m water depth. At the end, two proposals for platform types of different operating conditions for specific ice conditions are given.

As a first step the reader gets a view into the properties and different kinds of ice that affect an offshore structure in cold regions. Thereby the different kinds of occurring ice are introduced. For the further work only global loads due to first-year level ice are considered.

Afterwards different structure types are envisaged, which are already used in Arctic regions or which are considered in other work as concepts for ice infested regions. These different kinds of structures are the base for further evaluation and ice load calculations.

Subsequently different methods for reducing the ice loads on offshore structures and ships are presented. Thereby it is distinguished between active and passive methods. Active methods need additional energy to reduce the loads on structures and foundations, whereas passive methods include design considerations concerning the shape of the structure.

The final evaluation of the different structures to provide a drilling rig is focused on ice loads of first-year level ice. So, different calculation methods for the considered structure geometries are introduced. Thereby mainly methods in accordance with the ISO 19906 are considered, but also approaches for alternative calculation models are provided. Here also a method that orientates on the occurring specific failure mode for vertical structures, determined with help of the failure map of G. W. Timco, is developed. But the comparison with full scale measurement values and the other calculation methods show, that this method leads to unrealistic high results and needs improvement in further work. For running the calculations, three programs, written in the Software Matlab, are developed. These could also determine the occurring interaction type of the legs of a multiple leg structure, depending on the intrusion angle of the drifting ice.

To consider roughly the usage conditions for further calculations and evaluations, the chosen structures are separated into two groups. Group one considers long lasting exploration and following production at the same place whereas group two focuses only on exploration work

at the operation site and further production by other structures. The main differentiator is the size of the structure.

Finally a utility analysis is done to evaluate the different structures concerning the calculation results, but also more relevant general aspects, to provide a structure proposal of each group and presenting other influencing aspects.

Thereby the assumed conditions, weighting of aspects and rating of the utility analysis provides a multiple leg structure with vertical surfaces for group one and a round conical floating structure for group two. For the analysis it is assumed, that problems like structural vibrations, reported for multiple leg structures in Bohai Bay, could be captured. So they are not considered hereby.

Content

Acknowledgement.....	I
Abstract	II
Content	IV
Notation.....	VII
List of figures	XII
List of tables	XIV
1. Introduction	1
2. Fundamentals of ice	3
2.1 Different kinds of ice concerning Arctic structures	3
2.1.1 Sea ice	3
2.1.2 Icebergs	5
2.1.3 Topside icing	6
2.2 Mechanical properties of ice	7
2.2.1 Deformation during continuum behaviour	8
2.2.2 Fracture behaviour.....	11
2.2.3 Temperature correction	13
3. Possible structures for shallow waters	14
3.1 Fixed single leg structures/caissons	14
3.2 Fixed multiple leg structures	16
3.3 Jack up structures	17
3.4 Floating structures	18
4. Methods for reducing ice loads	21
4.1 Active methods for reducing ice loads	21

4.2 Passive methods for reducing ice loads.....	26
5. Ice load calculation models	29
5.1 Vertical structures	29
5.1.1 Failure modes	29
5.1.2 Pure creep	33
5.1.3 Buckling	34
5.1.4 Crushing	35
5.1.5 Korzhavin equation	36
5.1.6 Masterson	37
5.1.7 ISO 19906	37
5.1.8 Velocity correction.....	38
5.2 Sloped structures	39
5.2.1 Plastic method (cone structures).....	39
5.2.2 Elastic beam bending (wide structures)	42
5.2.3 Rubble high	45
5.2.4 Velocity effect	45
5.3 Treatment of multiple leg structures	47
5.4 Floating structures	51
6. Ice load calculations on chosen platforms.....	53
6.1 Introduction into calculation program.....	53
6.2 Comparison with measurement data	54
6.3 Calculations.....	59
7. Comparison of platforms.....	82
8. Conclusion and proposal	91
References	93

Appendix 1: Flow charts for structures with vertical surfaces	A 1
Appendix 2: Flow charts for structures with sloped surfaces	A 25
Appendix 3: Flow charts of floating structures	A 40
Appendix 4: Source code of velocity correction for wide sloping structures	A 42
Appendix 5: Multiple leg interaction scenarios	A 44
Appendix 6: CD - ROM	A 52
Appendix 5: Declaration	A 53

Notation

a	Exponent of Norton's law/power law creep
A	Contact area
A_E	Prefactor for Arrhenius activation energy law
A_j	Parameters for multiple leg interaction of sloped columns
B	Crystal type and temperature depending constant concerning Norton's law
b_f	statistical parameter for size effect
B_j	Parameters for multiple leg interaction of sloped columns
C	Stiffness tensor
c	Cohesion strength of ice rubble
C_{1-3}	Parameters for multiple leg interaction of sloped columns
C_R	Ice strength coefficient
d	Grain diameter
D	Structure diameter or leg diameter of structure at waterline
D_B	Diameter of submerged cylinder
d_r	Size of zone for crushing failure
D_T	Structure diameter or leg diameter of structure at top of cone
D_{WL}	Diameter of waterline
E	Modulus of elasticity
e	Porosity of the ice rubble
E_1	Complete elliptical integral of first kind
E_2	Complete elliptical integral of second kind
E_{fi}	Elastic modulus of fresh water ice
e_i	Porosity of ice
f	Geometrical parameter
$F_{non,h}$	Velocity factor for horizontal loads of downward breaking structures with respect to Lau et al.
$F_{non,M}$	Velocity factor with respect to Matskevitch

$F_{\text{non,u}}$	Velocity factor for horizontal loads of upward breaking structures with respect to Lau et al.
$F_{\text{non,v}}$	Velocity factor for vertical loads of downward breaking structures with respect to Lau et al.
Fr	Froude-number
G	Parameter for ice breaking component for sloped structures
g	Gravitational acceleration
g_r	Geometrical parameter
h	Thickness of ice cover
h_1	Reference thickness of 1 m
H_B	Horizontal load through breaking
h_C	High of submerged cylinder
H_L	Load to push the ice block up
H_P	Load to push sheet ice through ice rubble
h_r	Ice ride-up thickness
H_R	Horizontal load through ride-up
H_R	Load to push the ice block up through rubble
H_T	Load to turn the block at the top of the slope
h_V	Geometrical parameter
I	Indentation factor (ratio between indentation pressure $P/(Dh)$ and uniaxial strength)
k	Contact factor
k_1	Constant describing fracture behaviour
k_2	Constant describing fracture behaviour
KG	Distance between keel and centre of gravity
K_{IC}	Fracture toughness
K_Z	Factor for Masterson formula
l	Characteristic length concerning buckling
L_{1-4}	Characteristic distance between ice edges and column centre for multiple leg interaction

L_C	Characteristic length of ice sheet
l_C	Length of circumferential crack
m	Shape factor
m_{ISO}	Empirical constant concerning ISO 19906
n	Number of non-simultaneous failures
n_{ISO}	Empirical constant concerning ISO 19906
P	Load per unit width
P	Global load on indenter
P_B	Global load due to buckling
p_G	Global average ice pressure
p_G	Global average pressure on contact area of indenter with respect to the ISO
P_H	Global horizontal load on structure
P_{ISO}	Global load on indenter with respect to ISO
p_M	Global average pressure on contact area of indenter with respect to Master- son
P_{pc}	Global load due to pure creep
P_V	Global vertical load on structure
Q	Activation energy concerning Norton's law
R	Universal gas constant
R_C	Compressive strength against crushing failure
R_{Cg}	Uniaxial compressive strength of granular ice during continuum behaviour
R_C^H	Uniaxial compressive strength of columnar, orthogonal to column axis, ice during continuum behaviour
R_{CN}	Compressive strength against nucleation controlled fracture
R_F	Flexural strength
r_h	Rubble high
R_{TN}	Tensile strength against nucleation controlled fracture
S	Salinity
T	Temperature
T_0	Draught without pitch

T_{ij}	Design target no. j of category no. i
U	Ice drift velocity
U_0	Reference velocity
V_0	Normalizing volume constant
V_B	Vertical load through breaking
V_b	Brine volume
V_R	Vertical load through ride-up
V_t	Total brine and/or void volume
W	Rubble weight parameter
x	Parameter for ice actions on conical structures
Y	Coefficient concerning yield criterion

α	Slope angle of structure surface
β	Angle of the rubble with the horizontal
ε_0	Constant describing fracture behaviour
ε_e	Elastic strain
ε_{TN}	Critical strain for nucleation controlled tensile fracture
ε_{ve}	Viscoelastic strain
ε_{vp}	Viscoplastic strain
η_B	Lever arm of upsetting moment
η_{ve}	Dynamic viscosity during viscoelastic behaviour
η_{vp}	Dynamic viscosity during viscoplastic behaviour
λ	Scale
μ	Friction coefficient of structure-ice interaction
μ_i	Ice-to-ice friction coefficient
∇	Displaced volume
ν	Poisson's ratio
ξ	Relationship between horizontal and vertical forces
ρ_i	Density of ice
ρ_w	Density of water
σ	Stress
σ	Normal stress
σ_0	Constant describing fracture behaviour
σ_a	Stress by applied load
σ_c'	Net section stress for columnar ice
σ_g'	Net section stress for granular ice
σ_N	Critical stress for nucleation controlled tensile fracture
τ	Shear stress
φ	Angle of internal friction of ice rubble
ϕ	Pitch angle
ψ	Compatibility factor for indentation

List of figures

Figure 1: Regions with running oil activities, (1)	1
Figure 2: Change from ductile to brittle behaviour for uniaxial loading of pure ice. (3)	7
Figure 3: Applied stress.....	8
Figure 4: Resulting strain of a constant stress σ_a	8
Figure 5: Burgers model.....	10
Figure 6: Molikpaq platform in ice (1).....	14
Figure 7: Wake of Molikpaq platform (10).....	14
Figure 8: General view of movable drilling platform for different water depth (1)	15
Figure 9: Platform JZ20-2 MUQ and MNW at Bohai Bay, (13)	16
Figure 10: Piled structure at Cook Inlet,	16
Figure 11: Jack up platform with conical leg protection (15)	17
Figure 12: Sketch of Kulluk exploration vessel (16)	18
Figure 13: Kulluk on site during ice management (16)	18
Figure 14: Side view of Semi-submersible (17).....	19
Figure 15: Stena Icemax (20)	20
Figure 16: Stena Icemax model during stationkeeping tests in managed ice conditions (19) .	20
Figure 17: Shape of hull for ice breaking in transverse direction (23).....	22
Figure 18: Model tests for ice breaking in transverse direction (24)	22
Figure 19: Platform protection by microwave source; 1) Platform, 2) Leg, 3) Moving ice, 4) Moving microwave unit, 5) High-Voltage source, 6) Microwave radiation (30)	24
Figure 20: Operation vessel with disaggregation drums (31)	25
Figure 21: Indentation geometry, (3)	30
Figure 22: Principal failure mechanisms of laboratory indentation tests: a) creep; b) radial cracking; c) buckling; d) circumferential cracking; e) spalling; f) crushing , (3)	31
Figure 23: Failure modes dependent on indentation rate and aspect ratio (36)	32
Figure 24: Fracture with contact over n zones of width d_r (3)	36
Figure 25: Forces on upward-breaking cone (27), here t and t_R are equal to h and h_R	40
Figure 26: Rubble accumulation up and in front of structure (34), notation fitted	43
Figure 27: Coulomb-Mohr failure criterion (42).....	44

Figure 28: Idealized ice interaction of a multi leg platform (42)	47
Figure 29: Comparison of measurement pressure of level first year ice on Molikpaq with calculated values	54
Figure 30: General arrangement Kulluk vessel with inserted simplifications (red lines) and assumed main dimensions, (50) with modifications	56
Figure 31: Comparison of Upper bound values of measurement data and calculated values for Kulluk vessel	57
Figure 32: Normalized ice load vs. Ice drift speed, (16)	58
Figure 33: Top view Maersk XL Enhanced with inserted column distances assumed for calculations, (51) with modifications	65
Figure 34: Structure no. 3, group 1, intrusion angle: 10 °	70
Figure 35: Structure no. 3, group 1, intrusion angle: 30 °	70
Figure 36: Structure no. 3, group 1, intrusion angle: 45 °	71
Figure 37: Ice load versus ice drift velocity of selected structures of group one	72
Figure 38: Ice load versus ice drift velocity of selected structures of group two	73
Figure 39: Aspects of utility analysis	84
Figure 40: Group one, no. 17, intrusion angle: 10 °	A 44
Figure 41: Group one, no. 17, intrusion angle: 30 °	A 44
Figure 42: Group one, no. 17, intrusion angle: 45 °	A 45
Figure 44: Group two, no. 3, intrusion angle: 10 °	A 45
Figure 45: Group two, no. 3, intrusion angle: 30 °	A 46
Figure 46: Group two, no. 3, intrusion angle: 45 °	A 46
Figure 47: Group two, no. 5, intrusion angle: 10 °	A 47
Figure 48: Group two, no. 5, intrusion angle: 30 °	A 47
Figure 49: Group two, no. 5, intrusion angle: 45 °	A 48
Figure 50: Group two, no. 18, intrusion angle: 10 °	A 48
Figure 51: Group two, no. 18, intrusion angle: 30 °	A 49
Figure 52: Group two, no. 18, intrusion angle: 45 °	A 49
Figure 53: Group two, no. 28, intrusion angle: 10 °	A 50
Figure 54: Group two, no. 28, intrusion angle: 30 °	A 50
Figure 55: Group two, no. 28, intrusion angle: 45 °	A 51

List of tables

Table 1: Classification of icebergs by size (International Ice Patrol) (3).....	5
Table 2: Constants concerning creep behaviour of compression and tensile loading (3)	10
Table 3: Indentation rate for transition to brittle behaviour, dependent on scale (3), (37)	32
Table 4: Parameters for creep indentation (3).....	34
Table 5: Multiplication factor for four leg platforms with vertical surfaces (47)	48
Table 6: Multiplication factor for four leg platform with sloped surfaces, (42)	49
Table 7: Pitch angle for floater calculation	57
Table 8: Topside dimensions of Arctic drilling and production platforms	61
Table 9: Structure dimensions, group one.....	63
Table 10: Structure dimensions, group two, part one of three	66
Table 11: Structure dimensions, group two, part two of three	67
Table 12: Structure dimensions, group two, floater, part three of three	68
Table 13: Results of calculations, group one, structures with vertical surfaces, ice drift velocity: 0.05 m/s	75
Table 14: Results of calculations, group one, sloped caisson structures, ice drift velocity: 0.05 m/s	76
Table 15: Results of calculations, group one, sloped multiple leg structures, ice drift velocity: 0.05 m/s	77
Table 16: Results of calculations, group two, structures with vertical surfaces, ice drift velocity: 0.05 m/s	78
Table 17: Results of calculations, group two, caissons with sloped surfaces, ice drift velocity: 0.05 m/s	79
Table 18: Results of calculations, group two, multiple leg structures with sloped surfaces, ice drift velocity: 0.05 m/s	80
Table 19: Results of calculations, group two, floating structures, ice drift velocity: 0.05 m/s	81
Table 20: Comparison of structures for group one	88
Table 21: Comparison of structures of group two.....	89
Table 22: Comparison of group two structures	90

1. Introduction

The first exploitation of oil in the heavy ice infested areas began in the early 1970s in the Canadian Beaufort Sea, among others driven by the escalating oil price. Currently the worldwide increasing energy demand, climatic changes and the location of large hydrocarbon reservoirs give again rise to potentially economically viable exploration and production in the ice infested locations of the Arctic.

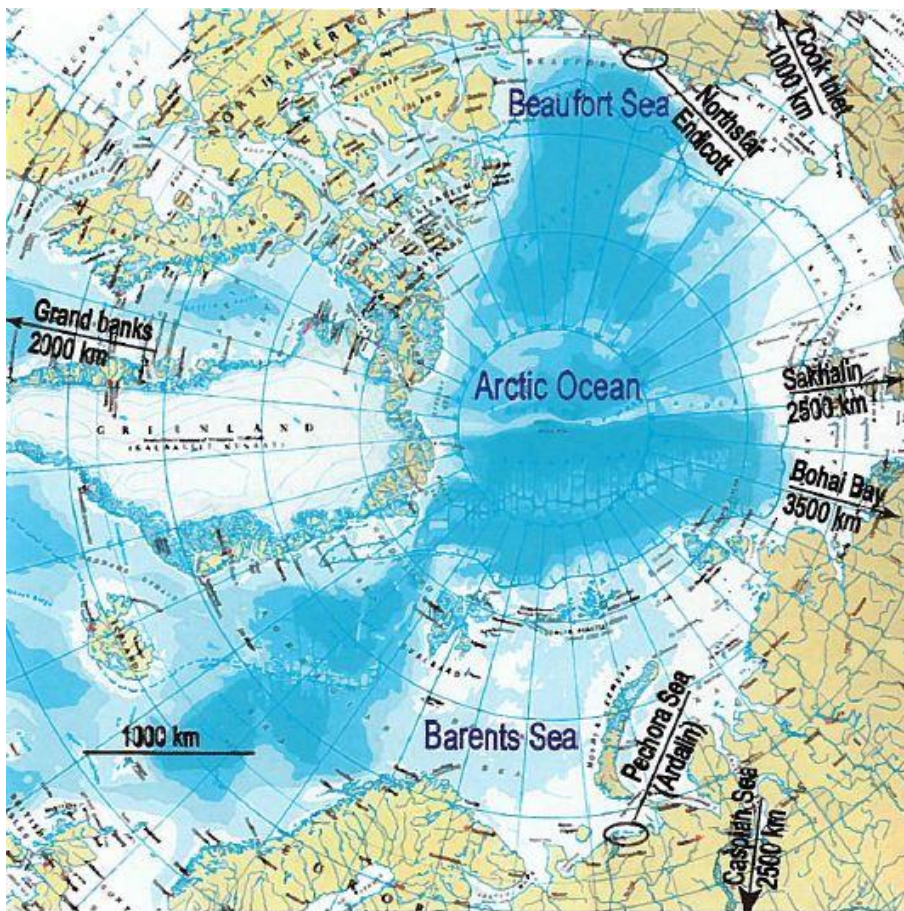


Figure 1: Regions with running oil activities, (1)

Even there are already a few oil activities running in cold regions the demand on technical optimisation is still strong since the extreme harsh environmental conditions, the weak infrastructure and limited knowledge about the ice as dominating load source.

A key parameter for safer and more cost-effective exploration is the choice and development of the right drilling rig. Thereby decreasing ice loads is one aspect that leads to minimize risk and could also decrease costs for station keeping applications or grounding.

The overall scope of this work is to give a proposal for a drilling rig in shallow waters (40 – 60 m). Therefor at first some fundamentals about the material ice, that influences an Arctic offshore structure and which are important for the further work, are presented. Subsequently, platformtypes that are used or could be used theoretically for drilling in ice covered shallow waters are introduced. Afterwards, nowadays operating and potential methods for reducing ice loads are given. As a main evaluation criterion the ice loads on different structure types are calculated.

Thereby only quasi-static global loads from first-year level sea ice by limit stress mechanism are considered. Quasi-static conditions amount that inertia effects of the influencing ice are neglected. Limit stress means that enough driving forces exist to envelope the structure and generate ice actions over the complete structure width (2).

Finally the platform types are evaluated with the help of an utility analysis and a proposal is given.

2. Fundamentals of ice

2.1 Different kinds of ice concerning Arctic structures

2.1.1 Sea ice

Development

To get sea ice, the water of an upper layer (10-20 m) has to be cooled down to $-1.9\text{ }^{\circ}\text{C}$ (if salinity equals 35 ppt.). In distinction to fresh water of lakes, where only the surface has to be cooled down, a layer has to be cooled down since the density of salt water (till salinity of 24.7 ppt.) continuously increases till it reaches its freezing point. So the water close to the freezing point will sink to a depth where water with same density is, respectively water with higher salinity and warmer water will rise to the surface.

If also the risen water is cooled down, crystals originate and float on the surface (grease ice). They will coalesce and form a solid surface, called ice rind, up to 5 cm thick. Because of waves this surface will easily break up and through abrasion round plates, between 0.3 m and 3 m of diameter, are formed, known as pancake ice. After a while this ice forms a stable layer, 5-30 cm thick, called young ice. It is composed of crystals about 1 mm in diameter, frozen together randomly, referred to as granular, frazil or T1-ice.

The ice crystals consist of pure ice, without salt. The salt of the sea water (5-10 ppt.) is stored in brines, together with air and gas and is embedded as pockets in the ice structure. (3)

First-year ice

After a first solid layer of ice is formed, the ice crystals grow structured downwards. They have a horizontal c-axis, because the highest thermal conductivity is perpendicular to the c-axis. So the emerged heat of the exothermic freezing process is transported most rapidly to the air. This ice is called columnar ice.

Landfast ice is located near to the shore and horizontally fixed. So it is possible to have a stable position to currents, if they occur. In this surrounding the c-axis is orientated nearly parallel to the current. The alignment increases with the depth of the ice cover. So the ice has a horizontal anisotropic behaviour. It is called S3-ice.

Further offshore, where the ice can drift around freely or where currents change, the c-axis is randomly arranged in a horizontal plane. So the ice has a transversely isotropic behaviour. It is called S2-ice.

If there is broken water, granular ice and other fragments of columnar ice from other places could be worked into the freezing process at any depth, so that there will be an ice layer with different kinds of ice and different material properties.

Also a lot of snow can accumulate on the ice cover. Thus, it could sink and the snow gets infiltrated of sea water. The developed ice is similar to granular ice. (3)

Through different stresses in the ice several actions can happen which will form special ice shapes:

If two ice covers hit against each other or high compressive stresses occur, compressive ridges can arise. It is a heap of rubble and freezes together. It contains of a “sail” (1-4 m above the surface) and a “keel” (5-10 m under the sea level, but strongly varying).

Shear movements in the ice cover can lead to shear ridges. They are more rarely formed out of a flat ice cover but can originate from compression ridges due to movement of two separated sheets of ice.

Also in young ice, normally up to 30 cm thickness, rafting can occur. Instead of breaking like in the compressive ridge, they over- and under ride each other.

First-year ice generally reaches a thickness of 1-2.5 m. (3)

Second-year ice and multi-year ice

Second-year ice survives the melting process in the summer. The warm environment leads to a lower salt content of the ice cover since brine pockets migrate to the warmer areas of the ice cover, in summer times at the top and bottom of the cover.

Also ridges are melting partly but refreeze in winter and “sails” and “keels” become coalesced hummocks and bummocks.

After surviving at least two seasons second-year ice becomes multi-year ice or old ice. Because of a difficult practical distinction, often second-year ice is called multi-year ice. In the Arctic the thickness reaches up about 2-6 m. The final thickness is defined by equilibrium between annual melting and annual freezing. In general multi-year ice is very irregular. But in more regular floes, annual layers from the freezing process can be observed.

Alexander Dummer	Project work	Investigation of Ice Interactions
MSF LS Ocean Engineering	handed in as	on Drilling Rigs in
University of Rostock	“Studienarbeit”	Shallow Water

Multi-year ridges have a horizontally wider keel as sail. In the Arctic (Queen Elizabeth Islands) a sail to keel ratio of about 1:5.6 by a keel depth of 36 m has been observed (4). (3) (5)

2.1.2 Icebergs

Icebergs originate from glaciers so they consist of pure freshwater ice from snowfall. If the ice breaks directly from the land-based ice cap or glacier into the sea, the iceberg has a cubical shape and diameters from 50-500 m. They are called blocky icebergs.

If the glacier flows from land into an embayment, extensive areas of landfast floating glacier ice, called ice shelf, will occur. Icebergs which break off from an ice shelf are called tabular icebergs. In general they have a thickness ratio of 1:10, but the largest ever observed one has a length of 160 km and a thickness of 500 m. The density of an iceberg depends of the region where it comes from.

Icebergs float around till they melt in warmer areas. Their trajectories are difficult to estimate because of unknown windages for wind and water currents. They also capsize often since their centre of gravity changes through melting. (3)

Icebergs can be classified by their size:

Table 1: Classification of icebergs by size (International Ice Patrol) (3)

Description	Height above sea level [m]	Length [m]	Approx. mass [t]
Growler	< 1.5	< 5	100
Bergy bit	1.5-5	5-15	1 000
Small berg	5-15	15-60	100 000
Medium berg	15-50	60-120	2 000 000
Large berg	50-100	120-220	10 000 000
Very large berg	> 100	> 220	> 10 000 000

Ice islands are similar to icebergs. They could break off from ice shelves of Ellesmere Island in the Arctic. Unlike by an iceberg, the ice shelve which originates an ice island does not contain ice of land based glaciers ice. It is more similar to multi-year ice with a thickness between 40-90 m with a low salinity. It is also in an equilibrium concerning freezing and melting and

Alexander Dummer	Project work	Investigation of Ice Interactions
MSF LS Ocean Engineering	handed in as	on Drilling Rigs in
University of Rostock	“Studienarbeit”	Shallow Water

samples showed that they are 1600-4200 years old. The calving islands are about 50 m thick and up 40 km in diameter. (3)

2.1.3 Topside icing

For the sake of completeness also topside icing is mentioned, whereas this work focuses more on floating ice. Topside icing leads to a higher centre of gravity and additional weight. This can cause heave, heel and trim on floating structures and additional loads on foundation and structure of based platforms.

Whereas icing on ships is mainly caused by freezing bow spray of wave slamming, fixed structures ice up through freezing droplets caused by wind waves. Icing occurs mainly by high wind speeds, air temperatures below the freezing point and water temperature below 6°C.

It is also caused by supercooled fog, freezing rain or drizzle and falling snow. (6) (7) (8)

2.2 Mechanical properties of ice

Ice is a polycrystalline material like metals but it behaves more complicated because it has relatively large grains and occurs close to its freezing point. Additionally sea ice has pockets with brine, air or solid salt. So the mechanical properties depend on time, direction and height of loading as well as on the type of ice and temperature/porosity. Depending on these parameters, ice switches from ductile to brittle behaviour. Sanderson (3) states that brittle behaviour occurs, if

- stresses exceeding a level of 5-10 MPa for uniaxial compression or 1-2 MPa for uniaxial tension
- strain-rates exceeding a level of approx.. 10^{-3} 1/s for uniaxial compression
- strain exceeding a level of approx. 1 %.

This can also be seen in figure 2, so in applications the most cases of impact are controlled by brittle behaviour where the strength is controlled by fracture. It can also be seen, that colder ice switches at higher values to brittle behaviour than warmer ice.

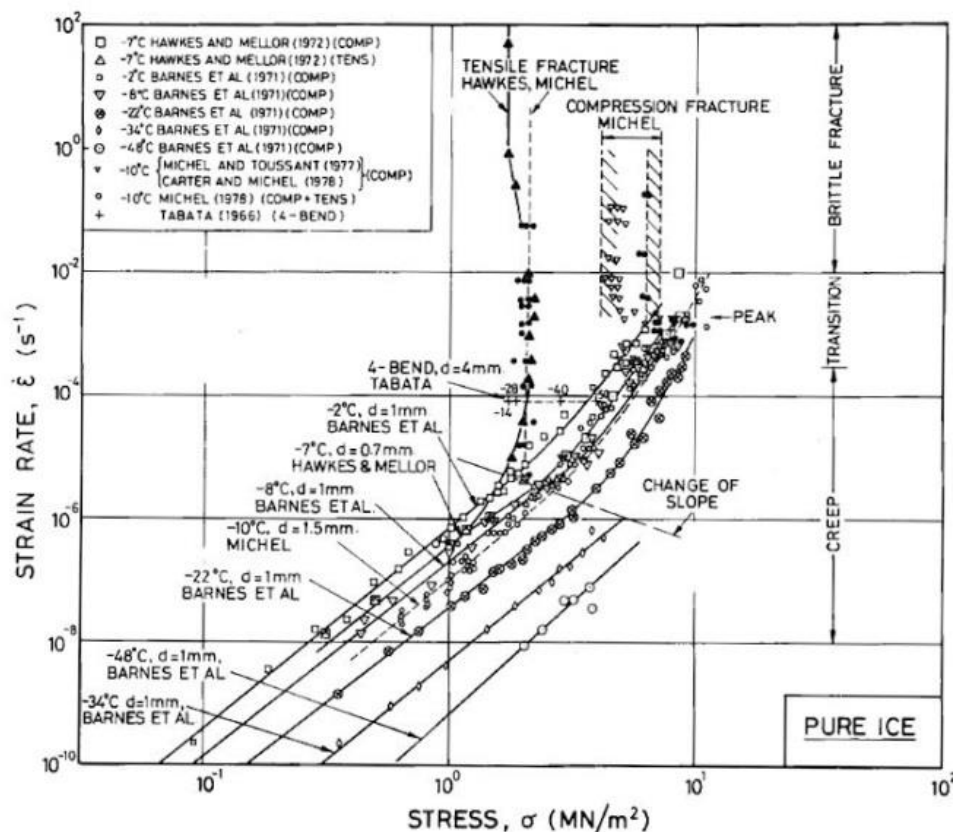


Figure 2: Change from ductile to brittle behaviour for uniaxial loading of pure ice. (3)

2.2.1 Deformation during continuum behaviour

If a constant load is applied to sea ice, it immediately comes to an elastic strain ε_e . Furthermore it starts a time dependent viscoelastic strain ε_{ve} and a time dependent, non-linear viscoplastic strain ε_{vp} at the same time. Subsequently the viscoelastic strain does not increase anymore and viscoplastic strain becomes noticeable. After a while tertiary creep occurs (dashed line in figure 3 and 4). Because this time range does not concern the treated topic, it will not be dealt with tertiary creep further more.

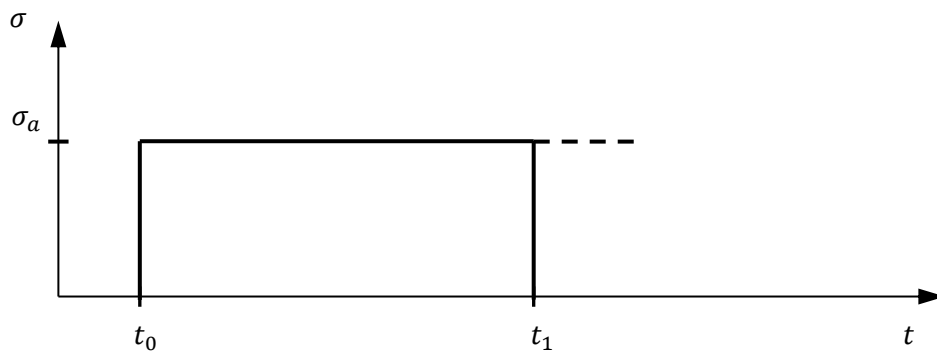


Figure 3: Applied stress

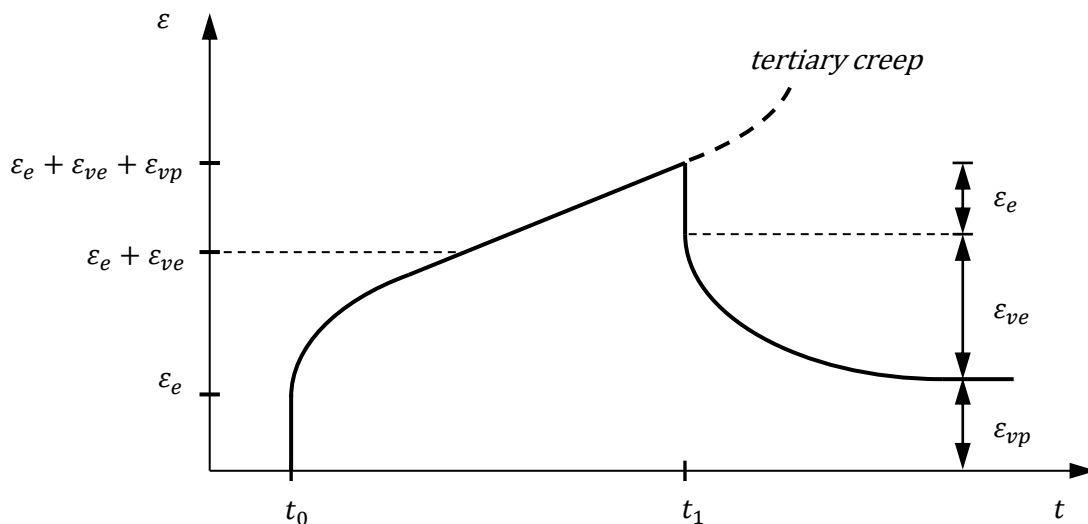


Figure 4: Resulting strain of a constant stress σ_a

Uniaxial elastic strain can be described by Hooke's Law:

$$\sigma = E \cdot \varepsilon_e \quad (2.1)$$

If three dimensions are considered, stress σ and elastic strain ε_e become tensors with six independent components and the modulus of elasticity E can be expressed as a 6x6 matrix, called stiffness tensor C . If isotropic granular ice is considered the matrix of C has only two independent variables: E and ν (Poisson's ratio). Because of the transversal isotropic behaviour of S2-ice it has 5 independent properties and the orthotropic S3-ice has 9 independent properties.

Viscoelastic strain is time dependent and can be described as follows:

$$\sigma = E \cdot \varepsilon_{ve} + \eta_{ve} \cdot \dot{\varepsilon}_{ve} \quad (2.2)$$

where η is the dynamic viscosity of ice. It is a reversible process but takes some time to reach the initial shape. Viscoelastic strain is also grain size dependent. It is called delayed elastic strain or primary creep too.

The deformation through viscoplastic strain (also called secondary creep) is permanent and can be expressed as follows:

$$\sigma = \eta_{vp} \cdot \dot{\varepsilon}_{vp}, \quad (2.3)$$

with the non-linear parameter η_{vp}

or as Norton's law:

$$\dot{\varepsilon}_{vp} = B \cdot \sigma^a \quad (2.4)$$

A value of 3 for the constant a can be chosen for the most strain-rates of ice. B is a crystal type and temperature dependent constant and can be calculated following the Arrhenius activation energy law:

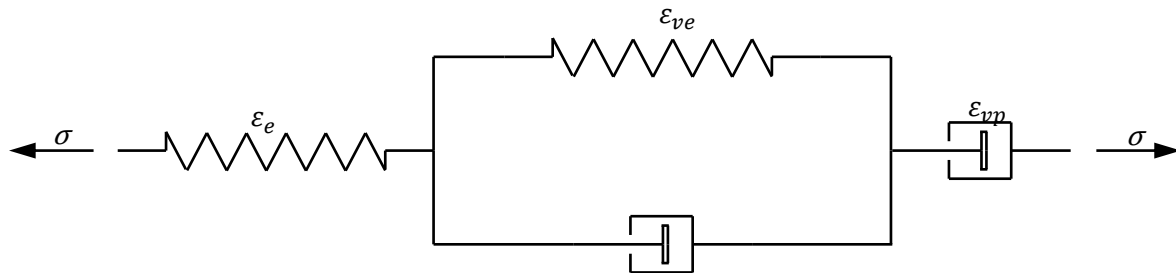
$$B = A_E \cdot e^{\frac{-Q}{RT}} \quad (2.5)$$

A_E is a prefactor, depending on crystal type and temperature, Q is the activation energy, R the universal gas constant and T the temperature here in Kelvin (see table 2).

Table 2: Constants concerning creep behaviour of compression and tensile loading (3)

	Granular ice		Columnar ice
	Above 265 K	Below 265 K	Simplified to all temperatures
$A_E \left[\frac{1}{MPa^3 \cdot s} \right]$	$7.8 \cdot 10^{16}$	$4.1 \cdot 10^8$	$3.5 \cdot 10^6$
$Q \left[\frac{kJ}{mol} \right]$	120	78	65
$R \left[\frac{J}{mol \cdot K} \right]$	8.314		

So the mechanical behaviour for a constant load can be summarized in the Burgers spring and dashpot model.

**Figure 5: Burgers model**

Compression tests

For strain-rates from 10^{-7} to 10^{-3} 1/s the uniaxial compressive strengths of columnar ice, loaded orthogonal to its column axis, can be described as follows (2):

$$R_C^H = 37 \cdot (\dot{\epsilon})^{0.22} \left(1 - \sqrt{\frac{e_i}{0.27}} \right) \quad (2.6)$$

and of granular ice as

$$R_{Cg} = 49 \cdot (\dot{\epsilon})^{0.22} \left(1 - \sqrt{\frac{e_i}{0.28}} \right) \quad (2.7)$$

where e_i is the porosity of ice. In this work gas pockets are neglected and it is set equal to the brine volume (see chapter 2.2.3).

Elastic modulus

In accordance to the ISO 19906:2010 the elastic modulus depends on total brine and/or void volume. Here it is assumed that the ice is free of air inclusions and only the brine volume (see chapter 2.2.3) is taken into account. So the elastic modulus results in

$$E = E_{fi}(1 - \sqrt{V_t})^4 \quad (2.8)$$

where E_{fi} is the elastic modulus of fresh water ice and here assumed to be 9.5 GPa, V_t is the total brine and/or void volume (0-1).

2.2.2 Fracture behaviour

If ice fails, it fails by a propagation controlled mechanism during ductile behaviour or a nucleation controlled mechanism during brittle behaviour.

The difference of the mechanisms is the size of the cracks. For propagation controlled failures already existing microcracks need additional load to grow till they are big enough that the ice fails. Nucleation controlled failures occur if microcracks arise and then steadily growing till they are large enough that the ice fails.

Which kind of control mechanism occurs depends also on the grain size and flaws in the ice during a specific strain-rate. Lee and Schulson observed, that for a strain-rate of 10^{-3} 1/s, nucleation controlled fracture occurs at grain sizes larger than 1.5 mm and for smaller grain sizes propagation controlled fracture occurs. (9)

For analysis of the fracture behaviour, linear elastic fracture mechanics is used.

Tensile fracture through nucleation

Cracks occur at a critical level of total strain or delayed elastic strain. Through the early stage of deformation stress concentrations on grain boundaries occur. To relieve this stress cracks nucleate which have approximately the same length as the grain diameter. This mechanism works for grain sizes higher than 1.5 mm. (3)

At high strain-rates ($10^{-6} \frac{1}{s}$) crack nucleation occurs at the following stresses (based on experimental data (9)):

$$R_{TN} = \sigma_0 + \frac{k_1}{\sqrt{d}} \quad (2.9)$$

$$\varepsilon_{TN} = \frac{\sigma_N}{E} = \varepsilon_0 + \frac{k_2}{\sqrt{d}} \quad (2.10)$$

The high strain-rates effect that purely elastic deformations occur.

σ_0 , ε_0 , k_1 and k_2 are calculated constants of experiments, they have only a small temperature dependency:

$$\begin{aligned} \sigma_0 &= 0.6 \text{ MPa}, & k_1 &= 0.02 \text{ MPa}\sqrt{m}, \\ \varepsilon_0 &= 6.3 \cdot 10^{-5}, & k_2 &= 2.1 \cdot 10^{-6} \sqrt{m}. \end{aligned} \quad (3)$$

Compressive fracture through nucleation

Also compressive fracture through nucleation occurs as a result of dislocation pile up at grain boundaries. As a limit criterion it is possible to say that cracks nucleate when the lateral tensile strain through Poisson ratio reaches the level of tensile fracture through nucleation:

$$R_{CN} = \frac{-R_{TN}}{\nu} = -\frac{1}{\nu} \left(\sigma_0 + \frac{k_1}{\sqrt{d}} \right) \quad (2.11)$$

σ_0 and k_1 are the same constants as in equation (2.9), ν is equal to 0.33. (3)

Flexural strength

The flexural strength is defined as the tension stress in the outer fibre of a bending ice sheet. On a basis of small scale tests the following formula is provided by the ISO:

$$R_F = 1.76 \cdot e^{-5.88 \cdot \sqrt{V_b}} \quad (2.12)$$

expressed in Megapascals, where V_b is the brine volume and takes into account the temperature dependence (see chapter 2.2.3).

2.2.3 Temperature correction

Different temperatures of the ice control the volume of brine pockets in it (see 2.1.1). So the porosity of the ice changes with temperature. Since brine pockets are not able to transfer stress, the remaining ice has to carry all the loads which lead to higher stress in it. This is called the net section stress and calculated for horizontal loading as follows:

Brine volume V_b

$$V_b = 0.001S(0.53 - \frac{49.2}{T}) \quad (2.13)$$

Where S is the gross salinity of the sea ice in ppt. and T is its temperature in °C.

Net section stress σ_c' for columnar ice

$$\sigma_c' = \frac{\sigma}{1 - \sqrt{\frac{V_b}{V_0}}} \quad (2.14)$$

Net section stress σ_g' for granular ice

$$\sigma_g' = \frac{\sigma}{1 - \frac{V_b}{V_0}} \quad (2.15)$$

V_0 is a normalizing constant and lies for columnar ice at approx. 0.1 and for granular ice at approx. 0.16 (3). So for considering temperature and salinity effects, the strength of the freshwater ice was set as maximum net section stress.

3. Possible structures for shallow waters

In the following potential structure types for ice covered shallow water (40 – 60 m depth) are introduced. For these types ice load due to level ice is calculated in the further part of this work.

3.1 Fixed single leg structures/caissons

Large structures for drilling and production

In the past a few structures (e.g. Molikpaq (delivered 1984), Hibernia (delivered 1997) or Prirazlomnoye (delivered 2010)) for drilling and production in arctic shallow waters were built. These are large gravity based caisson or multiple leg structures with diameters from 108 m (ice wall, leg diameter: 17 m) (Hibernia) or width of about 111 - 126 m (Molikpaq 111 m, Prirazlomnoye 126 m). They are protected by an additional vertical ice wall (Hibernia, high: 5 m about sea level, ground plan like a cog) or have a sloped or vertical hull, dimensioned strong enough for direct ice contact.



Figure 6: Molikpaq platform in ice (1)



Figure 7: Wake of Molikpaq platform (10)

Limited till water depth of 20 m artificial sand islands by drained sand were made. But these are not considered further since the water depth is not in the scope of this work and their costs increase exponential with water depth.

In the late 80s also sprayed ice islands were successfully used for exploration drilling. The production costs were only half of that from sand islands and they provide an environmental friendly way of construction. Because this principle works only for sub-zero temperatures and the construction by spraying becomes strongly reduced during air temperatures above $-20\text{ }^{\circ}\text{C}$ they are also not further considered in this work. (11), (12) in (13)

Conical structures

In shallow waters ice actions normally exceed wave actions at vertical sided structures. For decreasing the ice actions strongly and thereby slightly increasing the wave actions, conical structures can be considered.

In 1999 a fixed conical structure was developed which should be easy to build in shallow waters from 20 - 50 m and have low ice loads. It consists of a seabed foundation module (SFM) and an upper platform unit (UPU). The SFM can be easily towed to the operation side and be fixed by gravity basement or piles. Then the UPU can be adapted there afterwards.

Thus, only less construction time at the operational side is needed because the main work of building and fitting the two parts could be done in yards and towing operations are simpler as of a higher caisson consisting of one part. That fits also to an only short ice free available period. (1)

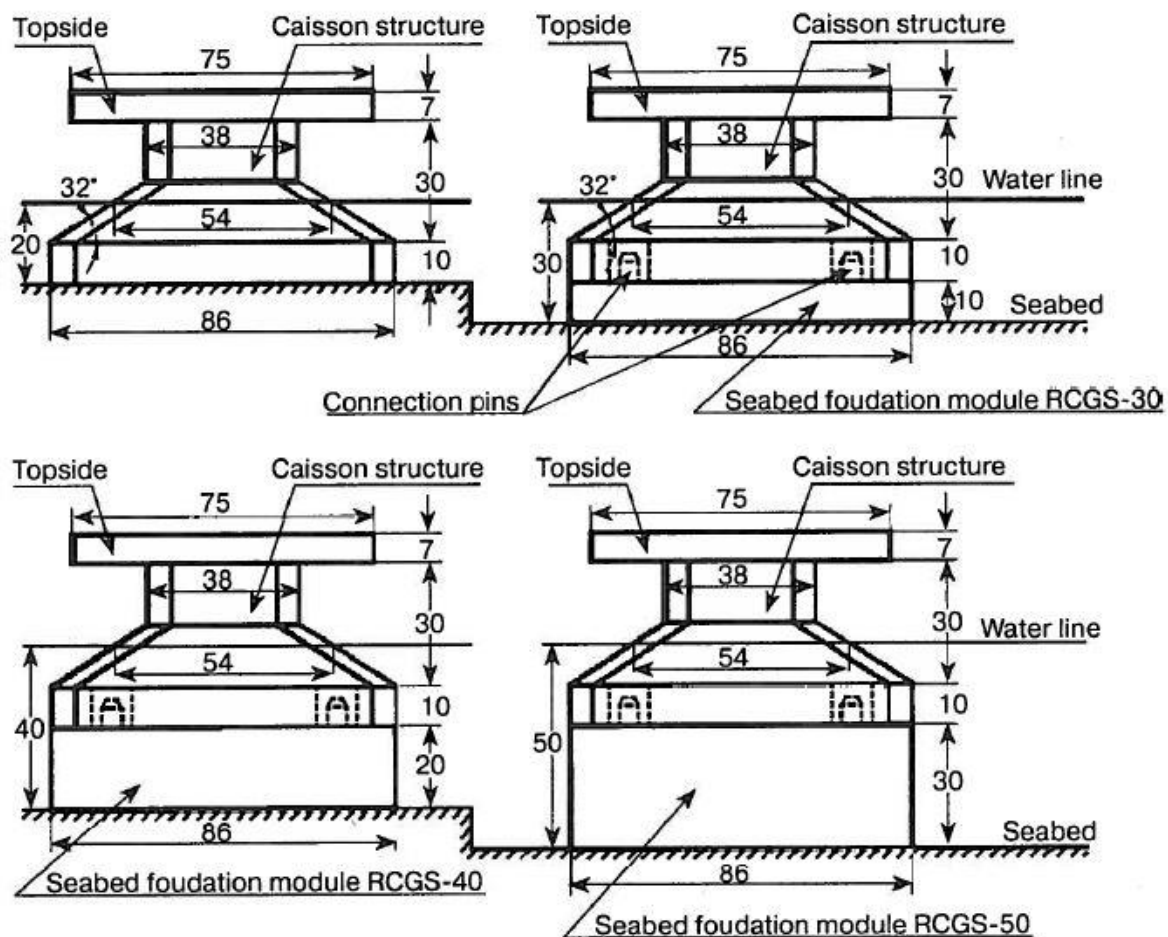


Figure 8: General view of movable drilling platform for different water depth (1)

3.2 Fixed multiple leg structures

In Sub Arctic regions like Cook Inlet, Alaska or Bohai Bay, China, piled structures have been used. For heavy ice conditions problems like fatigue damaged jackets due to ice induced dynamic vibrations in Bohai Bay were reported.

Ice accumulation between the legs have to be avoided by having a minimum distance between the legs of five to seven times the legs diameter and a sufficient depth of the cross stiffeners between the legs. To protect wells, risers or the drill string, they could be placed in the jacket legs. So even this structure does not seem to be capable of heavy ice conditions, in regions with less ice it could be the most economical in comparison with e.g. caisson structures.



Figure 9: Platform JZ20-2 MUQ and MNW at Bohai Bay, (13)

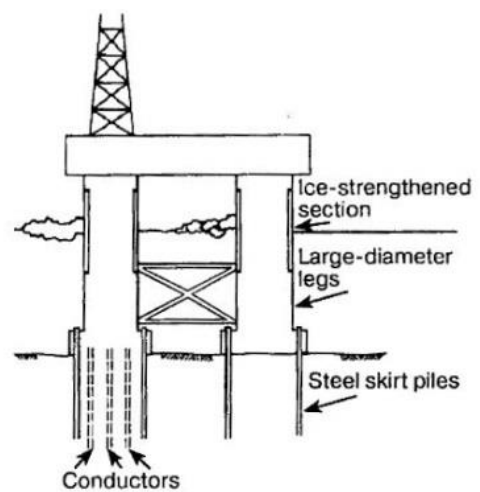


Figure 10: Piled structure at Cook Inlet,
(14) in (1)

3.3 Jack up structures

For small hydrocarbon reservoirs or following subsea installations it is more viable to use structures, which are simply removable and reusable at other areas. These criteria are fulfilled by jack up platforms.

As for all multiple leg structures the possibility of jamming between the legs has to be considered. Therefore also jack up structures with closed cylindrical surfaces and gear teeth at the legs instead of a jacket shaped legs should be used.

To reduce the load on the legs, downward breaking cones around the legs, near the bottom of the topside can be mounted. In case of an ice layer the topside can be lowered so that the cones are at the water level. Otherwise the topside is moved up, to reduce hydrodynamic impact through the cones and does not run risk to be affected by waves. (15)

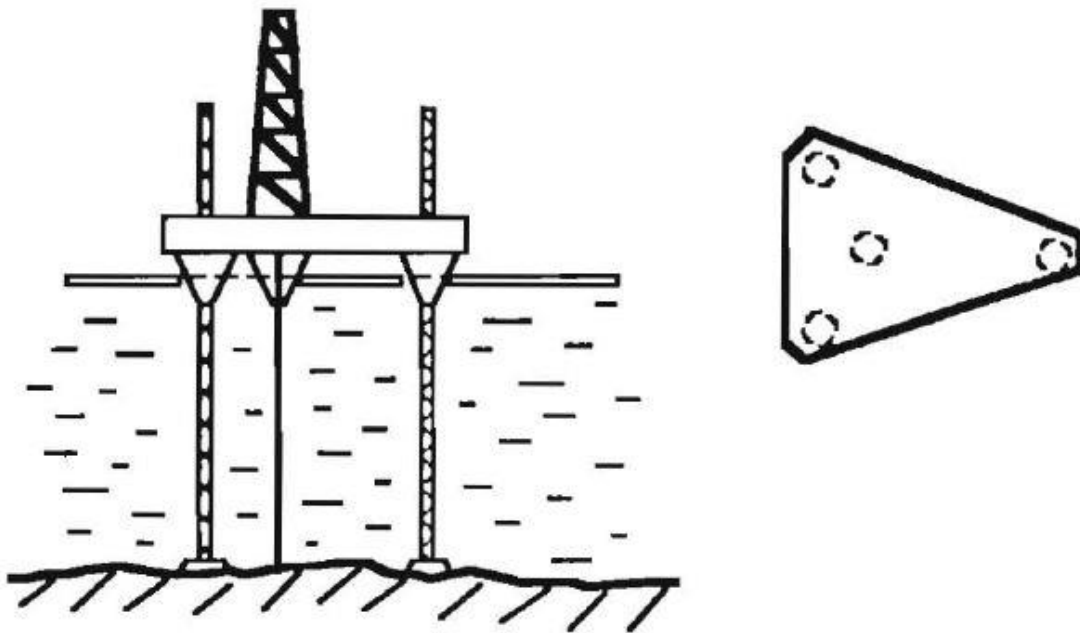


Figure 11: Jack up platform with conical leg protection (15)

3.4 Floating structures

As Jack-up platforms, floating structures have the advantage that they are more economical to install as fixed structures. Also floating structures give the chance of disconnection for not feasible ice conditions. They could be positioned by moorings or thrusters. Difficulties could rise to a higher demand on a small offset between ship and borehole in shallow water than in deep water. This occurs because at the borehole the maximum deflection of the drill string from the vertical position is about 6° . In combination with a high scatter of ice loads this leads to higher requirements to the station-keeping systems. Furthermore the thrusters have to resist ice impacts and the mooring lines near the water surface should be protected from ice to avoid accumulations and additional load.

Round floaters

A circular shape has the advantage that the vessel does not have the need of vane for changing ice drift directions but therefor has poorer sea keeping properties for ice free conditions.

In 1983 the Kulluk vessel (Deck diameter: 100 m, waterline diameter: 70 m, draft: 11.5-12.5 m, displacement: 28 000 t) entered the Beaufort Sea. It has a round conical hull, a protected submerged mooring system in the centre and no propulsion system. The mooring system was designed to resist global ice loads till 7.5 MN in working conditions by an offset of 5 % of the water depth (depth: 20 – 60 m) and 10 MN in survival conditions by an offset of 10 % of water depth. It was also fitted with a quick disconnection system. (16)

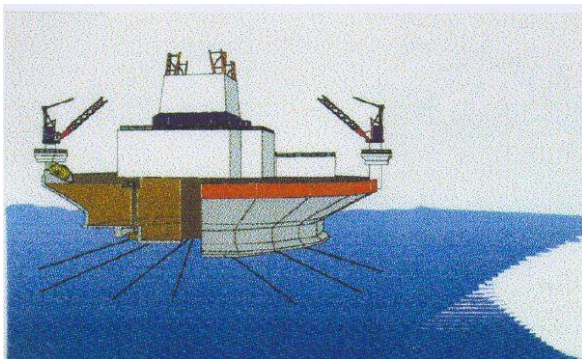


Figure 12: Sketch of Kulluk exploration vessel (16)



Figure 13: Kulluk on site during ice management (16)

Semi-submersibles

In general semi-submersibles are known for their good sea keeping properties. Even if during ice conditions the wave behaviour is not that important, it could be taken into account for operation during summer where no ice cover is present. It also enables a larger flexibility for possible operational areas. In comparison with e.g. ship shaped vessels, the semi-submersible is relative unsusceptible against changing in ice drift direction. As for all multiple leg structures also problems by additional forces due to jamming have to be considered.

In 1983 an ice resistant semi-submersible has been developed and tested in model tanks successfully even the ice loads were underestimated firstly. Attention was focused to have no struts or bracings trough the water plane to minimize ice interaction and rubble accumulation. To keep good sea keeping properties and also have the possibility to generate only low ice loads on the same platform, an additional draught for icebreaking modus was considered. At the upper ends of the columns downward cones are mounted. So if an ice cover exists and the wave amplitude is thereby lower that no need for a big distance between water plane and top-side is needed, the draught of the platform can be increased and the cones reaching the water/ice level. Furthermore an additional cone in the centre of the platform is mounted to protect the riser. (17)

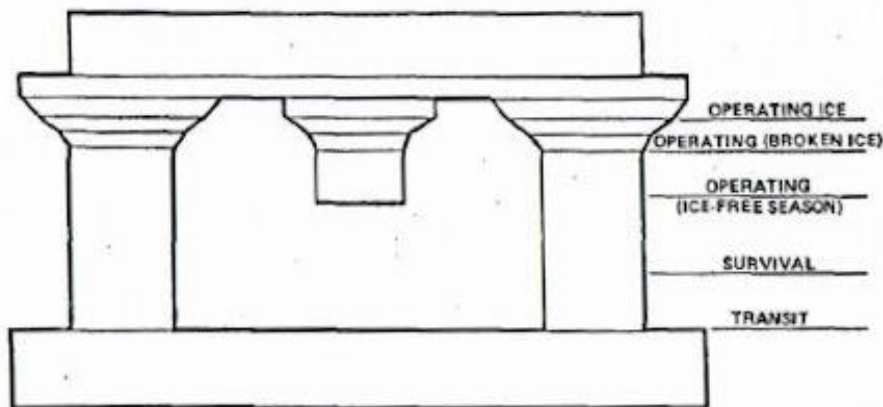


Fig. 4—Loading conditions

Figure 14: Side view of Semi-submersible (17)

Ship shaped vessels

The possibility of relative high transit velocities to the application sites and operations in deep water areas are in general the properties of drill ships.

During ice interaction from the front it can benefit from its relative small surface area at the front and a bow, shaped for effective ice breaking. However, if the drift direction changes and the vessel is limited against vane, the ice drifts against the broadside of the vessel and the loads increase very strongly. So the possibility to vane limits the ice capability.

Nevertheless, promising concepts to manage this problem, like at the Polar Research and (Scientific) Drill Vessel, “Aurora Borealis”, are developed (see chapter 4.1).

Also the first drillship with the IACS Polar Ice Class – PC 5, “Stena Icemax”, was launched in 2011 (Length: 228 m, breath: 42 m, draught: 12 m). PC 5 means, that it is suitable for year-round operation in medium first-year ice (till 1.2 m thick) which may include old ice inclusions. The support of at least two icebreakers for ice management is highly recommended. It is fitted with a dynamic positioning system with six azimuth thrusters of each 5.5 MW. (18)
(19)



Figure 15: Stena Icemax (20)



Figure 16: Stena Icemax model during stationkeeping tests in managed ice conditions (19)

4. Methods for reducing ice loads

For safe operation conditions the platform should be designed that only minor global loads on structure, foundation or station keeping systems occur to withstand the ice conditions. In the following section methods for reducing these loads are described. They are divided into active and passive methods. Active methods need additional energy during their usage and passive are design considerations.

4.1 Active methods for reducing ice loads

Ice Management

In front of the structure icebreaker can help to reduce the ice loads of incoming ice. They can break and thereby reduce the size of ice floes and ridges. Collision with large or non-manageable ice (e.g. multi-year ridges, icebergs) can be avoided by towing them away or re-directing by pushing with the wake of e.g. azimuth thrusters or the water cannon (21).

High improvements have been done by the use of azimuth thrusters than traditional propulsion to new icebreakers:

- “Ice can be broken by the wake of thrusters sometimes this can be even more efficient than breaking ice with the hull of the vessel.
- Ice can be cleared in a highly effective manner by the use of the wake of azimuth thrusters.
- The icebreaker can either stay stationary in moving ice whilst managing ice or move in a multitude of desired ways while doing so.
- The wake of the thrusters can dismantle large first year ridges by blowing away their keels, causing collapse due to lack of buoyancy.” (22)

Also ship shaped vessels for which vane is not possible because they are icebound could be extricated. Icebreaker could also observe the incoming ice conditions and send the data to the dynamic positioning system of the platform.

Depending on the ice conditions, type of platform and needs due to back-up level, redundancy and regulations different levels of ice management till two or more icebreakers working at the same time with available redundancy and back-up are possible. (1)

The advantages of azimuth thrusters lead also to the consideration to fit platforms like semi-submersible with them and managing ice by themselves while staying stationary.

Induced motions

From 2001 till 2012 ran a project for development of a new Polar Research and (Scientific) Drill Vessel, Aurora Borealis (Length: 199.95 m, breath: 49 m, draught: 13 m). During that, methods for breaking ice of 1 to 2 m thickness while station keeping with a Dynamic Positioning system were investigated. For breaking ice during station keeping, a combination of forced roll and pitch motions with a partly sloped hull was considered.

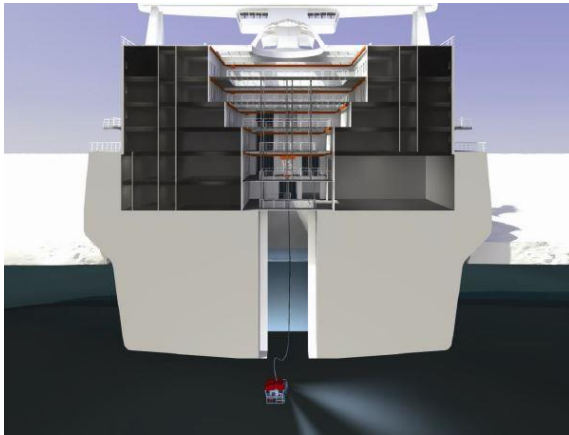


Figure 17: Shape of hull for ice breaking in transverse direction (23)



Figure 18: Model tests for ice breaking in transverse direction (24)

It was planned to realize the motions by pumping sea water between tanks at the port and starboard, respectively bow and stern, side of the vessel. For a heeling angle of $3 - 5^\circ$ the water is pumped in 60 to 100 s from one side to another per cycle. For pitch motions two times 750 t of water have to be pumped in 19 s maximum from one end to and to another. For the pitch motions two pumps of each 3 MW were considered. Model ice tests showed that this principle seems to work successfully till approximately 2 m thick ice. (23)

In 1979 also induced heave motions during development of a floating drilling, production and storage structure with an hourglass shape at the water plane were considered. The heave motions should be generated by periodic release of compressed air or gas, or hydraulic pull-down on vertical mooring lines. Scale model tests were made and the heave motions seemed to be an effective method of breaking ice sheet and ridges. (25)

Oscillating cones

Small icebreakers can increase their icebreaking capacities by generating additional pitch motions. This is done by using the so-called “Stampfanlage” which works with an eccentric rotation of masses in the forebody of the ship. This principle could be transferred to offshore structures with downward conical legs. The masses could be installed in floating conical collars, which are mounted around the vertical legs of the structure and are allowed to make horizontal and vertical oscillations. Frederking and Schwarz carried out model tests with oscillating cones in 1982 at the HSVA and observed that the mean horizontal force can be reduced by an amount of 33 % for pure vertical oscillations. For vertical and horizontal oscillations it has been even 66 %. The oscillations for these reductions were in the range between 1.3 and 2 Hz. (26) However, probably because e.g. of the difficult bearings of the cones this mechanism has not been applied to full scale structures till today.

Hull heating system

Especially for sloped structures the amount of friction between ice and the structure surface influences the global load because the ice has to be pushed up on the structures surface to fail (27). But also the load on structures with a vertical surface is influenced by friction, e.g. due to the sliding of ice at the side walls. The friction coefficient could be reduced by lubricating the surfaces with a water layer. This can be done by melting a part of the ice layer upon the structure. A heated outer surface prevent also from adfreezing of the ice and thereby jamming the platform during low ice velocities and tides. Because machineries at the platform producing a lot of waste heat this could be used to warm up the hull with less additional energy consumption. (28)

Air bubbles

Systems exist to keep water areas ice free by blowing out warm air out of pipes at the seabed. This method prevents from the formation of a new ice cover rather than destroying an existing one. So it works only for protected areas like bays or harbours were no ice of the neighbourhood drifts into the ice free area. (29)

Alexander Dummer	Project work	Investigation of Ice Interactions
MSF LS Ocean Engineering	handed in as	on Drilling Rigs in
University of Rostock	“Studienarbeit”	Shallow Water

High power microwaves

In 1995 Klyuchnik et al. investigated the destruction of sea ice during high power microwave radiation. The microwaves heat mainly the brine and for an effective destruction process sufficient large values of microwave power are needed. For protecting a leg like in figure 19, during ice velocities of 0.5 m/s and an ice thickness of 1 m, about 1MW for a frequency of 915 Hz should be necessary. Unfortunately the leg diameter is not clear. (30)

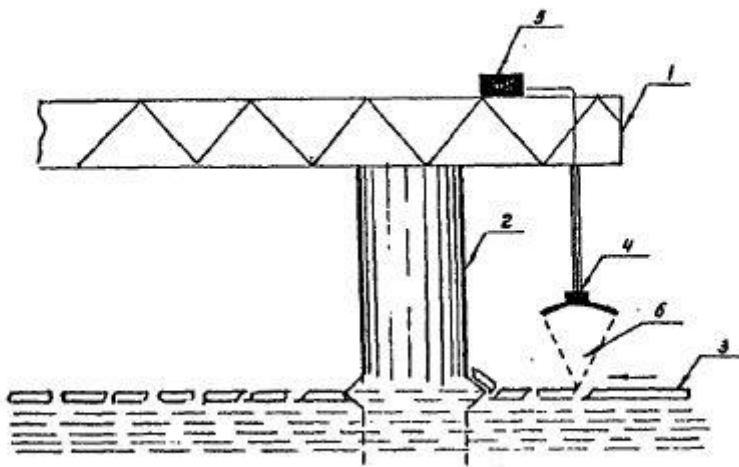


Figure 19: Platform protection by microwave source; 1) Platform, 2) Leg, 3) Moving ice, 4) Moving microwave unit, 5) High-Voltage source, 6) Microwave radiation (30)

This system could be interesting for mobile structures like Jack-ups that should be upgraded for ice infested areas because it seems to be relatively easy to install. Also as part-time operation for icebreaker to increase the icebreaking capacity on demand it could be interesting. Otherwise the risk for failure and costs for permanent operation due to the high demand of electrical energy are probably too high. It is not applied in field till today.

Disaggregation drums

Also devices for mechanical destruction of the ice cover have been invented. Disaggregation drums cut the ice in front of the structure which should be contra rotating and thereby eliminating a resulting torque. For clearing of the drums e.g. compressed air or exhaust of the engines should be used. (31)

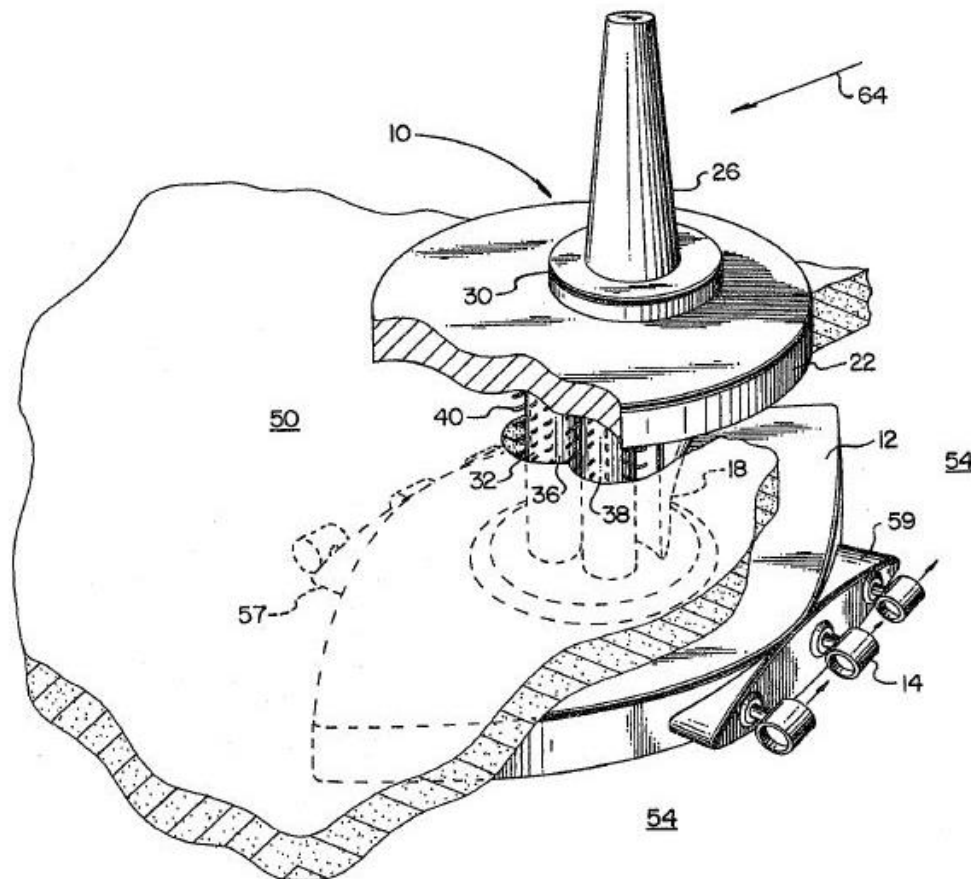


Figure 20: Operation vessel with disaggregation drums (31)

The reasons for no propagation of this method are probably a high attrition of the cutters, a high energy demand for an unnecessary high degree of destruction/pulverization of the ice cover and difficult possibility for redundancy of the cutting mechanism without ice management.

4.2 Passive methods for reducing ice loads

In accordance to the ISO the plane shape, in contrast to the plane dimensions, does not influence the global load much, except in situations where a corner of a rectangular structure is orientated towards the ice motion direction. So the waterplane shape has an influence from 10 to 15 % on the magnitude of global ice actions (32). Considering the size effect, the global average pressure for narrow structures is higher than for a wide one. (2)

Profile shape

In general the horizontal global loads can be reduced strongly by considering sloped structures instead of vertical structures. The reason is that the ice cover fails since bending failure instead of e.g. crushing failure. This can be transferred to cylindrical, resp. conical structures as well as on wide structures. Therefor additional vertical forces occur, which can lead to an additional overturning moment of the structure. (33)

A large amount of rubble that accumulates on the structures surface can cause so much additional load, that no reduction takes place any longer (2).

A significant difference of the horizontal load exists between downward breaking and upward breaking mode. During the upward breaking process the ice has to ride-up the structure, whereas during downward breaking it has to become submerged. Because the friction part of the horizontal load is influenced by buoyancy instead of weight, the force normal to the structure surface is lower for downward breaking structures. (27)

Also the vertical component is lower for downward breaking structures, but is also directed upwards. This reduces the effective shear resistance at the structure-seabed interface and thereby the resistance against translational displacement of the structure (2).

For shallow waters also the aspect of the possibility of jamming of ice ridges between the downward breaking cone and seabed should be considered, which leads also to increasing vertical forces (27).

This leads also to a larger action period as for vertical structures which often differs more from the structures natural period (33).

Multifaceted conical structures

During looking for a cost-effective and practical design, in the mid 1980's sloped structures with flat faces (facets) had been considered. Concerns appeared that the clearing forces would be greater than predicted by using the current theories.

It was found out that the facings have some effect on cracking patterns of ridges and ride-up process, but the theory gave reasonably comparable results. (34) (35)

Multiple legs

In general it can be said, that global horizontal loads are lower if only a smaller part of the ice cover needs to be destroyed. So structures with multiple legs for small waterplane areas and still great topsides come into play.

Model tests have shown that if the distance, orthogonal to the ice drift direction, between the surfaces of two legs is higher than five times a single leg diameter, the loads on a single leg can be calculated without taking into account the influence of another leg. So the global load on the whole platform is the sum of the single loads from each leg. For structures with three or four legs, the distance must be equal or greater than 7.3 times the leg diameter.

If the distance is lower, the load in the direction of ice velocity decreases, because the force vectors tend to rotate inwards up to 12° for two legs. But the individual load on each leg is the same.

Investigations for platforms with an aspect ratio (leg diameter divided by ice thickness) of mostly 7.5, showed that for a minimum global action the optimum leg spacing for a three-leg platform is 5.3 and for a four-leg platform is in the range from 2.5 till 4.

For some ice drift directions it is possible, that the legs in back of the forward legs are sheltered and have only contact with broken ice. Laboratory experiments showed that the loads on back legs never exceed 6 – 7 % of the actions on the front legs.

Nevertheless it should be taken into account, that rubble can accumulate between the legs and jamming occurs. Than the global load can exceed strongly the sum of single loads, calculated without jamming.

(3) (33)

Sloped multiple leg structures

Määttänen did scale model tests in 1992 with downward and upward breaking cones arranged in a triangular pattern. He varied cone spacing, direction of ice drift and ice velocity. During that he did not observe any jamming or pile-up, regardless of cone spacing. Also the loads never reached three times the single load, probably because of non-simultaneous occurrence of maximum force.

In contradiction to knowledge from vertical legs, he observed for upward breaking cones the highest ice load during minimum cone spacing. The minimum load was observed during spacing similar to the cone diameter. As explanation for higher loads he gave a higher clearing component, because the broken ice has to be pushed further out to pass the trailing cones.

The total load for upward cones increased about 20 % by changing the ice drift direction from one trailing and two front cones to two front cones and one trailing cones.

For downward breaking cones a clear minimum of load for a specific cone spacing and dependence of drift direction was not observed, but therefore higher velocity dependence. The loads of downward breaking were less than 40 % as during upward breaking.

(15)

5. Ice load calculation models

If ice surrounds a platform, driving forces like wind, currents or thermal expansion move it against the platform. Depending on several factors different failure modes occur.

5.1 Vertical structures

5.1.1 Failure modes

The occurring failure mode depends on the

- rate of indentation $\frac{U}{D}$
- aspect ratio $\frac{D}{h}$,
- shape of the indenter,
- absolute thickness and size of the ice cover,
- material properties like stiffness and strength of ice cover (depending on temperature, salinity and crystal orientation).

U is the velocity of the coming ice, D the diameter of the indenter and h the thickness of the ice cover. These modes are investigated in indentation tests, where an indenter moves against an ice cover (see figure 21). The indenter could represent a leg of a structure or the whole body of a structure.

Because of the surrounding ice which discourages the ice to deform, the indentation stress $P/(Dh)$ is higher than the strength from uniaxial tests (see table 4) depending on aspect ratio.

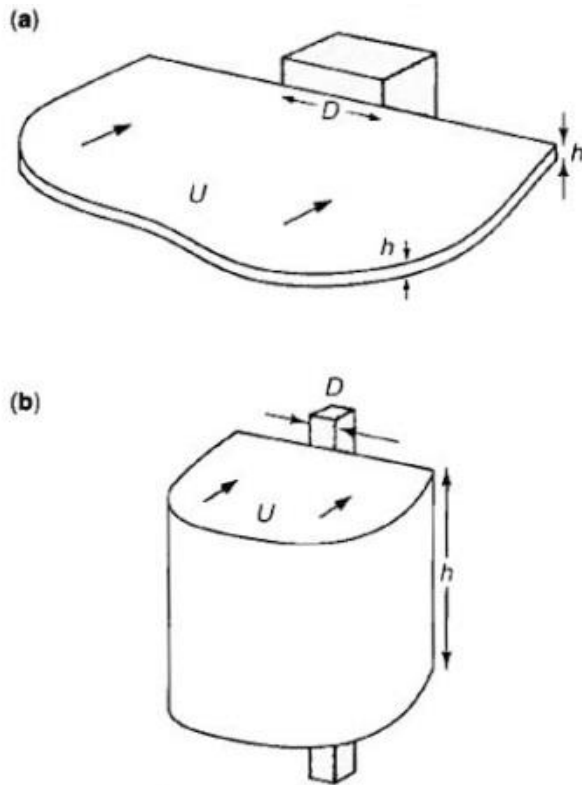


Figure 21: Indentation geometry, (3)

Different failure modes are shown in figure 22. In laboratory experiments and in the field it is possible that different modes occur at the same time (33). But for simplification this work regards only one mode per calculation. The modes a) to d) are called global failure modes whereas e) and f) are called local failure modes.

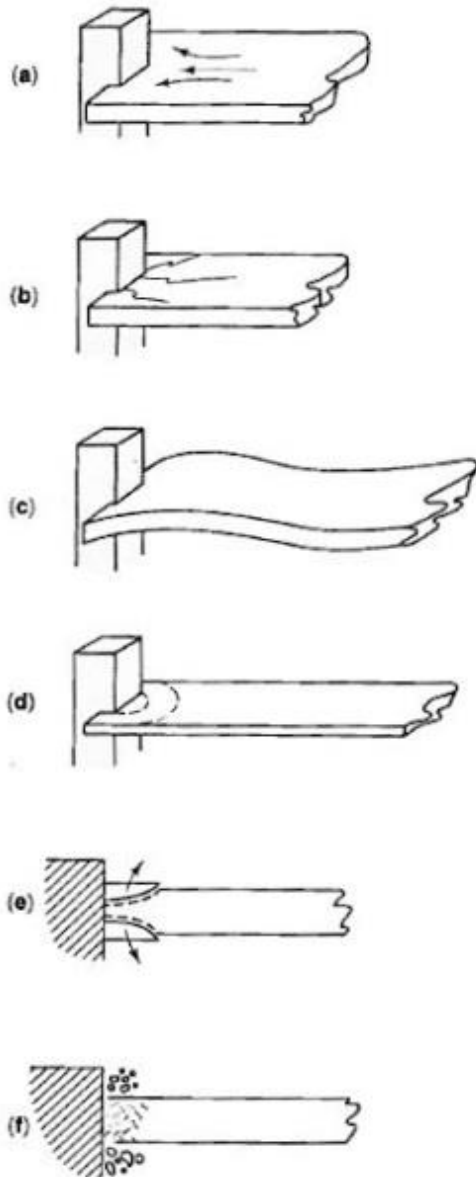


Figure 22: Principal failure mechanisms of laboratory indentation tests: a) creep; b) radial cracking; c) buckling; d) circumferential cracking; e) spalling; f) crushing , (3)

Figure 23 gives a rough overview of the circumstances when the different modes occur. There are no clear values for the transition between the different modes and is also a dependency of other factors like the absolute thickness of the ice cover. (3)

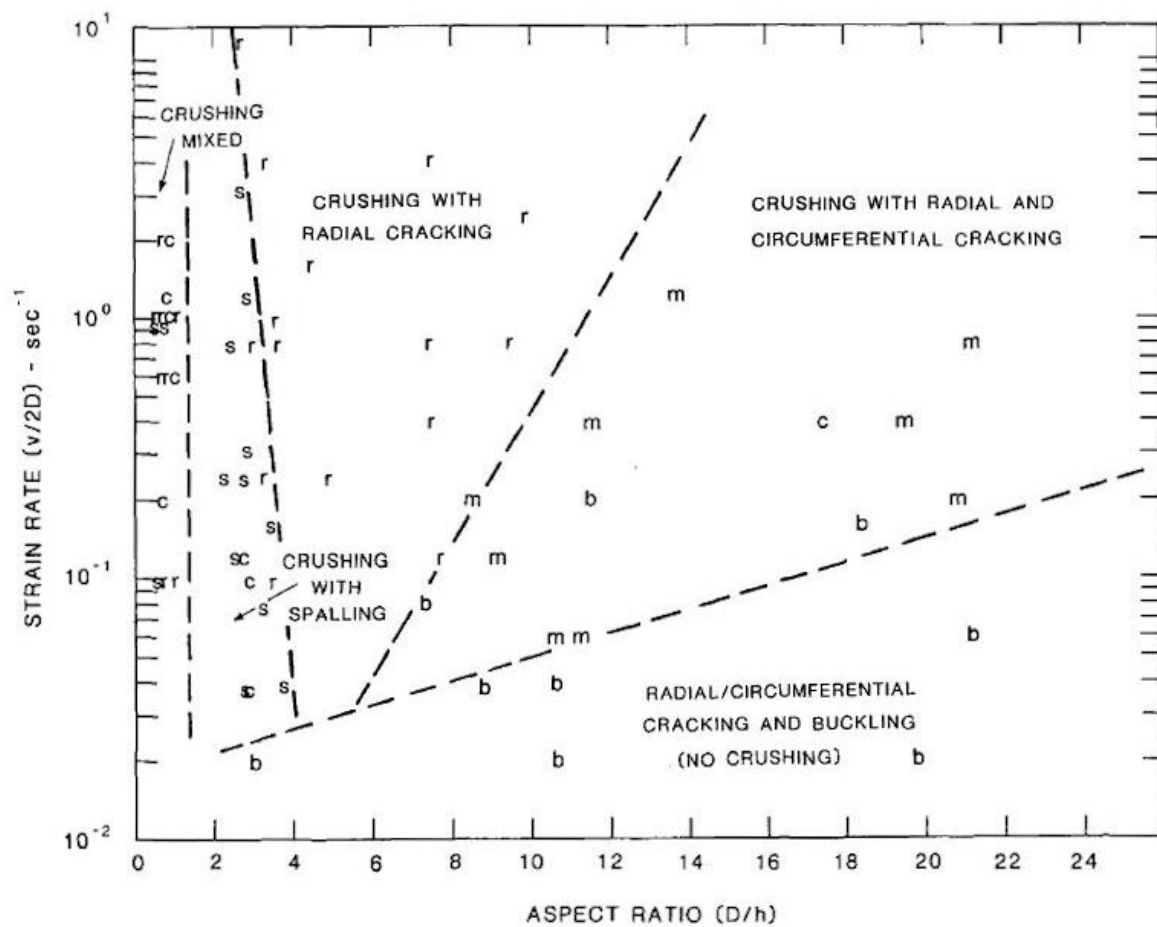


Figure 23: Failure modes dependent on indentation rate and aspect ratio (36)

Sanderson observed the transition from creep to fracture behaviour for following values:

Table 3: Indentation rate for transition to brittle behaviour, dependent on scale (3), (37)

Indentation strain rate ($U/2D$) [$1/s$]	Indenter diameter [m]
$10^{-4} - 10^{-2}$	~ 1
$10^{-5} - 10^{-4}$	~ 10
$10^{-7} - 10^{-6}$	~ 100

Although more theoretical formulas exist (see Schulson (37)) these values are chosen for a line of best fit and used as criterion for pure creep in 5.1.2 because of a lack of parameters for a general application of the other formulas.

5.1.2 Pure creep

In general it is unlikely that structures are exposed to pure creep conditions. Normally the natural driving forces affecting the ice are high enough to have a strain rate for a transition to fracture behaviour. Nevertheless it can occur, for example in landfast conditions when the ice melts and expands (3). Relying on medium scale tests the ISO simplified Sanderson's observation (see table 3) and says that creep occurs for ice velocities of less than 1 mm/s (2).

The indentation analysis can be done in two different ways, either the plastic limit analysis or the reference stress method. (3)

The latter method was chosen here, because it has the advantage that the deformation properties of the material ice can be modelled realistic, concerning Norton's power law for creep. But both methods do not incorporate brittle behaviour.

Assumptions

It will be assumed that the ice has a perfect contact to the structure surface. That can happen sometimes if the ice is adfrozen, besides the load is lower in the non-adfrozen case so the calculations have a higher safety factor. Also the ice should have an initial imperfection. During pure creep conditions no arising of cracks is taken into account.

The ice layers of granular and columnar ice are treated independently even they have different material properties and tend to bend under horizontal compression. However, the loads of the different layer are only added.

Calculation

As a first step the indentation strain-rate $\dot{\epsilon}$, depending on the velocity of the ice and the platform geometry, has to be calculated. Afterwards the global loads can be calculated from the nominal contact area and the stresses, which are depending on the indentation strain-rate.

$$\dot{\epsilon} = \frac{U}{I \cdot \psi \cdot D} \quad (5.1)$$

U is the velocity of the coming ice, I the indentation factor (ratio of indentation pressure $P/(Dh)$ and uniaxial strength R) and ψ the compatibility factor. They are chosen as follows:

Alexander Dummer	Project work	Investigation of Ice Interactions
MSF LS Ocean Engineering	handed in as	on Drilling Rigs in
University of Rostock	“Studienarbeit”	Shallow Water

Table 4: Parameters for creep indentation (3)

	Granular ice (isotropic)		Columnar ice (anisotropic)	
	I	ψ	I	ψ
D << h	2.97	0.45	4.12	0.45
D >> h	1.15	0.39	3.13	0.45

So the stress can be calculated from the indentation strain rate (see equation 2.4):

$$\sigma = \sqrt[3]{\frac{1}{A_E} \cdot \dot{\epsilon} \cdot e^{\frac{Q}{R \cdot T}}} \quad (5.2)$$

To get the right stress for the final load calculation, it has to be corrected for temperature and salinity like in chapter 2.2.3. Then the net section stress σ' can be used in combination with the contact area of the platform:

$$P_{PC} = I \cdot D \cdot h \cdot \sigma' \quad (5.3)$$

P_{PC} is the global load on the concerning platform by the specific ice layer (columnar or granular), D is the structure diameter which is in contact with the ice cover. So whether D is the diameter of a single leg or the whole platform depends on the structure type.

(3)

5.1.3 Buckling

To calculate loads due to buckling and to predict if buckling or crushing failure occurs, Sodhi and Harnza developed in 1977 a formula based on Finite Element calculations (38).

For these calculations the ice sheet was assumed to be an isotropic, homogenous and semi-infinite plate resting on an elastic foundation.

Rectangular elements were used for it and an adaption of the element size which depends on the distance from the load source was applied. Also three different buckling modes were considered.

The results were checked by comparison with available simply exact theoretical solutions and convergence tests concerning the mesh size up to 7×7 elements were made. To develop the formula a mesh of 6×6 elements was used for calculations with varying aspect ratios and the modulus of elastic foundation. (38)

The buckling action can be calculated as follows:

$$P_B = \rho_i \cdot g \cdot l^3 \left(\frac{D}{l} + 3.32 \left(1 + \frac{D}{4l} \right) \right) \quad (5.4)$$

where l is the characteristic length:

$$l = \sqrt[4]{\frac{E \cdot h^3}{12 \cdot \rho_i \cdot g (1 - \nu^2)}} \quad (5.5)$$

(33)

5.1.4 Crushing

It can be assumed that in every piece of ice is a statistical distribution of flaws of different size. So for bigger ice pieces there is a higher chance for finding bigger flaws. Also the possibility for ice non-homogeneity, non-simultaneous failure increases with bigger pieces. So it exists a size effect.

Another explanation could be made by dimensional analysis: The important parameter K_{IC} (see 2.12) which describes the fracture mechanism has a dimension $\text{kNm}^{-3/2}$. If a geometrical scaling law is used ($\frac{D_{max}}{D_{min}} = \lambda$) and all linear dimensions change proportionally by size, K_{IC} should be reduced by $\lambda^{3/2}$ for modelling D_{min} .

This fits to the values of the following statistically formula:

$$R_C \propto A^{\frac{-3}{2b_f}} \quad (5.6)$$

where A is the contact area and b_f is a statistical parameter equal to 3. So the global load results as

$$P = I \cdot R_C \cdot A^{-0.5} \cdot D \cdot h . \quad (5.7)$$

(3) (33)

5.1.5 Korzhavin equation

In 1962 K. N. Korzhavin developed an empirical formula:

$$P = I \cdot m \cdot k \cdot D \cdot h \cdot R_C \quad (5.8)$$

where P is the global load, I the indentation factor (possible to use values from plasticity theory: Table 4 in 5.1.2), m the structure's in plane shape factor ($m=1$ for a flat indentation, $m=0.9$ for a circular indentation), k the contact factor, D the structures diameter, h the ice thickness and R_C the uniaxial compressive strength.

Sanderson (3) recommends to use the equation as follows:

For creep indentation with perfect surface contact ($k=1$), which can happen if the structure is adfrozen, R_C can be calculated by the equations (2.6) and (2.7).

During fast fracture a large number n of non-simultaneous failures on small zones with the size d_r occur (see figure 24).

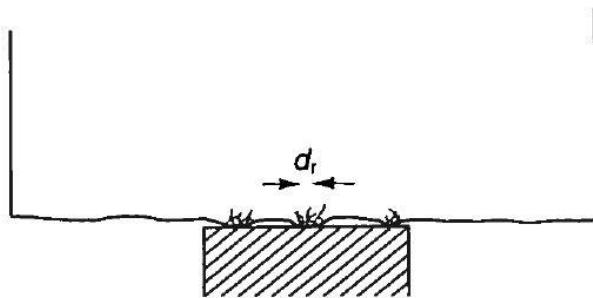


Figure 24: Fracture with contact over n zones of width d_r (3)

So equation (5.8) can be written as

$$P = n \cdot d_r \cdot I \cdot m \cdot h \cdot R_C \quad (5.9)$$

and k results as

$$k = \frac{n \cdot d_r}{D} \quad (5.10)$$

For R_C the equation (2.11) is used, and fitting it to indentation conditions I must be calculated by using the aspect ratio of d_r/h . Because of a lack of values of n and d_r , values of Table 4 are used for factor I .

Korzhavin recommended values for k in the range of 0.4 - 0.7 for D from 3-10 m. Blenkarn calculated for Cook Inlet a value of $k=0.5$. For wider structures of Molikpaq (Beaufort Sea) of about 120 m diameter and Hans Island Sanderson calculated values of $k=0.07$. (3)

Therefore a line of best fit was used from the values of Korzhavin and Sanderson.

Alexander Dummer	Project work	Investigation of Ice Interactions
MSF LS Ocean Engineering	handed in as	on Drilling Rigs in
University of Rostock	“Studienarbeit”	Shallow Water

Even the equation does not take much physical mechanisms into account it is used in the American API and Russian Code SNIP (33).

5.1.6 Masterson

In 2000 Masterson et al. published that for wide structures the ice thickness h is the main parameter. He developed a formula depending on the Freezing Degree Days [$^{\circ}\text{C}$] (the sum of daily degree below freezing point) of the evaluated region:

$$p_M = K_Z \cdot h^{-0.174} \quad (5.11)$$

K_Z is equal to

- 1.5 for 3000-4000 $^{\circ}\text{C}$
- 1.25 for 2000 $^{\circ}\text{C}$
- 1 for 1200 $^{\circ}\text{C}$

and it should be multiplied with the contact area of the structure.

(33)

5.1.7 ISO 19906

The ISO 19906:2010 (Petroleum and natural gas industries – Arctic offshore structures) gives a guideline how to calculate ice actions on structures. The proceeding to calculate global ice actions for vertical structures is described in part A.8.2.4.3.

The global ice load P_{ISO} follows from the global ice pressure averaged over the nominal contact area multiplied with the nominal contact area. The nominal contact area results from the structure width or diameter multiplied with the ice thickness:

$$P_{ISO} = p_G \cdot h \cdot D \quad (5.12)$$

The global average ice pressure in the ISO 19906 should be calculated by an empirical formula. The data for this formula is obtained from full-scale measurements in Cook Inlet, the Beaufort Sea and Bohai Sea and concerns a conservative limit for first-year and multi-year ice.

Alexander Dummer	Project work	Investigation of Ice Interactions
MSF LS Ocean Engineering	handed in as	on Drilling Rigs in
University of Rostock	“Studienarbeit”	Shallow Water

$$p_G = C_R \left(\frac{h}{h_1}\right)^n \left(\frac{D}{h}\right)^m \quad (5.13)$$

To take the temperature and salinity dependence in different areas into account the ice strength coefficient C_R varies depending on the region or could be calculated based on own measurements. In this work a value of 2.8 MPa for the Beaufort Sea is used.

n and m are empirical coefficients:

- $m_{ISO} = -0.16$,
- for $h < 1$ m: $n_{ISO} = -0.5 + \frac{h}{5}$,
- for $h \geq 1$ m: $n_{ISO} = -0.3$

h_1 is a reference thickness of 1 m. Equation 5.13 holds for rigid structures with aspect ratios D/h greater than 2 and a displacement of the waterline which results as a static response of the ice load less than 10 mm.

5.1.8 Velocity correction

A fitting of the ice loads to different ice velocities is done by several methods. At first by using different failure mode mechanisms at the corresponding strain rate (see figure 23).

A further method (in accordance to Bohon and Weingratten, (39)) is to adjust the compressive strength during continuum behaviour to the effective strain rate. Thereby the indentation strain rate can be fitted to the strain rate of uniaxial test depending on the aspect ratio:

$$\dot{\varepsilon} = \begin{cases} \frac{U}{4D}, & \text{if } \frac{D}{h} < 0.5 \\ U \cdot \frac{D}{h^2}, & \text{if } 0.5 \leq \frac{D}{h} < 2 \\ \frac{2U}{h}, & \text{if } \frac{D}{h} \geq 2 \end{cases} \quad (5.15)$$

But there is some doubt if this method could be used for big offshore structures with high aspect ratios, because these formulae are results of laboratory experiments.

As third method Korzhavin proposed 1962 that the ice action is proportional to $(U/U_0)^{-1/3}$, where U_0 is a reference velocity of 1 m/s (13). This dependence is also used in the API 95.

5.2 Sloped structures

In general sloped structures have a lower global load as vertical structures since the ice fails due to bending. Nevertheless it should be kept in mind that also loading scenarios from vertical structures can occur for large rubble accumulation around the structure. However, this is not part of this work.

For sloped structures the ISO 19906 provides two ways of estimating the ice loads while considering the main physical effects, either the theory of plasticity or the theory of elastic beam bending. Both are quasi-static solutions and do not consider the influence of ice velocity. So also the methods of chapter 5.2.4 are applied.

5.2.1 Plastic method (cone structures)

Concerning the plastic method for cones, the ISO and API-88 refers to the Paper of Ralston (27). He introduces into the plastic limit analysis of sheet ice loads.

This analysis idealizes the floating ice as an elastic-perfectly plastic plate resting on an elastic-perfectly plastic foundation. It is a pure bending analysis and the effect of in-plane forces on the moment capacity is neglected.

To calculate the deformation in front of the cone, moment yield criteria are used which describe the biaxial bending behaviour. Here the Tresca and Johansen criterion with equal upward and downward bending moment capacities are used. Also this is a simplification because of the composite of columnar and granular ice (see 2.2). The bending moment capacity is expressed in terms of flexural strength R_F , which is the elastic stress in the outer fibres of the ice when failure occurs.

The comparison by Ralston between loads calculated with the Tresca yielding criterion and the Johansen criterion shows that the choice of the yield criterion has only a minor influence. In general, calculations with the Johansen criterion give a higher load value than calculations with the Tresca criterion. (27) The ISO does not give a recommendation which criterion should be used or represents the material behaviour at its best and shows both calculation methods.

The calculation takes dissipation of energy due to the plastic hinge idealizations of circumferential and side cracks, foundation reaction, deformation in front of the cone and ride-up of ice.

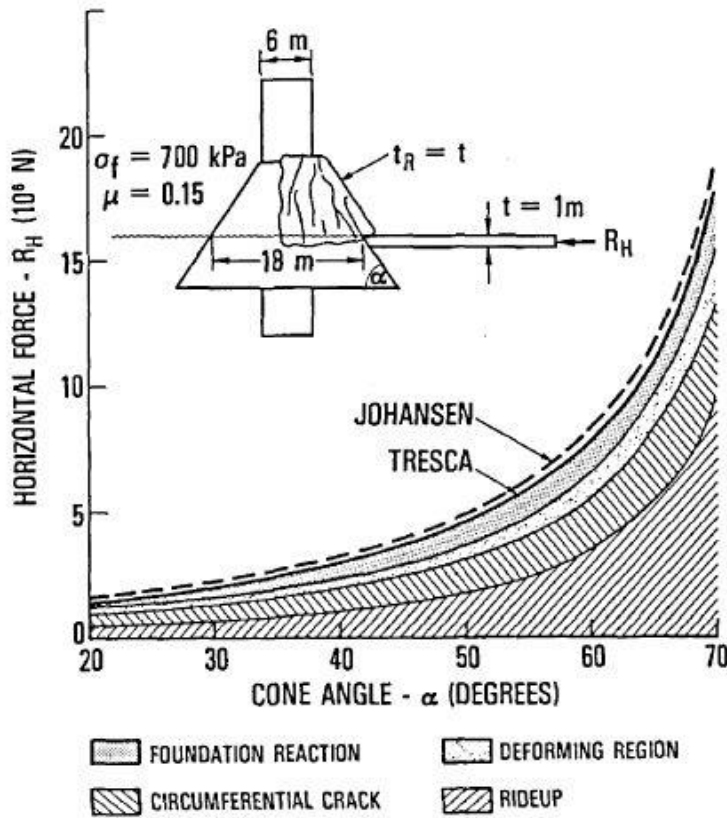


Figure 25: Forces on upward-breaking cone (27), here t and t_R are equal to h and h_R

Below is the calculation method, suggested by the ISO19906 for upward breaking structures. To get the loads for downward breaking structures ρ_I have to be replaced by $(\rho_W - \rho_I)$.

To take into account the structure geometry, first the parameters f , g_r and h_V are calculated:

$$f = \sin(\alpha) + \mu \cdot E_1 \cdot \cos(\alpha) \quad (5.16)$$

where E_1 is the complete elliptical integral of the first kind and μ is the friction coefficient between ice and structure,

$$g_r = \frac{\sin(\alpha) + \frac{\alpha}{\cos(\alpha)}}{\frac{\pi}{2} \sin^2(\alpha) + 2 \cdot \mu \cdot \alpha \cdot \cos(\alpha)} \quad (5.17)$$

$$h_V = \frac{f \cdot \cos(\alpha) - \mu \cdot E_2}{\frac{\pi}{4} \sin^2(\alpha) + \mu \cdot \alpha \cdot \cos(\alpha)} \quad (5.18)$$

where E_2 is the complete elliptical integral of the second kind.

$$E_1 = \int_0^{\pi/2} \frac{1}{\sqrt{1 - \sin^2(\alpha) \cdot \sin^2(\eta)}} d\eta \quad (5.19)$$

$$E_2 = \int_0^{\pi/2} \sqrt{1 - \sin^2(\alpha) \cdot \sin^2(\eta)} d\eta \quad (5.20)$$

The rubble weight parameter W is calculated as follows:

$$W = \rho_I \cdot g \cdot h_r \cdot \frac{D^2 - D_T^2}{4 \cdot \cos(\alpha)} \quad (5.21)$$

where ρ_I is the density of the ice, g the gravitational acceleration, D_T the top diameter of the cone and h_r the ride-up thickness. If the latter is assumed to be equal to a single ice sheet layer, the following express the horizontal and vertical components of ride-up action

$$H_R = W \cdot \frac{\tan(\alpha) + \mu \cdot E_2 - \mu \cdot f \cdot g_r \cdot \cos(\alpha)}{1 - \mu \cdot g_r} \quad (5.22)$$

$$V_R = W \cdot \cos(\alpha) \left(\frac{\pi}{2} \cdot \cos(\alpha) - \mu \cdot \alpha - f \cdot h_V \right) + H_R \cdot h_V \quad (5.23)$$

and the horizontal and vertical component of the breaking action

$$H_B = \frac{R_f \cdot h^2}{3} \cdot \frac{\tan(\alpha)}{1 - \mu \cdot g_r} \left(\frac{1 + Y \cdot x \cdot \ln(x)}{x - 1} + G \cdot (x - 1) \cdot (x + 2) \right) \quad (5.24)$$

$$V_B = H_B \cdot h_V \quad (5.25)$$

where Y is equal to 2.711 for using the Tresca yielding criterion or equal to 3.422 for using the Johansen yielding criterion, x can be calculated as follows

$$x = 1 + \frac{1}{\sqrt{(3G + \frac{Y}{2})}} \quad (5.26)$$

and G results as follows

$$G = \frac{\rho_I \cdot g \cdot D^2}{4R_f \cdot h} \quad (5.27)$$

The ride-up thickness h_r and thereby the load can increase through ice sheet rafting, rubble accumulations and jamming against the vertical structure part.

To get the total horizontal vertical forces the breaking and ride-up components are added:

$$P_H = H_B + H_R \quad (5.28)$$

$$P_V = V_B + V_R \quad (5.29)$$

5.2.2 Elastic beam bending (wide structures)

For calculating the ice load for wide structures the ISO refers to elastic beam theory by K. R. Croasdale et al. (40). It is recommended for wide structures and idealizes the process as an elastic beam on elastic foundation. The method offers also to consider the effects of rubble build-up in front of the structure in a way that is easy to use in probabilistic design load calculations. In addition to the plastic method it also makes allowance for in plane-forces by a simple iteratively re-adjust of the flexural strength:

$$R_f^{(1)} = \frac{P_H}{l_C \cdot h} + R_f \quad (5.30)$$

where l_C is the length of the circumferential crack

$$l_C = D + \frac{\pi^2}{4} L_C \quad (5.31)$$

and L_C is the characteristic length of an ice sheet or the length of the radial cracks

$$L_C = \sqrt[4]{\frac{E \cdot h^3}{12 \rho_W \cdot g \cdot (1 - \nu^2)}} \quad (5.32)$$

The horizontal action P_H consists of the breaking load H_B , the load component required to push the sheet ice through the ice rubble H_P , the load to push the ice blocks up the slope through the ice rubble H_R , the load required to lift the ice rubble on top of the advancing ice sheet prior to breaking it H_L and the load to turn the ice block at the top of the slope H_T .

$$H_B = 0.68 \cdot \xi \cdot \sigma_f \cdot \sqrt[4]{\frac{\rho_W \cdot g \cdot h^5}{E}} \left(D + \frac{\pi^2 L_C}{4} \right) \quad (5.33)$$

where ξ is the relationship between the horizontal and vertical forces

$$\xi = \frac{\sin(\alpha) + \mu \cdot \cos(\alpha)}{\cos(\alpha) - \mu \cdot \sin(\alpha)}$$

$$H_P = D \cdot r_h^2 \cdot \mu_i \cdot \rho_i \cdot g (1 - e) \left(1 - \frac{\tan(\beta)}{\tan(\alpha)} \right)^2 \frac{1}{2 \cdot \tan(\beta)} \quad (5.34)$$

where r_h is the rubble high, μ_i the ice-to-ice friction coefficient, e the porosity of the rubble. It is assumed that the rubble at a conical structure has a similar total porosity to the rubble of ridges, which is typical between 25 and 40 % (33).

The ice-to-ice friction coefficient depends on sliding velocity and ice temperature. It is calculated by a line of best fit from experimental data from Kennedy et al. (41)

Part of the rubble falls down from the sloping surface on the ice sheet during the ice sheet/structure interaction. It can be proposed that this rubble creates an

Alexander Dummer	Project work	Investigation of Ice Interactions
MSF LS Ocean Engineering	handed in as	on Drilling Rigs in
University of Rostock	“Studienarbeit”	Shallow Water

out-of-plane formation similar to a triangle with an angle of the rubble inclination to the horizon equal to β (33). The ISO advises to choose β not smaller than α minus 10° , so here was β assumed to be α minus 5° .

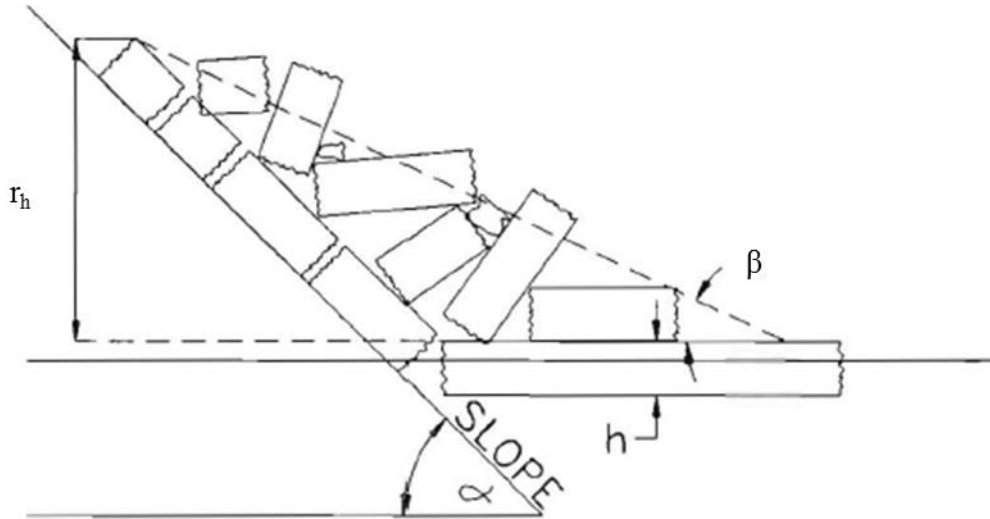


Figure 26: Rubble accumulation up and in front of structure (34), notation fitted

The further forces are calculated as

$$H_R = D \cdot P \cdot \frac{1}{\cos(\alpha) - \mu \cdot \sin(\alpha)} \quad (5.35)$$

where

$$P = 0.5\mu_i(\mu_i + \mu)\rho_i \cdot g(1 - e)r_h^2 \cdot \sin(\alpha) \cdot \left(\frac{1}{\tan(\beta)} - \frac{1}{\tan(\alpha)}\right) \left(1 - \frac{\tan(\beta)}{\tan(\alpha)}\right) + 0.5(\mu_i + \mu)\rho_i \cdot g(1 - e)r_h^2 \cdot \frac{\cos(\alpha)}{\tan(\alpha)} \left(1 - \frac{\tan(\beta)}{\tan(\alpha)}\right) + r_h \cdot h \cdot \rho_i \cdot g \frac{\sin(\alpha) + \mu \cdot \cos(\alpha)}{\sin(\alpha)} \quad (5.36)$$

$$H_L = 0.5D \cdot r_h^2 \cdot \rho_i \cdot g(1 - e)\xi \left(\frac{1}{\tan(\beta)} - \frac{1}{\tan(\alpha)}\right) \left(1 - \frac{\tan(\beta)}{\tan(\alpha)}\right) + 0.5D \cdot r_h^2 \cdot \rho_i \cdot g(1 - e)\xi \cdot \tan(\Phi) \left(1 - \frac{\tan(\beta)}{\tan(\alpha)}\right)^2 + \xi \cdot c \cdot D \cdot r_h \left(1 - \frac{\tan(\beta)}{\tan(\alpha)}\right) \quad (5.37)$$

where c is the cohesion strength of the ice rubble and Φ the angle of internal friction of the ice rubble in accordance with the Coulomb-Mohr failure criterion: $\tau = \sigma \cdot \tan(\Phi) + c$ (see figure 27).

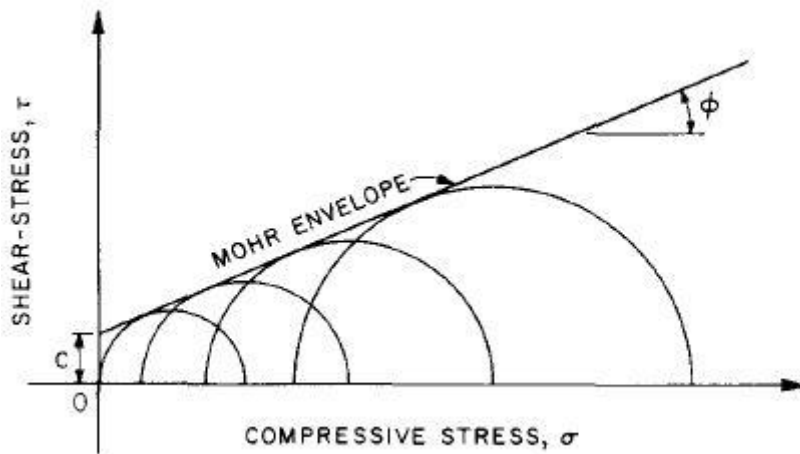


Figure 27: Coulomb-Mohr failure criterion (42)

The shear strength of ice rubble and thereby ϕ and c , are functions of time, normal pressure, porosity, shape and packing of the ice fragments, Ice/water/air temperatures and water salinity. Because the exact relationship is not known and also depends on operating side, mean values of strongly scattering experimental data, summarized in (42) were taken.

$$H_T = 1.5 D \cdot h^2 \cdot \rho_i \cdot g \frac{\cos(\beta)}{\sin(\beta) - \mu \cdot \cos(\beta)} \quad (5.38)$$

So the global horizontal action results as follows

$$P_H = \frac{H_B + H_P + H_R + H_L + H_T}{1 - \frac{H_B}{R_f \cdot l_C \cdot h}} \quad (5.39)$$

and the global vertical force as

$$P_V = \frac{P_H}{\xi} \quad (5.40)$$

As in the plastic method also this method can be adapted to downward breaking cones through changing the weight of the ice to buoyancy by replacing the ice density ρ_i by $(\rho_w - \rho_i)$.

5.2.3 Rubble high

In both calculation methods the high of rubble accumulation is considered. In 5.2.1 by considering the top cone diameter D_T , this is the diameter at the rubble high and in 5.2.2 directly by working with r_h . If the high of the structures neck is known, this can be used as r_h , otherwise Brown and Määttänen gave these formulae in 2002:

$$r_h = 3 + 4h \quad (5.41)$$

from measurements of the Kemi-1 lighthouse in the Gulf of Bothnia and

$$r_h = 7.6h^{0.64} \quad (5.42)$$

from measurements of the Confederation bridge in Canada.

(43) in (33)

5.2.4 Velocity effect

If the velocity of ice increases the ice sheet is not able to move up/down the sloped structure fast enough, because of inertia forces from rubble lying at the structure, friction and additional drag resistance of water for now submerged ice sheets at downward cones.

This leads to additional compressive stresses and can change the failure mode due to higher resistance against flexural failure to crushing, furthermore rubble originates.

Upward breaking wide structures

Shkhinek and Uvarova modelled the ice loads numerically for a wide upward breaking structure with several sloping angles under consideration of the latter points in 2001. They gave non-dimensional lines of best fit for the different angles of the ice loads where the failure mode changes from bending to crushing and calculated a velocity factor to quasi-static reference ice velocity of 0.05 m/s (see appendix 4). (44)

Their results showed a good agreement with experimental data and are therefore used here. For sloping angles between the angles, calculated from Shkhinek and Uvarova, values are obtained by calculating a line of best fit. This is a polynomial fitting of fourth order on the basis of least square fitting and is done by the Matlab order “polyfit”.

Upward breaking conical structures

In 2002 Matskevitch developed a formula for cones, relying on observation data for a cone with 60 ° slope angle:

$$F_{non,M} = \frac{P_V}{P_{0.5}} = \begin{cases} 1 & \text{if } U < 0.5 \frac{m}{s} \\ 1 + 0.5(U - 0.5) & \text{if } U > 0.5 \text{ m/s} \end{cases} \quad (5.43)$$

He used a velocity for quasi-static conditions of 0.5 m/s, so higher than Shkhinek and Uvarova. (33)

Lau et al. did scale model tests in 2000 for 45 ° and 60 ° sloping angle by considering Froude-similarity with ice thickness and velocity as characteristic parameter. They observed that the increasing of ice forces is also dependent on the ice thickness and that after a transition velocity the ice load does not increase any more. This is probably due to a changing in failure mode.

He developed empirical formulae for a ratio of horizontal ice load depending from Froude-number ($Fr = U/\sqrt{g \cdot h}$) to the horizontal ice load during quasi-static conditions

($U = 0.01$ m/s) for upward and downward breaking cones:

$$F_{non,u} = \frac{P_h}{P_{h,@U=0.01 \text{ m/s}}} = 1.03e^{0.77 \cdot Fr} \quad (5.44)$$

(45)

Downward breaking conical structures

Lau and Williams made scale model test in 1991 for downward breaking cones. In comparison with upward breaking ones they observed a higher velocity effect for downward cones. This could be explained by a higher influence of water drag and inertia forces because of more added mass. In his paper from 2000 they gave also an empirical formula for downward breaking cones depending on Froude-number:

$$F_{non,h} = \frac{P_h}{P_{h,@U=0.01 \text{ m/s}}} = 1.06e^{1.64 \cdot Fr} \quad (5.45)$$

(45)

For the velocity effect to the vertical forces, model test data from Lau and Williams (46) were used for deriving a line of best fit. The natural logarithmic function were taken from the data and then a polynomial function of third order was developed by using the Matlab order “polyfit”, which uses least square fitting.

Alexander Dummer	Project work	Investigation of Ice Interactions
MSF LS Ocean Engineering	handed in as	on Drilling Rigs in
University of Rostock	“Studienarbeit”	Shallow Water

This leads to

$$F_{non,v} = \frac{P_v}{P_{v,U=0.01 \text{ m/s}}} = e^{1.27Fr^3 - 2.81Fr^2 + 2.82Fr - 0.05} \quad (5.46)$$

Even the influence of degree of cone angle and structure diameter needs more investigations, (5.45) and (5.46) are used in this work since a lack of other investigations.

5.3 Treatment of multiple leg structures

Like in chapter 4.2 was mentioned, the load on a single leg, standing in a cluster of piles, differs from a free standing single leg. For calculation, the load of a single leg of a structure can be multiplied by factor that covers the influence on the ice layer by the surrounding legs. Afterwards all loads from the single legs can be summed up. The total load is also multiplied by a reduction factor that takes into account that peak loads on the single legs do not occur in the same moment.

For calculating the factor of the single legs, the interaction is idealized and divided in different categories like in figure 28:

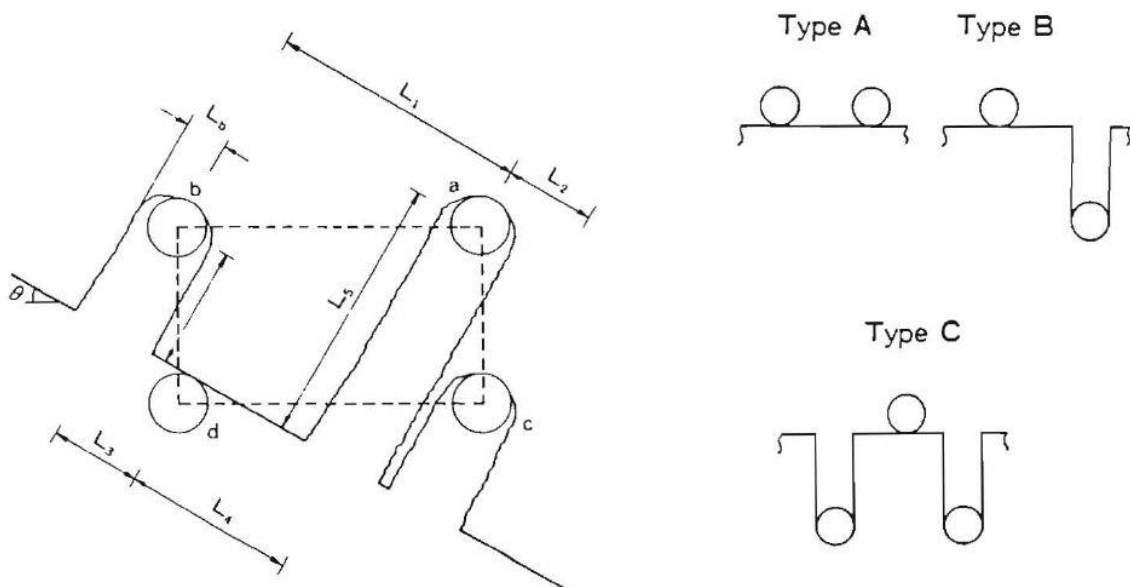


Figure 28: Idealized ice interaction of a multi leg platform (42)

Then the factors are calculated by empirical formulae, developed from scale model tests and depending on the column diameter, distance of the free ice layer edge to the column centre and number of interacting free ice layer edges:

Alexander Dummer	Project work	Investigation of Ice Interactions
MSF LS Ocean Engineering	handed in as	on Drilling Rigs in
University of Rostock	“Studienarbeit”	Shallow Water

Vertical columns:**Table 5: Multiplication factor for four leg platforms with vertical surfaces (47)**

f_a	Assumed condition
$0.125 \left(\frac{L_1}{D} - 1 \right) + 0.5$	$1 < \frac{L_1}{D} < 5$
1	$\frac{L_1}{D} \geq 5$
f_b	
$0.58 \left(\frac{L_2}{D} \right)$	$0 \leq \frac{L_2}{D} < 1$
$0.083 \left(\frac{L_2}{D} - 1 \right) + 0.58$	$1 \leq \frac{L_2}{D} < 6$
1	$\frac{L_2}{D} \geq 6$
f_c	
f _b with L ₂ = L ₄	$5D < L_3$
Smaller value of load either with type B or buckling is chosen	$2D < L_3 < 5D$
Buckling failure	$L_3 < 2D$

- L₁ is the distance between the centres of the two legs (type A)
- L₂ is the distance between the centre of the leg and the free end of the ice cover (type B)
- L₃ is the distance between the two free ends (type C)
- L₄ is the shorter distance from the centre of the leg to the free end of the ice cover (type C)

Sloped columns

For sloped structures the factor can be calculated by

$$f_j = (A_j + \frac{B_j \cdot C_1 \cdot C_2}{C_3}) / (1 + \frac{C_1 \cdot C_2}{C_3}) \quad (5.47)$$

where $j = a$ for type A interaction and $j = b$ for type B interaction

- $C_1 = 2.431$ for type A interaction
- $C_1 = 2.416$ for type B interaction
- $C_2 = R_f \cdot h$ (5.48)

- $C_3 = \rho_i \cdot g \cdot (D^2 - D_T^2)$ (5.49)

Table 6: Multiplication factor for four leg platform with sloped surfaces, (42)

Type A interaction	Ratio of distance to free ice edge to column diameter
$A_a = 0.18 \cdot \left(\frac{L_1}{D} - 1\right) + 0.462$	$1 \leq \frac{L_1}{D} \leq 4$
$A_a = 1$	$\frac{L_1}{D} > 4$
$B_a = 0.04 \cdot \left(\frac{L_1}{D} - 1\right) + 0.88$	$1 \leq \frac{L_1}{D} \leq 4$
$B_a = 1$	$\frac{L_1}{D} > 4$
Type B interaction	
$A_b = 0.45 \cdot \left(\frac{L_2}{D} + 0.5\right)$	$-0.5 \leq \frac{L_2}{D} < 0.5$
$A_b = 0.194 \cdot \frac{L_2}{D} + 0.36$	$0.5 \leq \frac{L_2}{D} \leq 3$
$A_b = 1$	$\frac{L_2}{D} > 3$
$B_b = 0.85 \cdot \left(\frac{L_2}{D} + 0.5\right)$	$-0.5 \leq \frac{L_2}{D} < 0.5$
$B_b = 0.1 \cdot \frac{L_2}{D} + 0.80$	$0.5 \leq \frac{L_2}{D} \leq 2$
$B_b = 1$	$\frac{L_2}{D} > 2$

The meaning of L is the same as for vertical structures above. Because buckling for sloped structures rarely occurs and only bending failure is considered, type C interaction are always treated as type B interaction by considering the smaller distance to the free ice edge.

Kato et al. observed that the forces and induced moments, normalized by the forces of an independent leg, for downward breaking structures are twice as large as for upward breaking structures. The magnitude was approximately the same. During the model test the size of the failed ice blocks from downward breaking cones were bigger than for upward breaking cones and always deep jamming occurred between the legs of the downward breaking cones and led to a higher load. (48)

Määttänen (15) observed no jamming and a total load reduction till 40 % for downward breaking cones during scale model test with a structure of three upward or downward cones, while varying cone spacing velocity and intrusion angle. Nevertheless, here the factors of table 6 are multiplied by two for downward breaking cones.

Even the values were determined by experiments with structures of four columns, it is assumed here that the values could be used also for structures with less or more columns. This is done because for all type of structures one interaction type could be determined for every column by the geometric criteria for the interaction types. Furthermore it is always assumed that the distance to the forward ice sheet interaction is negligible. So here only the properties of the ice sheet abeam of the concerning column in ice drift direction are considered. To consider the influence of prior ice interaction more, further research has to be done.

Also depending on the leg distances a larger amount of ice can accumulate between the legs and jamming occurs. Than the effective diameter increases to the whole structure diameter and the global loads can be much higher. (3)

5.4 Floating structures

In contrast to fixed structures, floating structures, hold in position by moorings or thrusters, are much more compliant. This leads to a distinct dynamic behaviour and ice loads give rise to motions like heave e.g. caused by the weight or buoyancy of ice in contact with sloped structures, surge e.g. caused by the time and ice load dependent behaviour of the positioning system and point of breaking, pitch e.g. caused by an additional moment due to the ice load and so forth. All these motions also again influences the ice loads.

Conical floater

Because the dynamic behaviour depends also strongly on the specific geometry with its hydrodynamic properties and the positioning system of the chosen platform, in this work only quasi-static pitch behaviour is considered.

This is again simplified by keeping the length of the lever arm of the horizontal ice forces constant, equal to the draught of the platform. So no influence of pitch to the lever arm is considered and for vertical ice forces equal to half of a diameter of the waterline without pitch correction. Furthermore vertical forces and hydrodynamic aspects of the mooring are neglected.

A changing parameter is the effective sloping angle, between the hull of the platform and the waterplane at the forward side, which also influences the ice loads and is calculated iteratively corresponding to the pitch. Also the thereby changing upsetting moment was calculated iteratively.

For taking the equilibrium of moments at the middle of the keel, where also the working point of the moorings is assumed, the following equation is solved:

$$P_H \cdot T_0 + P_V \cdot \frac{D_{WL}}{2} + KG \cdot \sin \varphi \cdot \nabla \cdot \rho_W \cdot g - \eta_B \cdot \nabla \cdot \rho_W \cdot g = 0 \quad (5.50)$$

where KG is the distance between keel and centre of gravity, ∇ the displaced volume, η_B the lever arm of the upsetting moment and φ the pitch angle. P_H , P_V and η_B depend on φ .

For calculating the centre of buoyancy the structure is cut into slices. In case of a fully submerged slice it has the plane shape of circle. If the waterline goes through a slice it has the shape of a circular segment. Then the centroids of the submerged volumes of the slice are calculated and summarized. After turning the coordinate system around point of origin with

the abscissa parallel to the water plane, the lever arm of the upsetting moment is taken as the distance on the abscissa to the keel.

Semisubmersibles

For simplification it is assumed that semisubmersibles can be treated as fixed and rigid structures. So no pitch correction is considered and they are calculated with the methods of the previous chapters. The calculations of the round floater at the end of chapter 6.3 shows, that with a low centre of gravity or small sloping angles the resulting pitch is only small.

So it is here assumed, that the additional deviation of load due to negligence of pitch is acceptable in the total accuracy of load calculations for semisubmersibles. Other uncertainties in load prediction occur e.g. due to jamming possibility (see chapter 5.3).

Ship shaped floaters

Ship shaped floaters are not further treated here for calculations to restrain the scope of this work. For further interests it is referred to the work of G. Lindqvist in 1989 He gave a straightforward method for calculation of ice resistance of ships (49).

6. Ice load calculations on chosen platforms

6.1 Introduction into calculation program

The calculations are realised by four separated programs written in Matlab. One is used for fixed vertical structures, one for fixed sloped structures and two for round floating structures. Thereby the first two consider also multiple leg structures.

Platform dimensions are set in the function files

“structure_geometry_vertical”,
 ”structure_geometry_sloped” or
 ”floater_geometry”

and assumed conditions, like the range of ice drift velocity, intrusion angle and so on, are set in the files

“environmental_properties_vertical_structures”,
 “environmental_properties_sloped_structures” or
 ”environmental_properties_floater”.

The script files, which have to be started to run the programs, are called

“Start_ice_load_calculations_sloped_structures”,
 “Start_ice_load_calculations_vertical_structures”,
 “Start_ice_load_calculations_floater_plastic” for use of plastic limit theory or
 “Start_ice_load_calculations_floater_elastic” for use of elastic beam bending theory.

For fixed structures a calculation parameter can be customized in the script files to determine what kind of modifications to the main calculation theories should be applied, e.g. choosing a temperature or velocity correction. For floating structures the velocity correction can be shut off by changing the velocity correction factor “f_vh(i)” or “f_vv(i)” equal to 1 in the script files.

After calculation the results are exported into an Excel file for better clearness.

For more details the flow charts of scripts and functions can be seen in the appendix.

6.2 Comparison with measurement data

Before calculating the ice loads to different structures types, it has to be checked if the calculation methods and the program lead to similar results of measured loads. Therefore available values from structures of the literature were chosen and compared to calculated values.

Vertical structures

For comparison with vertical full scale measurements, the data of Molikpaq structure from Sanderson and Jefferies is chosen. As calculation parameter a width of the base, 111 m, is set. Because not always a specific value of drift speed is given in the data sources, no velocity correction is applied. In general the speed is about 0.1 m/s.

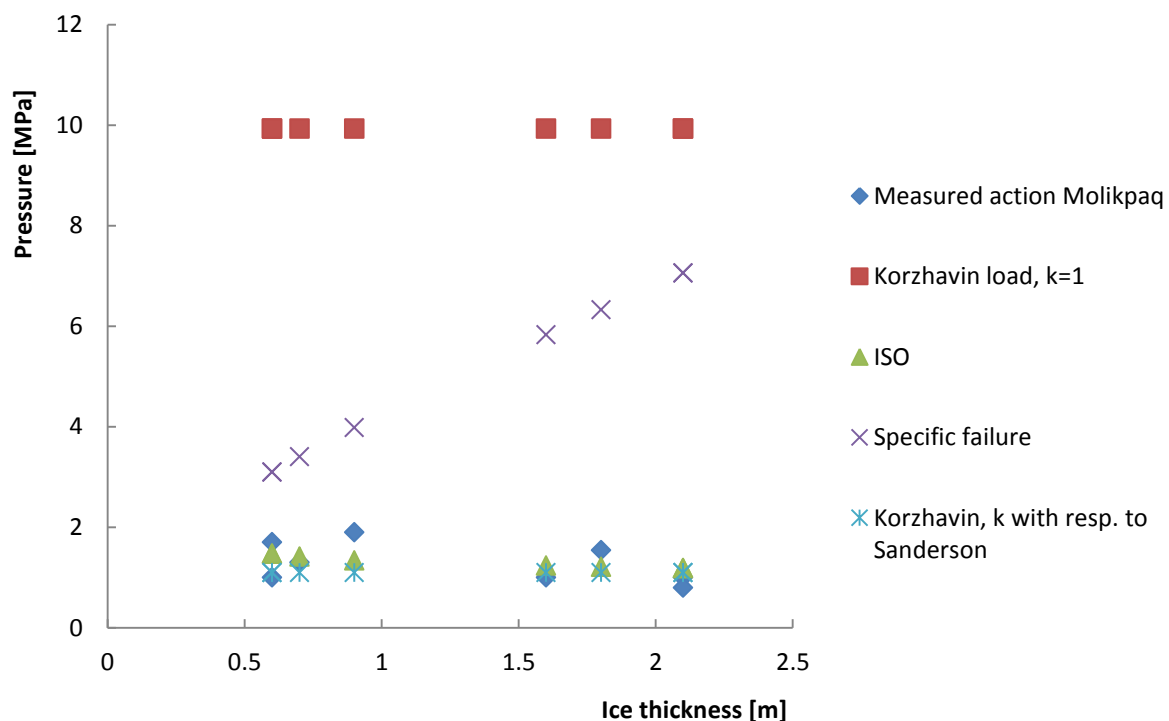


Figure 29: Comparison of measurement pressure of level first year ice on Molikpaq with calculated values

It can be seen in figure 29 that the values of the calculations in accordance to the ISO and to Korzhavin with the contact factor of Sanderson, here 0.07, fits best to the measurement values.

For using the specific failure calculations, buckling failure is assumed to occur because of the high aspect ratio and transition to crushing criteria as linear equation. That leads to an increase of pressure in the calculations with increasing ice thickness. However, this mechanism

does not seem to occur in reality and it becomes obvious, that the calculation model of choosing the specific failure mechanism needs more selection criteria, e.g. like the absolute thickness of the ice cover or absolute size of structure.

Important to notice is that sometimes an underestimation of the pressure seems to occur with the ISO or Korzhavin/Sanderson calculation method. But thereby it should be considered that the measured pressure values come from Medorf panels that covered only 10 % of the contact area. So for calculating a global load from the measurement values, the size effect has to be considered. The calculated pressure values are all derived from calculated global loads with the full contact area and thereby partly considering the size effect.

After all, the calculation method with respect to the ISO is chosen for further platform evaluation of structures with vertical surfaces.

Sloped structures

An upper bound line of measured data from the Kulluk vessel (16) with the following characteristic is chosen:

- Displacement: 28 000 t
- Sloping angle: 31.4 °
- Waterline diameter: 70 m
- Draught: 12.5 m
- Diameter of submerged cylinder (D_B): 43.3 m
- Height of submerged cylinder (h_C): 4.3 m
- Distance between keel and centre of gravity (KG): 10 m

Thereby the dimensions of the submerged cylinder are only calculated values because of a lack of data. The cylindrical shape at the bottom is assumed, because the real structure has also there partly sloped surfaces. This was simplified as well as the existence of the moonpool in the centre of the structure is neglected.

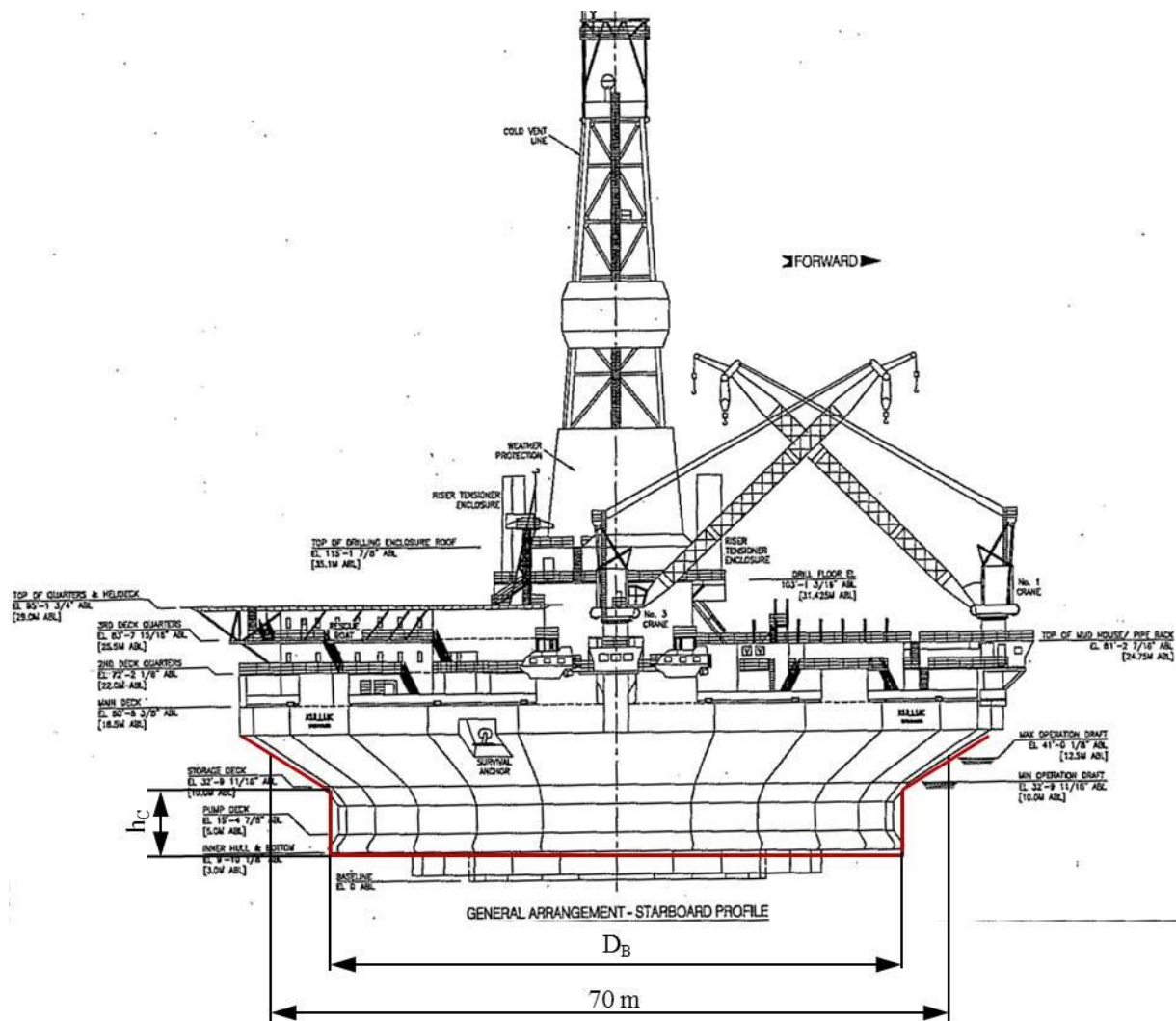


Figure 30: General arrangement Kulluk vessel with inserted simplifications (red lines) and assumed main dimensions, (50) with modifications

The load is calculated with the plastic limit theory for cones and with the elastic beam theory for wide structures. Thereby a flexural strength of 500 kPa and friction for conditions of -10° is assumed. For calculating as a wide structure the slope angle was averaged over the half of the cone in ice drift direction. So instead of a sloping angle of 31.4° an angle of 48.4° was used.

Additional the pitch angle is calculated and added to the slope angle during calculations:

Table 7: Pitch angle for floater calculation

Ice conditions	Plastic limit method	Elastic beam method
h=0.2 m, U=0.05 m/s	0.8 °	0.9 °
h=0.2 m, U=0.65 m/s	1.4 °	1.6 °
h=1 m, U=0.05 m/s	2.6 °	2.6 °
h=1 m, U=0.65 m/s	2.8 °	2.8 °

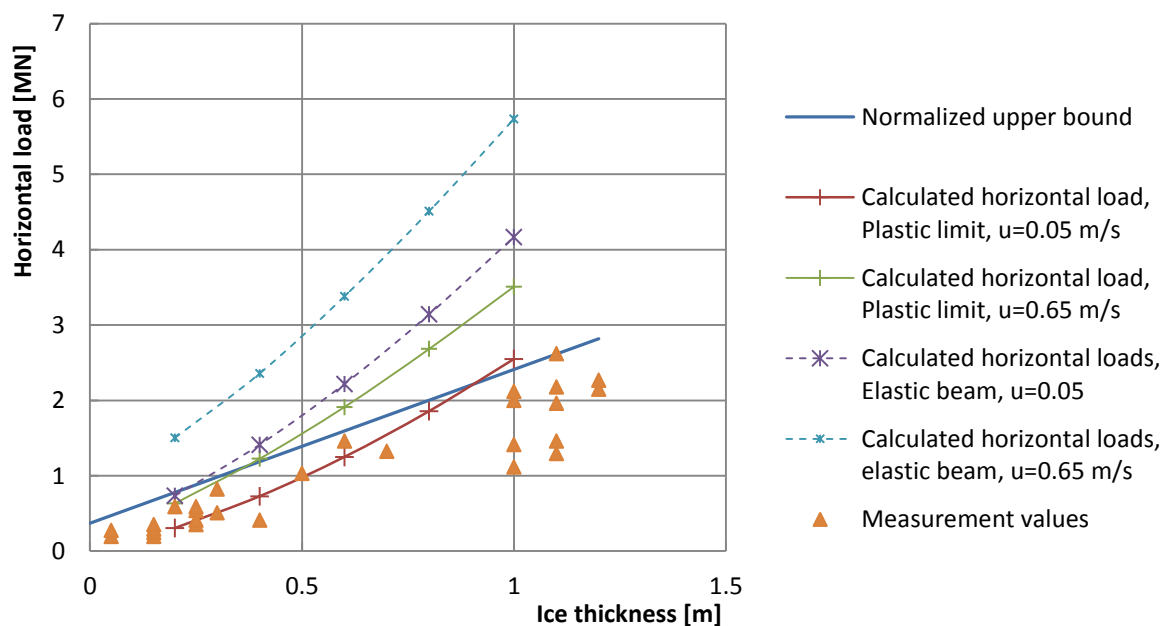


Figure 31: Comparison of Upper bound values of measurement data and calculated values for Kulluk vessel

In figure 31 it can be seen that all calculations are lying in a similar range and the deviation becomes greater with increasing ice thickness for using elastic beam theory and plastic beam theory with velocity correction to 0.65 m/s. The calculations with the plastic limit methods lead to more similar results as elastic beam theory for floating cone structures. Thereby for smaller ice thickness the results of higher drift speed fits better to the upper bound values as the very low drift speeds. For increasing ice thickness this relationship inverts.

It has to be mentioned that the upper bound line is not the mean of the measured data, but the mean added two times the standard deviation.

The higher load of thin ice sheets could probably not be explained by a velocity effect. In figure 32 Wright normalized the loads to 1 m thick ice and it could no velocity dependence be observed. The velocity correction in chapter 5.2.4 was developed on scale model tests and takes only ice thickness as a size parameter into account. Probably because of the size effect of ice this dependence could not be observed on this full scale data from downward breaking cones. Also the velocity factor in this velocity range is close to one and therefor the velocity effect is small, so maybe not visible in the scatter of data. Also the accuracy of the load measurements is maybe not high enough to make the velocity effect visible. However, the load was measured at the mooring system.

Other reasons for deviation could also be a different geometry in the submerged part and different mass and buoyancy distribution of the real structure and irregularities in the ice cover.

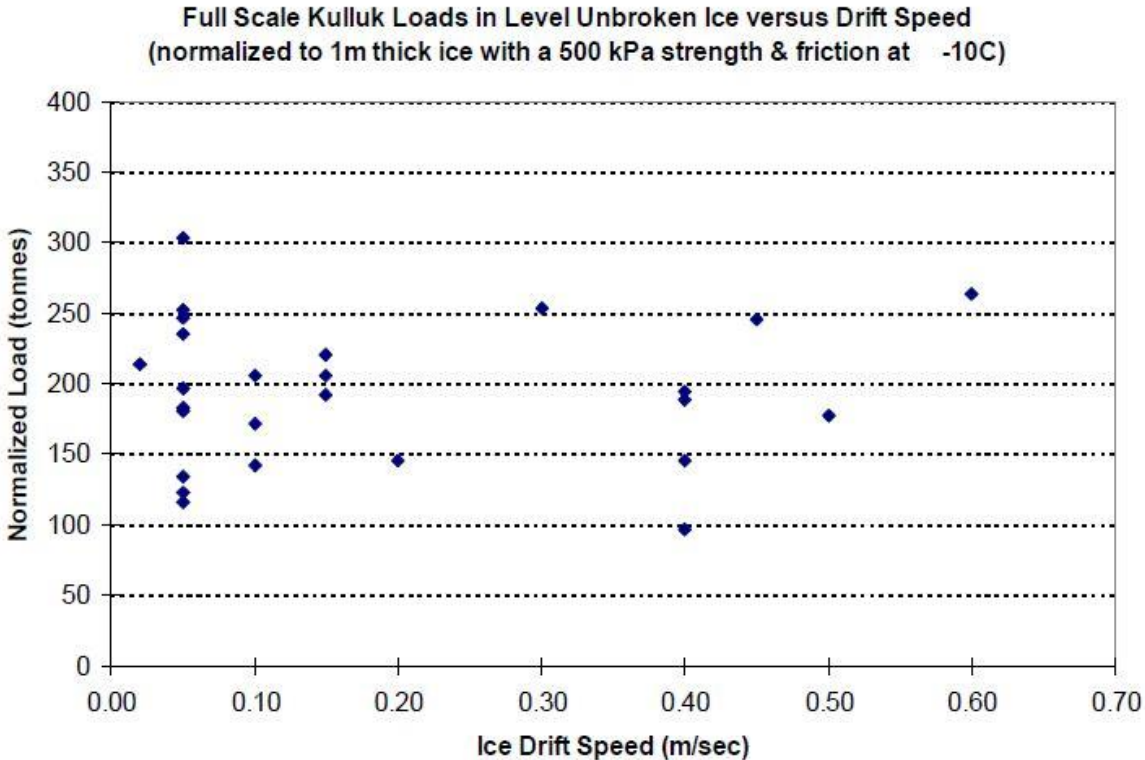


Figure 32: Normalized ice load vs. Ice drift speed, (16)

6.3 Calculations

Chosen ice conditions

For all calculations first year S2-ice is chosen. It is assumed, that it is free of any ridges and has no inclusions of any other kind of irregular ice, e. g. through rough weather condition during the freezing process.

The calculations are made for 0.8 m thick ice, wherefrom a part of 0.1 m is assumed to have a granular structure. It is supposed that the mean temperature of the ice cover is $-10\text{ }^{\circ}\text{C}$ and the salinity of the melt water of the ice cover is 6 ppt. For calculating the compressive fracture strength with respect to equation (2.11), a grain diameter of 10 mm over both layers and a Poisson's ratio of 0.3 are assumed.

This leads after temperature and salinity correction to a

- compressive fracture strength of 1.46 MPa for the columnar ice layer,
- compressive fracture strength of 2.12 MPa for the granular ice layer,
- flexural strength of 0.61 MPa and an
- elastic modulus of 4.28 GPa

of the ice cover.

For calculations with respect to the elastic beam bending theory following parameters of rubble are assumed:

- Internal friction angle: 38.0 °
- Cohesion: 823 Pa
- Porosity: 0.325

Thereby the values are averages of experimental values listed in (42). As mentioned in 5.2.2 the values are strong scattering but were used since no more specific information are available.

Calculations are done for the ice drift velocities of 0.05, 0.25 and 0.45 m/s and intrusion angles of 0 ° , 10 ° , 30 ° and 45 ° . While changing the intrusion angle, the width of rectangular caisson is not fitted since simplification and the different ice drift directions is only relevant for multiple leg structures.

For structures with vertical surfaces the velocity correction with respect to Korzhavin is only applied while using the Korzhavin load calculation model for the global load. Since the velocity factor $(U/U_0)^{-1/3}$ has a high influence for this velocity range (about factor 2.7 for 0.05 m/s) and the ISO does not recommend a velocity correction this way of proceeding is chosen.

Alexander Dummer	Project work	Investigation of Ice Interactions
MSF LS Ocean Engineering	handed in as	on Drilling Rigs in
University of Rostock	“Studienarbeit”	Shallow Water

During calculations with the specific failure mode the velocity effect is captured by the choice of failure mode. So also here no correction with respect to Korzhavin is applied.

For sloped structures the ISO does not recommend a velocity correction. However, it is applied since it can be seen that it has only minor influence to the calculated load in this velocity range and is for cone structures more independent of the major calculation method as e.g. the Korzhavin velocity correction.

Structure dimensions

As already mentioned in chapter 3, there are several possible principles for providing a drilling rig in ice infested areas. Before focusing on environmental conditions, a closer look at the framework conditions has to be taken to determine the size of the structure. Here two possible scenarios are considered:

- It is clear that the location could also be used for production facilities afterwards, and that it should be possible to drill several wells at the same time (Group one).
- The drilling rig should be removed after finishing work and e.g. subsea installations are considered afterwards (Group two).

As constant parameters for all structures of each group the footprint of the topside structure is taken and/or it is orientated on dimensions of existing structures or concepts.

Group one dimensions

To get a value of the footprint for group one, the mean of Molikpaq, Hibernia and Prirazlomnoye platform is chosen.

Table 8: Topside dimensions of Arctic drilling and production platforms

Name	Length [m]	Width [m]	Area [m ²]
Hibernia (51)	98	34	3332
Molikpaq (52)	73	73	5329
Prirazlomnoye (1)	126	126	15876

This results in 8179 m², so the structure is assumed to have a squared plane shape with a length of 90 m of the topside.

It is assumed that the high from the water line to the end of the sloped surface, respectively the high to the neck of the cone, is equal to the rubble high from chapter 5.2.3. This is done to have enough space for rubble till it falls down and submerges. So the rubble is not enforced to fall down earlier since the vertical part of the structure begins and the influence to the bending failure mechanism is minimized. Since no information is available about the dependency on slope angel, equation (5.42) is chosen for every sloping angle with an assumed maximum ice thickness of 1.5 m. This results to a high of 9.9 m. The horizontal length of the sloped surface depends on high and sloping angle.

For low slope angles the high of the neck of the cones is reduced since for multiple leg structures the single waterline diameter becomes too big and does not fit any longer under the dimensions of the topside. So the high is fitted that similar horizontal length of the sloped part result as of the concept in figure 8, chapter 3.1. The structure of figure 8 has also a small slope angle. So for a slope angle of 30° a high of the neck of the cones of 5 m is chosen and for 40° a high of 7 m.

The high of the structure above waterline depends beside ice conditions, volume requirements inside the structure, e.g. for oil storage, also from expectable wave high during the ice free season. Since the total high, where the topside starts, is not considered in the calculation models, it is not further considered here.

For piled structures a leg diameter of 15 m is assumed. This is 2 m less than from the Hibernia platform. Because this platform is located in water depth of 80 m and the legs have to carry higher forces as in shallow waters, it is assumed, that the diameter could be reduced.

Floating structures of the size to belong into group one are not considered here because this work focuses on drilling rigs. Large reservoirs, for which floating structures are considered, e.g. the Terra Nova field, could be developed by floating structures of group two and afterwards a Floating Production Storage and Offloading Vessel could be installed.

A summary of the used dimensions of group one is given in table 9.

Alexander Dummer	Project work	Investigation of Ice Interactions
MSF LS Ocean Engineering	handed in as	on Drilling Rigs in
University of Rostock	“Studienarbeit”	Shallow Water

Table 9: Structure dimensions, group one

Structure number	Slope angle [m]	Width of vertical part of structure [m]	Width of sloped part at waterline [m]	Cone high [m]	Distance between legs [m]
Vertical caisson					
1	90	90	-/-	-/-	-/-
Vertical multiple leg structures					
2	90	15	-/-	-/-	50
3	90	15	-/-	-/-	60
4	90	15	-/-	-/-	70
Sloped caissons					
5	30	90	124.1	9.9	-/-
6	40	90	113.5	9.9	-/-
7	50	90	106.5	9.9	-/-
8	60	90	101.4	9.9	-/-
9	70	90	97.2	9.9	-/-
Sloped multiple leg structures					
10	30	15	32.3	5	50
11	30	15	32.3	5	60
12	30	15	32.3	5	70
13	40	15	31.7	7	50
14	40	15	31.7	7	60
15	40	15	31.7	7	70
16	50	15	31.5	9.9	50
17	50	15	31.5	9.9	60
18	50	15	31.5	9.9	70
19	60	15	26.4	9.9	50
20	60	15	26.4	9.9	60
21	60	15	26.4	9.9	70
22	70	15	22.2	9.9	50
23	70	15	22.2	9.9	60
24	70	15	22.2	9.9	70

Group two dimensions

For sloped caissons of group two the dimensions of the movable drilling rig concept from figure 8 in chapter 3.1 are assumed in a squared manner. Thereby the width of the middle column of 38 m and a width of 54 m at water level is taken. For this water level width, the high of 20 m restricts the maximum sloping angle to approximately 65° . For vertical surfaces the width of 38 m is taken.

The dimensions of the semisubmersible are orientated towards the concept in chapter 3.4. So the column diameter of the vertical part of the legs is set to 14.5 m and the vertical part of the protecting column in the centre is assumed to have a diameter of 10 m. Since semi submersibles need a low centre of gravity and have not such deep heavy structure parts as gravity based structures, it is assumed that they could not have as high topsides as grounded structures. As a consequence it is assumed to have a similar footprint of the topside as the structures of group one. So the same leg distances as for multiple structures in group one are assumed.

For floating structures the dimensions were chosen with respect to the Kulluk vessel. Thereby the diameter of the waterline, 70 m, and the mass of 28 000 t are taken constant. The slope angle varies from 30 ° to 60 °. To keep the shape of a sloped column in the water line and a vertical cylindrical part at the bottom, the draught has to be decreased if the mass is taken constant. While decreasing draught also the vertical position of the centre of gravity is fitted.

Table 10: Structure dimensions, group two, part one of three

Structure number	Slope angle [°]	Width of vertical part of legs [m]	Width of vertical part of protection cone [m]	Width of sloped part of legs at waterline [m]	Width of sloped part of protection cone at waterline [m]	Cone high [m]	Distance between legs [m]
Vertical caissons							
1	90	38	-/-	-/-	-/-	-/-	-/-
Vertical multiple leg structures (Semisubmersibles)							
2	90	14.5	10	-/-	-/-	-/-	50
3	90	14.5	10	-/-	-/-	-/-	60
4	90	14.5	10	-/-	-/-	-/-	70
Vertical multiple leg structures (Jack ups)							
5	90	30	10	-/-	-/-	-/-	140; 120; 65
Sloped caissons							
6	30	38	-/-	54	-/-	4.6	-/-
7	40	38	-/-	54	-/-	6.7	-/-
8	50	38	-/-	54	-/-	9.5	-/-
9	60	38	-/-	54	-/-	13.9	-/-
10	65	38	-/-	54	-/-	17.2	-/-

Table 11: Structure dimensions, group two, part two of three

Structure number	Slope angle [°]	Width of vertical part of legs [m]	Width of vertical part of protection cone [m]	Width of sloped part of legs at waterline [m]	Width of sloped part of protection cone at waterline [m]	Cone high [m]	Distance between legs [m]
Sloped multiple leg structures (Semisubmersibles)							
11	30	14.5	10	31.8	27.3	5	50
12	30	14.5	10	31.8	27.3	5	60
13	30	14.5	10	31.8	27.3	5	70
14	40	14.5	10	31.2	26.7	7	50
15	40	14.5	10	31.2	26.7	7	60
16	40	14.5	10	31.2	26.7	7	70
17	50	14.5	10	31	26.5	9.9	50
18	50	14.5	10	31	26.5	9.9	60
19	50	14.5	10	31	26.5	9.9	70
20	60	14.5	10	25.9	21.4	9.9	50
21	60	14.5	10	25.9	21.4	9.9	60
22	60	14.5	10	25.9	21.4	9.9	70
23	70	14.5	10	21.7	17.2	9.9	50
24	70	14.5	10	21.7	17.2	9.9	60
25	70	14.5	10	21.7	17.2	9.9	70
Sloped multiple leg structures (Jack ups)							
26	30	30	10	47.3	27.3	5	140; 120; 65
27	40	30	10	46.7	26.7	7	140; 120; 65
28	50	30	10	46.5	26.5	9.9	140; 120; 65
29	60	30	10	41.4	21.4	9.9	140; 120; 65
30	70	30	10	37.2	17.2	9.9	140; 120; 65

Table 12: Structure dimensions, group two, floater, part three of three

Structure number	Draught [m]	Slope angle [°]	KG [m]
31	12.5	30	10
32	10	40	10
33	8	50	10
34	8	50	7.5
35	8	60	7.5

Ice loads

In the following tables (13 to 19) the calculated ice loads of group one and two are presented. All shown results are for an ice drift speed equal to 0.05 m/s and intrusion angles of 0 °, 10 °, 30 ° and 45 °.

The interaction type and thereby the sub factor changes with respect to chapter 5.3. In general it can be seen, that multiple leg structures have the lowest load if the intrusion angle leads to a maximum sheltering effect to the behind legs. For squared structures with four legs this occurs for small intrusion angles. The highest loads result of an intrusion angle of 30 °. Here often all legs have contact with the ice cover over the complete leg diameter. For 45 ° again sheltering effects influence the load of squared structures and lead to a decrease in load.

It can also be observed, that for this structure dimensions a decreasing leg distance leads to load reduction. This happens due to the assumed inward turning force vectors during type A interaction and of earlier starting sheltering effects by higher column diameter to column distance ratio. Exemplary interactions can be seen in the following figures. Thereby the red circles are the legs of the structure, the blue lines are the ice edges and the interaction type refers to chapter 5.3, respectively the flow chart in the appendix. Further figures of other structure types can be found in the appendix.

The calculation model of Masterson is not used for further calculation since this work focuses on calculations with general cases of ice cover thickness and ice drift velocity for several regions. So, here are no Freezing Degree Days known, but it could be used as an additional model for calculations of more specific operation sides. However, if 2000 FDD are assumed it leads to a pressure of 1.29 MPa for wide structures.

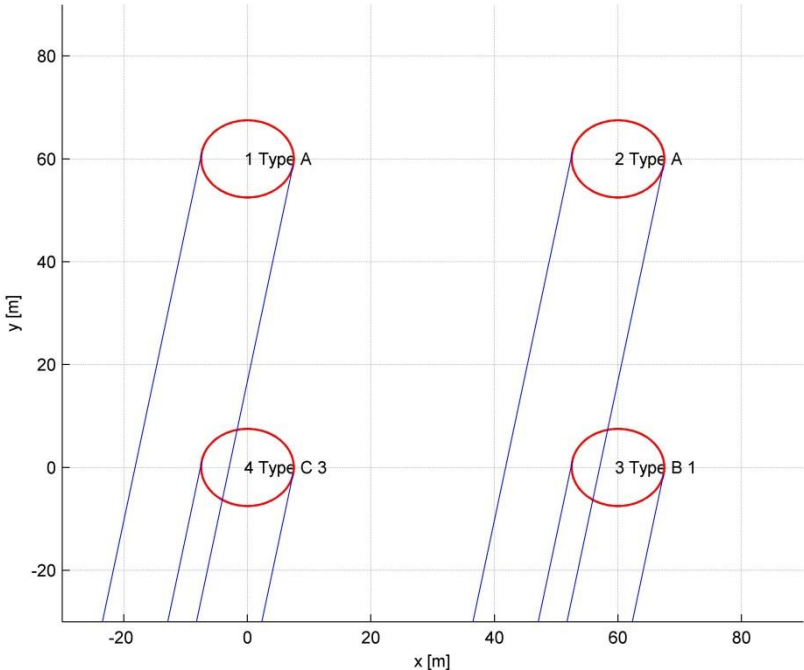


Figure 34: Structure no. 3, group 1, intrusion angle: 10 °

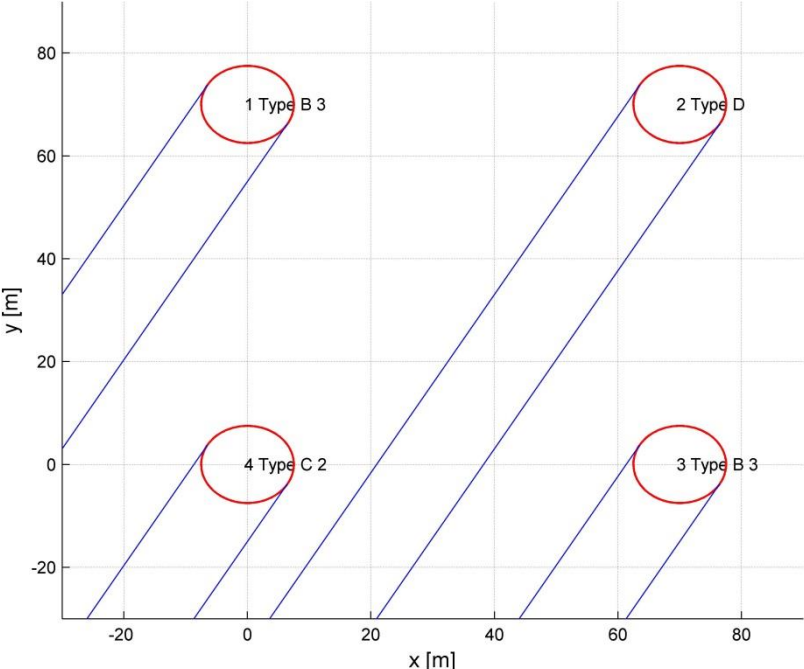


Figure 35: Structure no. 3, group 1, intrusion angle: 30 °

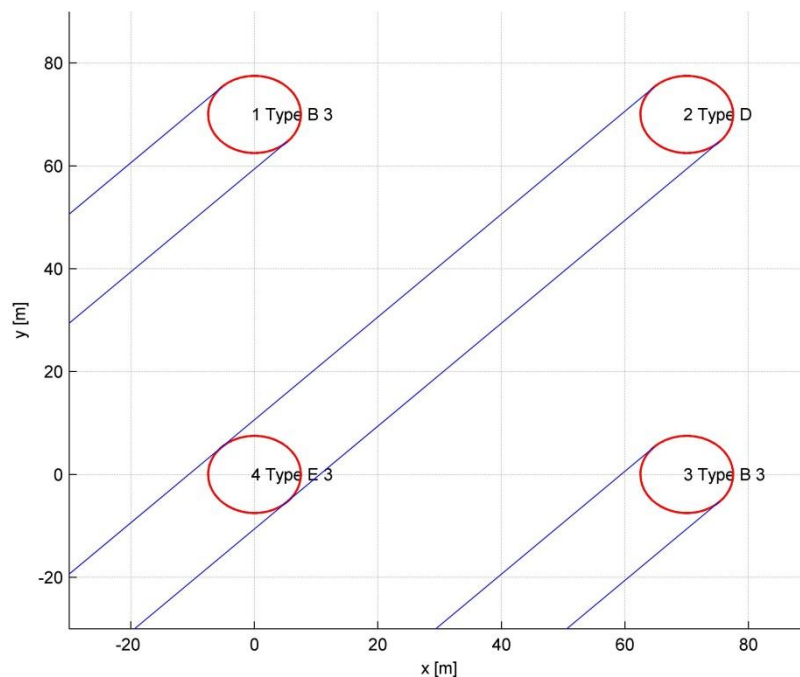


Figure 36: Structure no. 3, group 1, intrusion angle: 45 °

The loads of the structures due to further ice drift velocities increase with respect to the calculation models in chapter 5. Thereby the increasing velocity leads to an increase of load by sloped structures. Like figure 37 and 38 show exemplary and also becomes clear from the equations in chapter 5, the different calculation models of velocity correction for sloped structures increase for the chosen velocity range in a similar manner. The load of vertical structures where the velocity correction with respect to Korzhavin is applied decreases with increasing velocity.

The different directions of load changing by the velocity corrections of vertical and sloped structures result of their different breaking mechanisms, respectively the underlying empirical observations in the calculation models. Whereas the decrease of load on vertical structures relies probably on ductile to brittle transition and thereby a decrease of compressive strength, the increase of sloped structures results from more additional forces, e.g. due to inertia, etc. (see chapter 5.2.4).

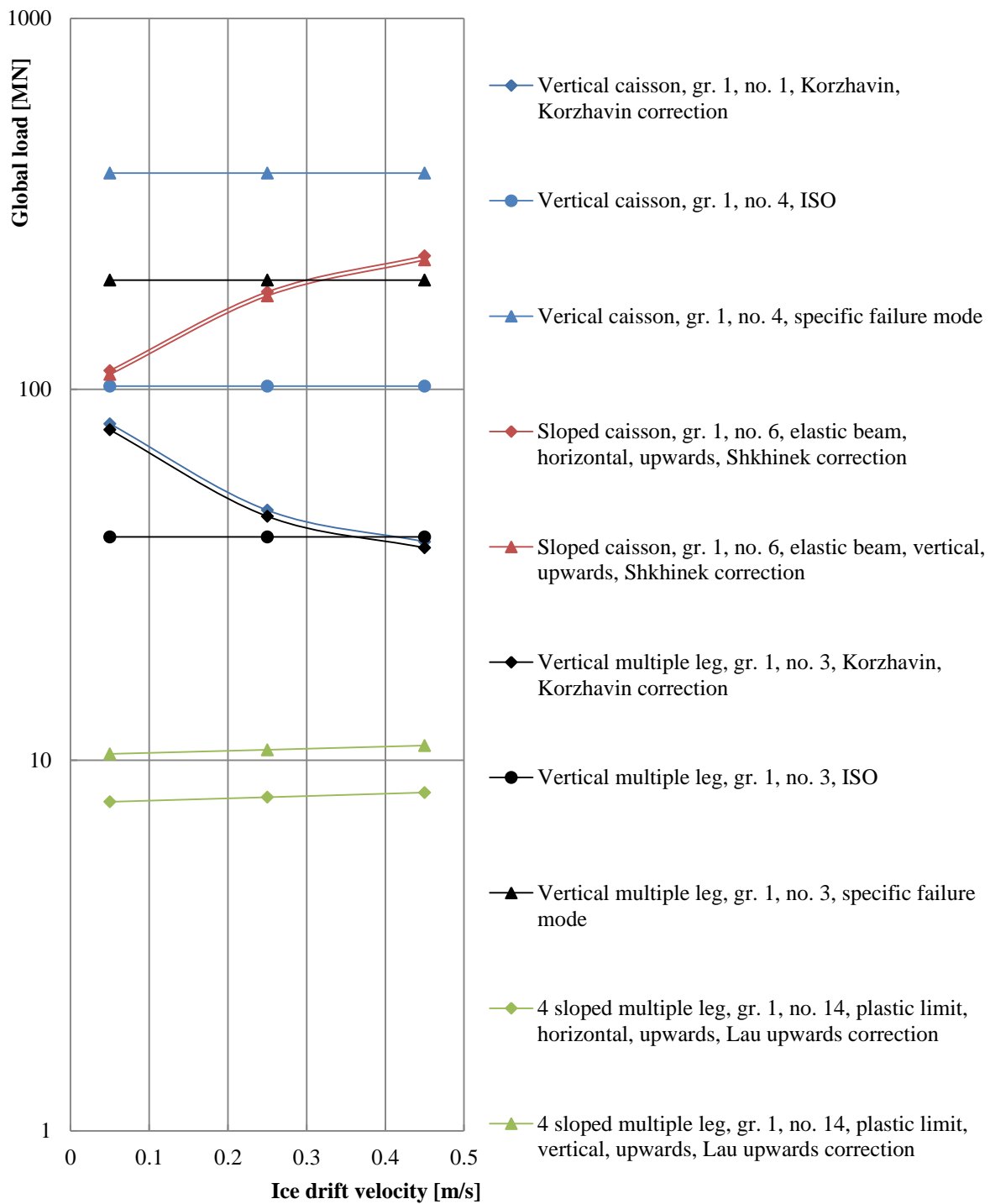


Figure 37: Ice load versus ice drift velocity of selected structures of group one

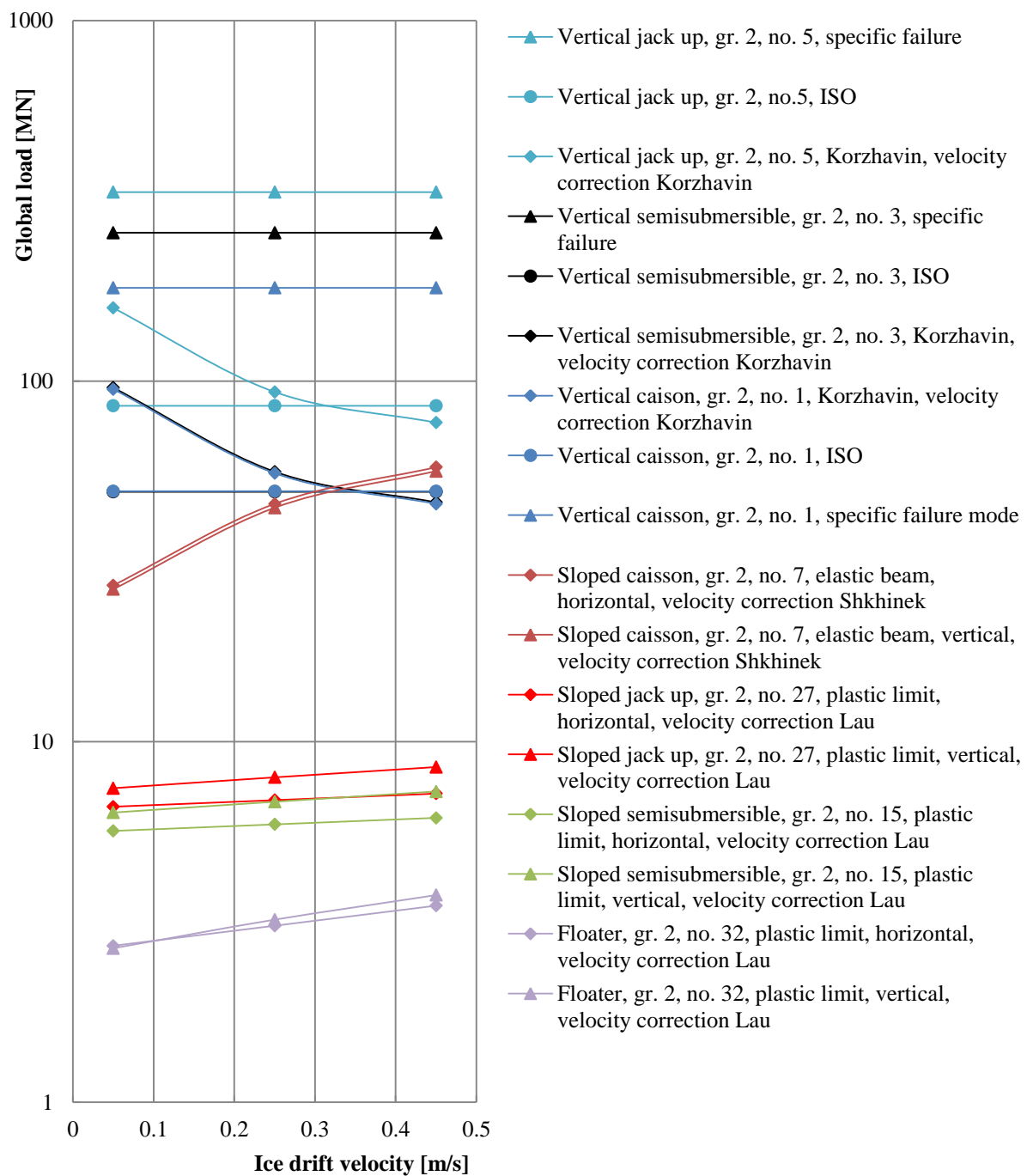


Figure 38: Ice load versus ice drift velocity of selected structures of group two

Since the difference of load due to velocity change has only a small part of the total amount of loads in the chosen velocity range for the most structures, here only the loads for a velocity of 0.05 m/s are shown. The further results can be found at the enclosed CD-ROM.

While looking at the loads of structures with vertical surfaces it can be observed that the high of the resulting loads have a settled order with respect to the calculation model. Thereby the results of the Korzhavin method with respect to the contact factor of Sanderson lead to the lowest results. With a small difference the loads, calculated with respect to the ISO, follow and high loads result of the calculation model which choses the specific failure mode.

The low loads of the Korzhavin equation result of a low contact factor with respect to the observations of Sanderson since it is assumed that in the chosen velocity range no pure creep occurs. The high loads of the specific failure mode, results of the assumed requirements for each failure mode. These lead here always to the conjecture that buckling occurs.

The figures 37, 38 and the following tables show that in general multiple leg structures result in lower loads than caisson structures and structures with sloped surfaces in lower loads than structures with vertical surfaces. The lowest load occurs at a round floating structure.

A reason for the relatively small difference between the sloped and vertical caisson structures of group one results of the different size of waterline diameter. Sloped structures need a wider waterline width if the same size of the vertical part, that provides the topside, should be reached. So, even structures with smaller slope angles can result in higher ice loads.

Loads to sloped caissons show also a strong dependency on velocity. That leads even to higher loads of the sloped caisson after a certain velocity, than of vertical caissons in group two, while using the velocity correction with respect to Shkhinek and Korzhavin.

Group one ice loads

The tables 13 to 15 show the results for selected calculation models of group one during an ice drift speed of 0.05 m/s:

Table 13: Results of calculations, group one, structures with vertical surfaces, ice drift velocity: 0.05 m/s

Structure number	Intrusion angle: 0 °			Intrusion angle: 10 °			Intrusion angle: 30 °			Intrusion angle: 45 °		
	Korzhavin [MN]	ISO [MN]	Specific failure mode [MN]	Korzhavin [MN]	ISO [MN]	Specific failure mode [MN]	Korzhavin [MN]	ISO [MN]	Specific failure mode [MN]	Korzhavin [MN]	ISO [MN]	Specific failure mode [MN]
Vertical caisson												
1	81	102	383	81	102	383	81	102	383	81	102	383
Vertical multiple leg structures												
2	71	36	180	68	35	171	396	159	344	96	49	243
3	78	40	197	80	41	203	117	60	296	99	51	251
4	84	43	214	92	47	233	121	62	307	102	52	259

Table 14: Results of calculations, group one, sloped caisson structures, ice drift velocity: 0.05 m/s

Structure number	Intrusion angle: 0 °		Intrusion angle: 10 °		Intrusion angle: 30 °		Intrusion angle: 45 °	
	Elastic beam theory, upwards, horizontal load [MN]	Elastic beam theory, upwards, vertical load [MN]	Elastic beam theory, upwards, horizontal load [MN]	Elastic beam theory, upwards, vertical load [MN]	Elastic beam theory, upwards, horizontal load [MN]	Elastic beam theory, upwards, vertical load [MN]	Elastic beam theory, upwards, horizontal load [MN]	Elastic beam theory, upwards, vertical load [MN]
Sloped caissons								
5	237	329	237	329	237	329	237	329
6	112	110	112	110	112	110	112	110
7	52	36	52	36	52	36	52	36
8	28	12	28	12	28	12	28	12
9	47	12	47	12	47	12	47	12

Table 15: Results of calculations, group one, sloped multiple leg structures, ice drift velocity: 0.05 m/s

Structure number	Intrusion angle: 0 °		Intrusion angle: 10 °		Intrusion angle: 30 °		Intrusion angle: 45 °	
	Plastic limit theory, upwards, horizontal load [MN]	Plastic limit theory, upwards, vertical load [MN]	Plastic limit theory, upwards, horizontal load [MN]	Plastic limit theory, upwards, vertical load [MN]	Plastic limit theory, upwards, horizontal load [MN]	Plastic limit theory, upwards, vertical load [MN]	Plastic limit theory, upwards, horizontal load [MN]	Plastic limit theory, upwards, vertical load [MN]
Sloped multiple leg structures								
10	5.2	10.0	5.3	10.2	6.3	12.0	6.5	12.2
11	5.3	10.3	5.6	10.7	7.1	13.3	6.6	12.5
12	5.5	10.6	5.8	11.1	7.2	13.5	6.7	12.7
13	7.5	10.1	7.6	10.3	9.1	12.1	9.4	12.4
14	7.7	10.4	8.0	10.8	10.3	13.6	9.6	12.6
15	8.0	10.7	8.4	11.3	10.5	13.8	9.8	12.9
16	11.3	10.5	11.6	10.8	13.9	12.8	14.3	13.1
17	11.7	10.9	12.2	11.3	15.9	14.4	14.6	13.4
18	12.1	11.2	12.8	11.8	16.2	14.7	15.0	13.7
19	15.2	9.1	15.9	9.5	20.4	12.0	18.8	11.1
20	15.7	9.4	16.8	10.0	20.8	12.3	19.2	11.4
21	16.3	9.7	17.7	10.5	21.6	12.8	19.7	11.6
22	24.7	8.2	26.5	8.8	32.5	10.7	29.9	9.9
23	25.6	8.5	28.0	9.2	33.9	11.2	30.7	10.1
24	26.4	8.7	29.5	9.7	34.9	11.5	31.4	10.4

Group two ice loads

The tables 16 to 19 show the results for selected calculation models of group two during an ice drift speed of 0.05 m/s:

Table 16: Results of calculations, group two, structures with vertical surfaces, ice drift velocity: 0.05 m/s

Structure number	Intrusion angle: 0 °			Intrusion angle: 10 °			Intrusion angle: 30 °			Intrusion angle: 45 °		
	Korzhavin [MN]	ISO [MN]	Specific failure mode [MN]	Korzhavin [MN]	ISO [MN]	Specific failure mode [MN]	Korzhavin [MN]	ISO [MN]	Specific failure mode [MN]	Korzhavin [MN]	ISO [MN]	Specific failure mode [MN]
Vertical caisson												
1	95	50	181	95	50	181	95	50	181	95	50	181
Vertical multiple leg structures (Semisubmersibles)												
2	88	45	237	382	152	329	394	159	354	96	49	250
3	96	49	258	98	50	263	109	56	285	99	51	258
4	104	53	270	110	57	295	116	60	305	103	53	266
Vertical multiple leg structures (Jack ups)												
5	160	85	343	174	93	381	146	78	321	154	83	323

Table 17: Results of calculations, group two, caissons with sloped surfaces, ice drift velocity: 0.05 m/s

Structure number	Intrusion angle: 0 °		Intrusion angle: 10 °		Intrusion angle: 30 °		Intrusion angle: 45 °	
	Elastic beam theory, upwards, horizontal load [MN]	Elastic beam theory, upwards, vertical load [MN]	Elastic beam theory, upwards, horizontal load [MN]	Elastic beam theory, upwards, vertical load [MN]	Elastic beam theory, upwards, horizontal load [MN]	Elastic beam theory, upwards, vertical load [MN]	Elastic beam theory, upwards, horizontal load [MN]	Elastic beam theory, upwards, vertical load [MN]
Sloped caissons								
6	25	35	16	23	16	23	16	23
7	27	26	16	16	16	16	16	16
8	25	17	15	10	15	10	15	10
9	21	10	17	8	17	8	17	8
10	26	9	34	12	34	12	34	12

Table 18: Results of calculations, group two, multiple leg structures with sloped surfaces, ice drift velocity: 0.05 m/s

Structure number	Intrusion angle: 0 °		Intrusion angle: 10 °		Intrusion angle: 30 °		Intrusion angle: 45 °	
	Plastic limit theory, downwards, horizontal load [MN]	Plastic limit theory, downwards, vertical load [MN]	Plastic limit theory, downwards, horizontal load [MN]	Plastic limit theory, downwards, vertical load [MN]	Plastic limit theory, downwards, horizontal load [MN]	Plastic limit theory, downwards, vertical load [MN]	Plastic limit theory, downwards, horizontal load [MN]	Plastic limit theory, downwards, vertical load [MN]
Sloped multiple leg structures (Semisubmersibles)								
11	4	6	3	6	4	7	4	7
12	4	6	4	6	4	7	4	7
13	4	6	4	6	4	7	4	7
14	6	6	5	6	6	7	6	7
15	6	6	6	6	6	7	6	7
16	6	6	6	6	6	7	6	7
17	8	6	7	6	9	7	9	7
18	8	7	8	6	9	7	9	7
19	8	7	8	7	9	7	9	7
20	11	6	11	6	12	6	12	6
21	12	6	12	6	12	6	12	6
22	12	6	12	6	13	7	12	6
23	19	6	19	6	20	6	20	6
24	20	6	20	6	21	6	20	6
25	20	6	21	6	21	6	20	6
Sloped multiple leg structures (Jack ups)								
26	5	7	5	8	4	7	5	7
27	7	7	7	8	6	7	7	7
28	10	8	10	8	9	7	10	8
29	14	7	14	7	13	7	14	7
30	23	7	24	7	21	6	23	7

Table 19: Results of calculations, group two, floating structures, ice drift velocity: 0.05 m/s

Structure number	Plastic limit analysis, downwards, horizontal [MN]	Plastic limit analysis, downwards, vertical [MN]	Pitch [°]	High of cylindrical shape [m]
31	1.9	2.8	2.6	5.2
32	2.7	2.7	4.5	2.2
33	6.3	2.2	17.9	5.0
34	4.6	2.1	13.3	5.0
35	11.6	2.5	13.8	2.7

7. Comparison of platforms

To evaluate the different structure types a utility analysis is done. The aspects of safety, operating, costs and influence to environment are included (see figure 39). Thereby the focus lies on the safety category due to ice loads.

Every aspect is rated by points from the number of structures of each group till one. Thereby the highest number is the best value. So the structures are graded in a kind of comparison to each other instead of giving absolute values, e.g. from one to ten. A negative aspect of this rating system is that it does not cover or quantify how much better one solution in comparison to another solution is. But since in a general case often no precise, certain and quantifiable information about the differences between the varying solutions of each aspect are available, this procedure is chosen.

Some aspects are only mentioned for sake of completeness and cannot be evaluated in the range of this work, since the above mentioned reasons, so they are all rated equal. The other aspects are always rated with respect to the shape or working principle of the different structure or how shape and working principle influence the aspect. If structures are rated equal since a lack of information or since equal skills, the grade is the mean between the next upper and lower value. Thereby the distance between the next upper and lower value is the number of equal rated structures.

A higher value means here, that the probability for occurrence of failure or accidents is lower, the consequences of failure does not change or influence the normal working principles much, the costs are lower or the environment is less affected.

The aspects are weighted by the number on the right half in the circle of figure 39. The number in the left half is the weighting of the aspects in the corresponding category. The specific weighting of the aspects in practice is individual and depends on the company policy of owner, operator and customers, operation site and legal regulations, so it could only be assumed here. Since the work focuses on ice loads which are covered by the safety category, these points are weighted stronger as the other ones.

The difference between the aspects is justified by the duration or effort of the specific event. Thereby, aspects that are related to events which take a bigger part of lifetime than other aspect are weighted stronger. That means that accessibility for maintenance work is weighted lower as accessibility for operation since it is assumed that maintenance work takes not such a

Alexander Dummer	Project work	Investigation of Ice Interactions
MSF LS Ocean Engineering	handed in as	on Drilling Rigs in
University of Rostock	“Studienarbeit”	Shallow Water

big part of the lifetime of the structure as operation. Aspects that are related with more effort are also weighted stronger than aspects with less effort. So, costs for maintenance are weighted lower as operation costs since it is assumed that the amount of maintenance costs on total costs is lower as for operation costs.

This utility analysis makes no claims of being complete in the sense of resulting in a structure recommendation for every case of Arctic shallow water conditions. Instead it gives an overview of potential aspects and influence by the choice of structure type to them. These could be considered by a further analysis with more respect to the specific operating conditions.

Here a multiple leg structure with vertical surfaces for group one and a round floating structure for group two have the best results (see tables 20 to 22).

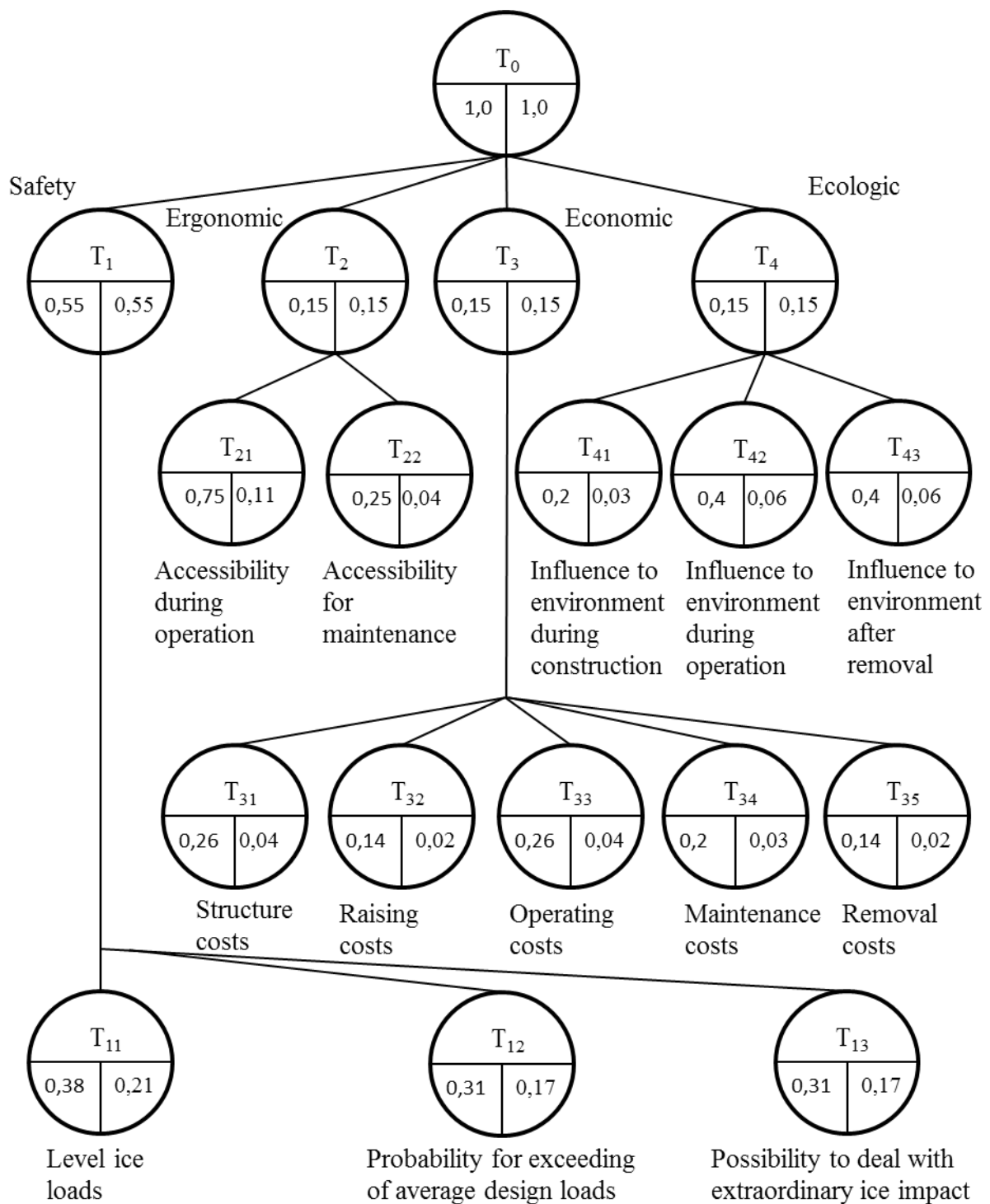


Figure 39: Aspects of utility analysis

Safety aspects

- Under the aspect T_{11} the structure is rated in accordance to the level ice loads calculated in the previous chapters. Thereby in general on sloped structures work less loads than on ones with vertical surfaces and structures with multiple legs have lower loads since caissons have a greater projected area in ice drift direction by the same topside dimensions. Thereby values of multiple leg structures with leg distances lying in the average of the investigated ones are considered and other intrusions angles than 0° , even that could lead to strongly increasing loads, are neglected.
- The probability for exceeding the average design load T_{12} concerns ice load events that are difficult to predict. This could be rubble accumulation and jamming between the columns of a multiple leg structure or adfreezing of rubble on top of the surface of a sloped structure so that no bending failure mechanism occurs any longer. In case of these interaction events the loads increase strongly and exceed the loads calculated of the aimed failure mechanism. While designing a structure, the prediction of appearance of these events and load due to them is relative uncertain but have to be considered. So the chance for over or under estimation is high. Because of that, structures, like the caisson with vertical surfaces, that operate always with failure mechanisms that lead to higher ice loads and cannot increase so strongly anymore are rated better.
- By extraordinary ice impacts in aspect T_{13} the occurrence of e.g. heavy ice bergs or large multi-year ridges is considered. Thereby it is assumed that the appearance exceeds the maximum considered ice impact that is manageable by the platform itself. For this situation fixed structures need ice management support and an outage leads to contact with the ice and thereby damage of the structure. Floating structures are assumed to be fitted with a quick disconnection system. So also ice management is considered to reduce expensive downtime but in case of an outage some chance is available to avoid the impact. So floating structures are rated better in this category.

Alexander Dummer	Project work	Investigation of Ice Interactions
MSF LS Ocean Engineering	handed in as	on Drilling Rigs in
University of Rostock	“Studienarbeit”	Shallow Water

Ergonomic aspects

- If upward sloped structures should be accessed by a supply vessel, in general a larger distance has to be spanned to reach the deck of the vessel as for vertical structures. The crane boom has to overhang the sloped surface and a bigger part behind since the water depth increases only with respect to the slope angle. That makes delivery of a sloped structure more difficult. So upward sloped structures are not rated as good as vertical structures in T_{21} . If the topside of the structure overhangs the base, this problem is reduced. Floating structures are also not as good to access as fixed structures since more motions occur. So, fixed upward sloped structures are rated equal as floating downward sloped structures.
- Maintenance work in T_{22} is related to outer work like painting, hull repairs and so on. Thereby vertical surfaces can be reached much simpler by working on a hanging rig near the surface. A large part of the outer maintenance work of floating structures can be done in a drydock of a yard between different explorations. So fixed sloped structures are rated worst and floating structures best.

Economic aspects

- Since sloped structures and floaters have a more complicated shape it is assumed that they have higher building costs than e.g. vertical caissons. So they get fewer points in T_{31} than a vertical caisson.
- Raising costs in T_{32} are rated on dependency of the duration of the offshore construction site since this determines the year around construction timeframe and effort. So floaters that are kept on station by dynamic positioning or moorings get more points than a structure that needs a foundation. Fixed structures with lower ice loads get also more points than structures with higher ice loads because they need more effort concerning the foundation.
- Operating costs in T_{33} are varying strongly with respect to demand on ice management and operating site. Since no reasonable assumption can be made here, every type of structure is rated equal and the aspect is mentioned for the sake of completeness. It could be possible that fixed structures with no necessary station keeping system have

Alexander Dummer	Project work	Investigation of Ice Interactions
MSF LS Ocean Engineering	handed in as	on Drilling Rigs in
University of Rostock	“Studienarbeit”	Shallow Water

lower operating costs but thereby so many other factors influence this point that a detailed determination is behind the scope of this work.

- Like in aspect T₃₄ no clear rating is done here because of the variety of influencing parameters. Sloped structures have more area of abrasion since the ice is gliding over a bigger surface. So concerning this point at sloped structures could maybe arise more maintenance costs. Also on floating structures maybe higher maintenance costs occur since a more complicated station keeping system.
- Floating structures are rated better concerning aspect T₃₅ since after their operating period no long lasting demolition work at the offshore site has to be done.

Ecologic aspects

- Influence to environment is rated concerning noise and duration of the activities at the construction site. So T₄₁ is rated better for floating structures as for fixed structures. This point covers also the influence during rebuilding.
- The influence on environment during operation cannot be rated profound in the coverage of this work. T₄₂ differs only slightly between the different structures and depends more on other aspects than on shape. It could be assumed that fixed structures could be rated better since no noise pollution through thrusters is present. But instead other noise sources like structure vibrations and crushing sounds could make them negligible. So every structure is rated equal.
- Aspect T₄₃ covers the remaining situation after removal of the structure. Also this point cannot be clarified only by structure shape, so every structure is rated equal. For further rating the size of the footprint of the base or effect by remaining anchorages in the ground could be considered. Also the consequences of necessary holes or structures to protect the subsea installation from iceberg scouring could be considered in the more specific analysis.

Group one

Table 20: Comparison of structures for group one

Criterion	Loading	Sloped Caisson		Vertical Caisson		Sloped multiple leg		Vertical multiple leg	
		Perfor- mance	Loading x performance	Perfor- mance	Loading x performance	Perfor- mance	Loading x performance	Perfor- mance	Loading x performance
Level ice loads	0.22	2	0.418	1	0.209	4	0.836	3	0.627
Probability for exceeding the average design load	0.17	3	0.5115	4	0.682	1	0.1705	2	0.341
Possibility to deal with extraordinary ice impact	0.17	2.5	0.4263	2.5	0.4263	2.5	0.4263	2.5	0.4263
Accessibility during operations	0.11	1.5	0.165	3.5	0.385	1.5	0.165	3.5	0.385
Accessibility for maintenance	0.04	1.5	0.06	3.5	0.14	1.5	0.06	3.5	0.14
Structure costs	0.04	2	0.08	4	0.16	2	0.08	2	0.08
Raising costs	0.02	2	0.04	1	0.02	4	0.08	3	0.06
Operating costs	0.04	2.5	0.1	2.5	0.1	2.5	0.1	2.5	0.1
Maintenance costs	0.03	2.5	0.075	2.5	0.075	2.5	0.075	2.5	0.075
Removal costs	0.02	2.5	0.05	2.5	0.05	2.5	0.05	2.5	0.05
Influence to environment during construction	0.03	2.5	0.075	2.5	0.075	2.5	0.075	2.5	0.075
Influence to environment	0.06	2.5	0.15	2.5	0.15	2.5	0.15	2.5	0.15
Influence to environment after removal	0.06	2.5	0.15	2.5	0.15	2.5	0.15	2.5	0.15
Sum	1.00		2.3008		2.6223		2.4178		2.6593

Table 21: Comparison of structures of group two

Criterion	Loading		Sloped movable drilling rig		Vertical movable drilling rig		Jack up with cones		Jack up without cones	
	Performance	Loading x performance	Performance	Loading x performance	Performance	Loading x performance	Performance	Loading x performance	Performance	Loading x performance
Level ice loads		0.22	4	0.88	3	0.66	5	1.1	1	0.22
Probability for exceeding the average design load		0.17	5.5	0.908	7	1.155	1.5	0.248	3.5	0.578
Possibility to deal with extraordinary ice impact		0.17	1.5	0.248	1.5	0.248	5	0.825	5	0.825
Accessibility during operations		0.11	2.5	0.275	6.5	0.715	2.5	0.275	6.5	0.715
Accessibility for maintenance		0.04	1	0.04	2	0.08	5	0.2	5	0.2
Structure costs		0.04	3	0.12	7	0.28	3	0.12	3	0.12
Raising costs		0.02	2	0.04	1	0.02	6.5	0.13	6.5	0.13
Operating costs		0.04	3.5	0.14	3.5	0.14	3.5	0.14	3.5	0.14
Maintenance costs		0.03	3.5	0.105	3.5	0.105	3.5	0.105	3.5	0.105
Removal costs		0.02	1.5	0.03	1.5	0.03	5	0.1	5	0.1
Influence to environment during construction		0.03	1.5	0.045	1.5	0.045	5	0.15	5	0.15
Influence to environment during operation		0.06	3.5	0.21	3.5	0.21	3.5	0.21	3.5	0.21
Influence to environment after removal		0.06	3.5	0.21	3.5	0.21	3.5	0.21	3.5	0.21
Sum		1.00		3.25		3.898		3.813		3.703

Table 22: Comparison of group two structures

Criterion	Loading	Semisubmersible with sloped legs		Semisubmersible with vertical legs		Round floater	
		Performance	Loading x performance	Performance	Loading x performance	Performance	Loading x performance
Level ice loads	0.22	6	1.32	2	0.44	7	1.54
Probability for exceeding the average design load	0.17	1.5	0.248	3.5	0.578	5.5	0.908
Possibility to deal with extraordinary ice impact	0.17	5	0.825	5	0.825	5	0.825
Accessibility during operations	0.11	2.5	0.275	2.5	0.275	2.5	0.275
Accessibility for maintenance	0.04	5	0.2	5	0.2	5	0.2
Structure costs	0.04	3	0.12	3	0.12	3	0.12
Raising costs	0.02	4	0.08	4	0.08	4	0.08
Operating costs	0.04	3.5	0.14	3.5	0.14	3.5	0.14
Maintenance costs	0.03	3.5	0.105	3.5	0.105	3.5	0.105
Removal costs	0.02	5	0.1	5	0.1	5	0.1
Influence to environment during construction	0.03	5	0.15	5	0.15	5	0.15
Influence to environment during operation	0.06	3.5	0.21	3.5	0.21	3.5	0.21
Influence to environment after removal	0.06	3.5	0.21	3.5	0.21	3.5	0.21
Sum	1.00		3.983		3.433		4.863

8. Conclusion and proposal

From the last chapters it comes clear, that the chosen ice load calculation models show a high scatter and so still a lot of uncertainty in load prediction even for specific ice conditions exists. The different aspects of the utility analysis show that no perfect structure, fitting best for all aspects in the Arctic regions, can be found from the evaluated ones. This statement is supported by the variety of existing structure types of the different regions. Nevertheless, general tendencies could have been observed for different structures.

For group one the results of the utility analysis are quite close. With the chosen weightings a multiple leg structure with vertical surfaces should be considered, similar to structures in Cook Inlet.

It has to be mentioned, that challenges by damage due to structural vibrations, like report for structures in Bohai Bay, are not considered and assumed to be manageable. Besides, also to the caisson structure Molikpaq serious events due to ice induced vibrations were reported.

Further it could be investigated how high the additional load due to jamming is and how it could be avoided. In case of considering heavily ice infested operation sides the behaviour due to ridges and their influence to the occurrence of jamming could be considered. Also the applicability of active methods for reducing ice loads should be investigated by a further and more detailed utility analysis. The probability of exceeding the average design load of sloped structures could also be decreased by considering e.g. a hull heating system to avoid adfreezing and too much rubble on top of the structure surface.

For group two the utility analysis results clearly in a round floating structure. This is provided in practice by the successful operations of the Kulluk vessel. Since ship shaped drillships are not considered the analysis is not quite complete. So in future works it could be supplemented with experiences of the new “Stena Icemax”. However, probably also in the near future round floaters need less ice management than ship shaped drillships since they do not need to vane. So for pure Arctic operations round floaters keep still better usable.

For group two, floating structures are also provided by the assumption that it is maybe more economical to accept in unusually heavy ice conditions the risk of downtime during survival modus of the structure, instead of designing the structure for normal operations during long term low probability events. So floating structures could be simpler evacuated. Afterwards

they could also return faster back to operation side and continuing work. So they are not running seriously risk to be damaged during the heavy ice event.

In the future, additionally to a more detailed and versatile utility analysis, also the ice load calculation program could be improved. It has some difficulties for multiple leg structures with tight standing columns of high diameter. It could happen that the wrong interaction type is determined in these conditions. So the interaction type should be checked to plausibility in the issued figure. However, this occurs only in conditions that are anyhow untypical leg diameter to leg distance ratios.

A lot of further work can also be done by improving the specific failure calculation model. Thereby more failure modes could be added which also occur parallel and the determination of choosing the right failure mode needs further revision.

The output file and user-friendliness could also be improved, e.g. by having the possibility of setting a range of different ice thicknesses and intrusion angles for calculations, like the way it is for ice drift velocities, instead of always changing the thickness or angle manually in single steps.

The program of the floating structures could be improved by implicating the possibility to consider more geometric shapes easily. Also the solver of the equation of moment equilibrium could be changed to a more sophisticated one to decrease calculation time. Furthermore, it would also be interesting to take into account more hydrodynamic effects of the structures.

Finally the accuracy of the calculation models, especially for vertical surfaces, need more research and improvement, to lead to more reliable and less scattering results, with more physical background instead of mainly empirical observations.

References

1. **Gudmestad, O. T., et al.,** *Engineering Aspects Related to Arctic Offshore Developments*. St. Petersburg : LAN, 2007. ISBN 978-5-8114-0723-1.
2. **ISO 19906 Petroleum and natural gas industries.** *ISO 19906 Petroleum and natural gas industries - Arctic offshore structures*. 2010.
3. **Sanderson, T. J. O.** *Ice Mechanics Risks to Offshore Structures*. London, Great Britain : Graham and Trotman Limited, 1988. ISBN 0 86010 785 X.
4. **Dickins and Wetzel.** 1981.
5. **Timco, G. W. and Burden, R. P.** *An analysis of the shape of sea ice ridges*. Ottawa, Ont. KIA 0R6 Canada; Nfld. AIB 3X5 Canada : Canadian Hydraulics Centre, National Research Council; Memorial University, St. John's, 1996.
6. **Fett, R. W., Englebretson, R. E. and Perryman, D. C.** *Forecasters Handbook for the Bering Sea, Aleutian Islands, and Gulf of Alaska*. [red.] Marine Meteorology Division, Monterey Naval Research Laboratory. 1993, ss. 7-1 - 7-12.
7. **Jones, Kathleen F. and Andreas, Edgar L.** *Sea Spray Concentration and the Icing of Fixed Offshore Structures*. CRREL and North West Research Associates, Inc. USA, Hanover and USA, Lebanon : s.n., 2012.
8. **William, L. and Thomas, III.** *Bering Sea Topside Icing Probabilities for Two Naval Combatants*. David Taylor Research Center, Ship Hydrodynamics Dept. USA, Maryland, Bethesda : s.n., 1991.
9. **Lee, R. W. and Schulson, E. M.** *The Strength and Ductility of Ice under Tension. Proceeding of the 5th International Symposium on Offshore Mechanics and Arctic Engineering*. 1986, Vol. IV.
10. **Timco, G. W., et al.,** *Ice damage zone around Molikpaq: Implications for evacuation systems. Cold Regions Science and Technology*. 2006, 44, ss. 67-85.
11. **Instanes, A.** *An environmental study of the mechanical behaviour of spray ice. Dr. in dissertation, The Norwegian Institute of Technology*. 1993.
12. **Masterson, D. M., et al.,** *Beaufort Sea Exploration: Past and Future. Proceedings Offshore Technology Conference*. 1991, OTC 6530.

13. **Løset, S.** Science and Technology for Exploration of Oil and Gas - An Environmental Challenge. *European Networking Conference on Research in the North*. 1995.
14. **Gerwick, B. C. and Morris, M. D.** *Construction of marine and offshore structures*. New York/London/Washington : Crc Pr Inc, 2000. ISBN 0-8493-7485-5.
15. **Määttänen, Mauri.** *Ice Force Interaction Effects in Multi-Legged Conical Structures*. Banff, Alberta : IAHR Ice Symposium, 1992.
16. **Wright, B.** Evaluation of Full Scale Data for Moored Vessel Stationkeeping in Pack Ice. *Working Report 26-200 for the Program of Energy, Research and Development*. 1999.
17. **Corona, E. N. and Yashima, N.** Development of a Novel Ice-Resistant Semisubmersible Drilling Unit. *Offshore Technology Conference*. 1983, Vol. III, OTC 4602.
18. **Hals, T. and Efraimsson, F.** DP Ice Model Test of Arctic Drillship. *Dynamic Positioning Conference*. 2011.
19. **Liljeström, G.** Stena Drilling gearing up for the next Arctic challenge. *Lighthouse Cargo Ship Theme Day*. 10 December 2009.
20. shipspotting.com. [Internett] [Siter: 04 March 2013.] www.shipspotting.com.
21. [Internett] 2013. <http://www.hibernia.ca/photos.html>.
22. **Keinonen, A. J.** Ice Management for Ice Offshore Operations. *Offshore Technology Conference*. 2008.
23. **Deter, Dietmar, Doelling, Willy and Lembke-Jene, Lester.** Stationkeeping in Solid Drift Ice. *Dynamic Positioning Conference*. Paper, 2009.
24. **Deter, Dieter.** Stationkeeping in Solid Drift Ice. *Dynamic Positioning Conference*. Presentation, 2009.
25. **Gerwick, Jr., B. C. and Jahns, H. O.** Conceptual Design of Floating Drilling Production and Storage Caisson for Arctic Waters. *Proceedings of 5th POAC Conference*. 1979.
26. **Frederking, R. and Schwarz, J.** Model Tests of Ice Forces on Fixed and Oscillating Cones. *Cold Regions Science and Technology*. 1982, Vol. 6.
27. **Ralston, T. D.** Plastic Limit Analysis of Sheet Ice Loads on Conical Structures. *Symp. Physics and Mechanics of Ice*. 1990.
28. **DePriester, C. L.** *Hull Heating System for an Arctic Offshore Production Structure*. 4,335,980 United States, 22 June 1982.
29. **Mäkitalo, L. I. and Sandkvist, J.** Combination of Warm Water Outlets and Air Bubbler Curtains for Ice-Reducing Purpose - Full Scale Tests. *POAC Conference 1985*. 1985, Vol. II.

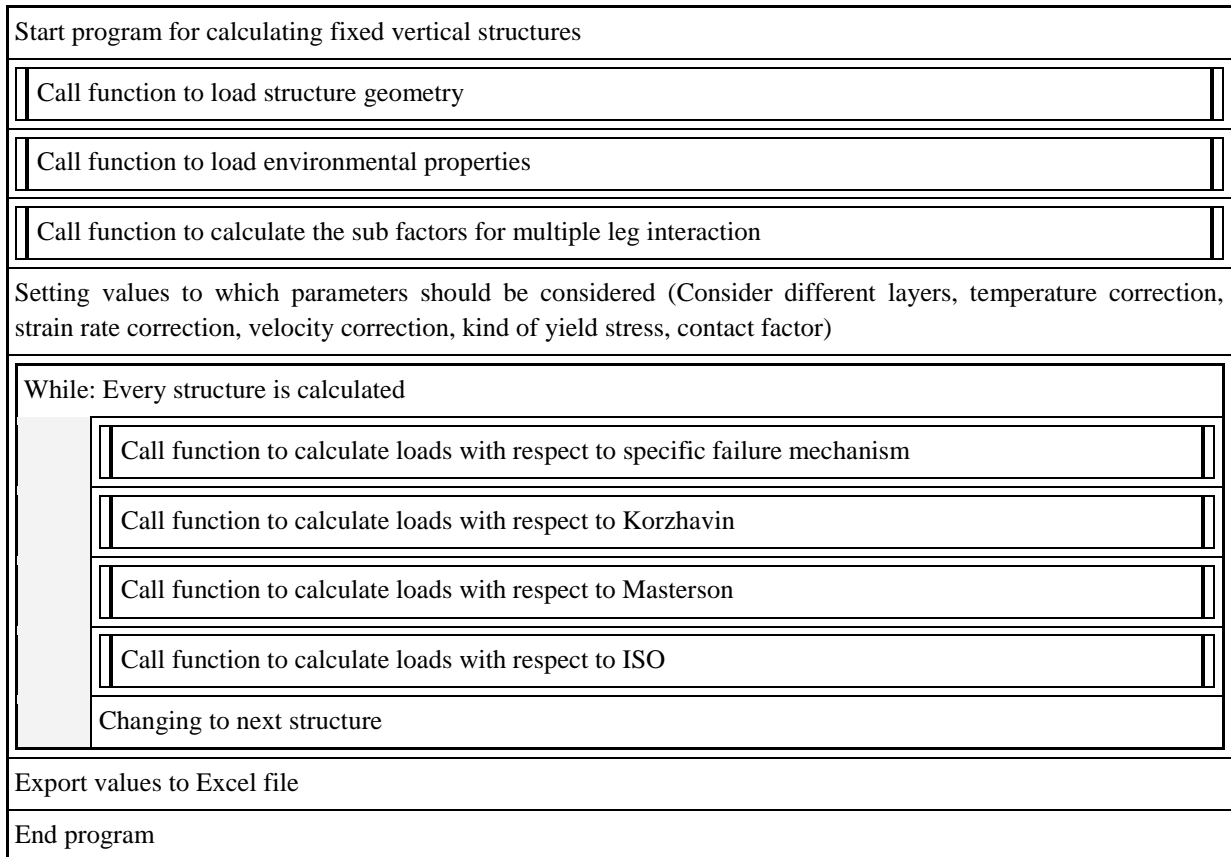
Alexander Dummer	Project work	Investigation of Ice Interactions
MSF LS Ocean Engineering	handed in as	on Drilling Rigs in
University of Rostock	“Studienarbeit”	Shallow Water

30. **Klyuchnik, A. V., Motorin, N. G. and Podkopayev, V. D.** Sea Ice Destruction under High Power Microwave Radiation. *Proceedings of the 13th Conference on Port and Ocean Engineering under Arctic Conditions*. 1995, Vol. IV.
31. **Morgan, G. W. and Berry, H. J.** *Operation Vessel for Ice Covered Sea*. 295, 498 Canada, 1976.
32. **Korzhasin, K. N.** *Action of ice on engineering structures*. s.l. : Publishing House of Siberian Branch of USSR Academy of Sciences, 1962.
33. **Løset, Sveinung, et al.,** *Actions from Ice on Arctic Offshore and Coastal Structures*. St. Petersburg : LAN, 2006. ISBN S-8114-0703-3.
34. **Croasdale, K. R. and Muggeridge, D. B.** A Collaborative Research Program to Investigate Ice Loads on Multifaceted Conical Structures. *Proceedings of the 12th POAC Conference*. 1993, Vol. II, ss. 475-486.
35. **Lau, M., et al.,** Model Ice Forces on a Multi-Faceted Cone. *Proceedings of the 12th POAC Conference*. 1993, Vol. II, ss. 537-546.
36. **Timco, G. W.** Indentation and Penetration of Edge-Loaded Freshwater Ice Sheets in the Brittle Range. *Offshore Mechanics and Arctic Engineering Symposium*. 1986, ss. 444-452.
37. **Schulson, E. M. and Duval, P.** *Creep and Fracture of Ice*. Cambridge, New York, Melbourne, Madrid, Cape Town, Singapore, Sao Paulo : Cambridge University Press, 2009. ISBN-13 978-0-511-53983-1.
38. **Sodhi, D. S. and Hamza, H. E.** Buckling Analysis of a Semi-Infinite Ice Sheet. *Proceedings of the POAC Conference*. 1977, Vol. I, ss. 593-604.
39. **Bohon, W. M. and Weingratten, J. S.** The Calculation of Ice Force on Arctic Structures. *Civil Engineering in the Arctic Offshore. Proceedings of the Conference "Arctic Offshore '85"*. 1985, ss. 456-464.
40. **Croasdale, K. R.** A Method for the Calculation of Sheet Ice loads on sloping structures. *IAHR Ice Symposium*. 1994.
41. **Kennedy, F. E., Schulson, E. M. and Jones, D. E.** The friction of ice on ice at low sliding velocities. *Philosophical Magazine A*. 2000, 80:5, ss. 1093-1110.
42. **Ettema, R. and Urroz, G. E.** On Internal Friction and Cohesion in Unconsolidated Ice Rubble. *Cold Regions Science and Technology*. 1989, 16, ss. 237-247.

43. **Brown, T. G. and Määttänen, M.** Comparison of Kemi I and Confederation Bridge Cone Ice Loads Measurement Results. *Proceedings of the IAHR Conference*. 2002, ss. 503-512.
44. **Shkhinek, K. and Uvarova, E.** Dynamics of the Ice Sheet Interaction with the Sloping Structure. *Proceedings of the 16th International Conference on Port and Ocean Engineering under Arctic Conditions*. 2001, Vol. II, ss. 639-649.
45. **Lau, M. R., et al.**, Influence of Velocity on Ice-Cone Interaction. *IUTAM Symposium on Scaling Laws in Ice Mechanics and Ice Dynamics*. 2000, ss. 127-134.
46. **Lau, M. and Williams, F. M.** Model Ice Forces on a Downward Breaking Cone. *The Proceeding of the 11th POAC Conference*. 1991, Vol. I, ss. 167-184.
47. **Kato, Kazuyuki.** *Total Ice Force on Multi Legged Structures*. Ship and Marine Technology Dept., Research Institute Ishikawajima-Harima Heavy Ind. Co., Ltd. Japan : IAHR Ice Symposium 1990, 1990.
48. **Kato, K., et al.**, Model Experiments for Ice Forces on Multi Conical legged Structures. *Proceedings of the Fourth International Offshore and Polar Engineering Conference*. 1994, Vol. II.
49. **Lindqvist, Gustav.** A Straightforward Method for Calculation of Ice Resistance of Ships. *The 10th International Conference on Port and Ocean Engineering under Arctic Conditions*. 1989.
50. **McDonald, RD.** Oil-Electric. [Internett] [Sitert: 08 March 2013.] <http://2.bp.blogspot.com/-Pwpl7Kq-JYk/UUpqqKv9H0I/AAAAAAAAAN2Y/CfUbj9lWk9w/s1600/KULLUK-PLAN.jpg>.
51. **Structurae - Internationale Datenbank für Ingenieurbauwerke.** Structurae - Internationale Datenbank für Ingenieurbauwerke. [Internett] [Sitert: 15 March 2013.] <http://de.structurae.de/structures/data/index.cfm?id=s0003251>.
52. **Sakhalin Energy.** *Sakhalin Energy*. [Internett] 15 March 2013. <http://www.sakhalinenergy.ru/docs/FactLists/English/MOLIKPAQ.pdf>.
53. **Maersk Drilling.** Maersk Drilling. [Internett] 10 03 2003. www.maerskdrilling.com/Documents/PDF/Drillingrigs/Specific-Rigs/XL-Enhanced-1.pdf.
54. **Yufeng, Tian and Huang, Yan.** The dynamic ice loads on conical structures. *Ocean Engineering*. 2013, 59, ss. 37-46.

Appendix 1: Flow charts for structures with vertical surfaces

Script to calculate fixed vertical structures



Function to load dimensions of fixed vertical structures

Start function to load structure geometry, input: -/-
Set leg diameter
Set distance between centres of abreast columns
Set distance between centres of consecutive columns
Set shape parameter to 0 for rectangular indenter or to 1 for a circular indenter
Set number of columns
End function, output: Leg diameter, distance between centres of abreast and consecutive columns, shape of column, number of columns of each structure

Function to load environmental properties for structures with vertical surfaces

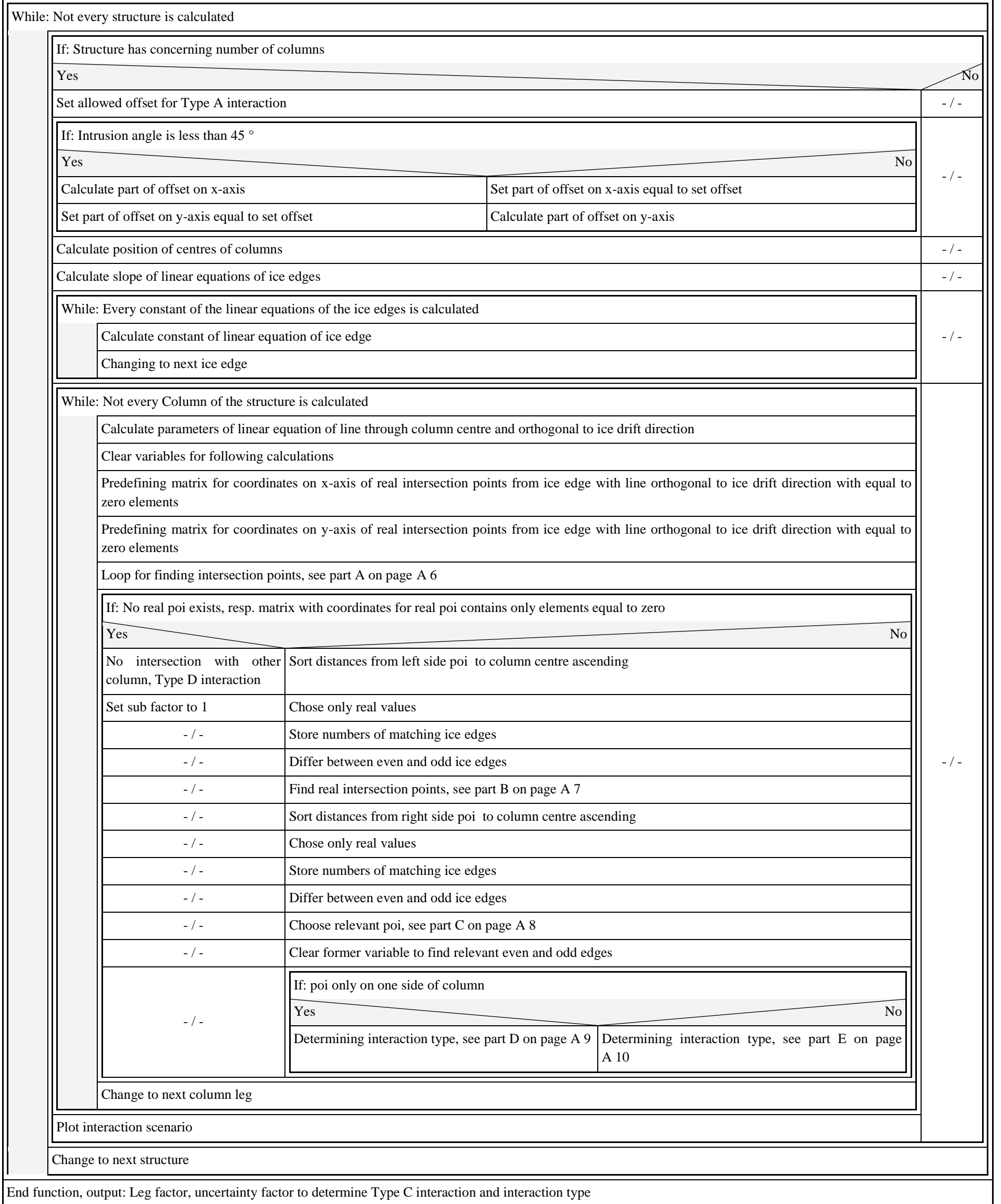
Start function to load environmental properties, input: Calculation parameter	
Set number of freezing degree days	
Set ice drift speed	
Set intrusion angle	
Set ice mean temperature	
Set thickness of ice cover	
Set salinity of ice cover	
If: Thickness of ice cover is less than 0.3 m	
Yes	No
Set content of columnar ice to zero	Set content of columnar ice while considering 0.3 m granular ice cover
If: Mean temperature is less than $-8\text{ }^{\circ}\text{C}$	
Yes	No
Set activation energy for granular ice to 78000 J/mol	Set activation energy for granular ice to 120 000 J/mol
Set crystal type depending constant to $4.1 \cdot 10^8\text{ } 1/(\text{MPa}^3 \cdot \text{s})$	Set crystal type depending constant to $7.8 \cdot 10^{16}\text{ } 1/(\text{MPa}^3 \cdot \text{s})$
Set activation energy for columnar ice to 65000 J/mol	
Set crystal type depending constant for columnar ice to $3.5 \cdot 10^6\text{ } 1/(\text{MPa}^3 \cdot \text{s})$	
Set mean density of ice to 900 kg/m^3	
Calculate brine volume []	
Temperature correction:	
Yes	No
Calculate brine volume	Set brine volume to 0
Calculate elastic modulus [Pa]	
Set Poisson ratio to 0.33	
Set grain diameter	
Calculate Compressive strength with respect to Sanderson	
Set gravitational acceleration	
Set universal gas constant	
End function, output: Freezing degree days, velocity, intrusion angle, temperature, salinity, crystal type depending constants and activation energy of columnar and granular ice, density of ice, Poisson ratio, elastic modulus, content columnar ice, ice thickness, universal gas constant, gravitational acceleration, compressive strength	

Function to calculate leg factors of structures with vertical surfaces

Start function, Input: Column diameter, distance between abreast columns, distance between consecutive columns, number of legs, intrusion angle theta
Set reduction factor to consider non simultaneous failure
Predefining matrix for leg factor
Predefining matrix for uncertainty factor for buckling failure possibility
Predefining matrix for interaction type
Call function to calculate leg factors of rectangular structures with five vertical columns
Multiply leg factor with reduction factor
Call function to calculate leg factors of rectangular structures with four vertical columns
Multiply leg factor with reduction factor
Call function to calculate leg factors of triangular structures with four vertical columns
Multiply leg factor with reduction factor
Call function to calculate leg factor of structures with one vertical column
Add leg factors to predefined matrix
Add uncertainty factors to predefined matrix
Add interaction type factors to predefined matrix
End function, output: Leg factors for single legs, uncertainty factors for single legs, interaction type factors for single legs

Function to calculate interaction types of structures with four or five columns, respectively three or four legs

Start function, input: Leg diameter, distance of centres of abreast columns, distance of centres of consecutive columns, number of legs, predefined matrix for leg factors, predefined matrix for uncertainty factor, predefined matrix for interaction type, intrusion angle



Part A of flowchart to calculate interaction types of structures with four or five columns, respectively three or four legs

While: Not every point of intersection (poi) between orthogonal line and different ice edges is calculated	
Calculate coordinate on x-axis of poi with ice edge	
Calculate coordinate on y-axis of poi with ice edge	
If: poi is on already existing ice edge resp. poi is left or in allowed offset of starting point from ice edge and poi belongs not to ice edge of calculated leg	
Yes	No
Store position of real poi on x-axis in predefined matrix	Store distance from poi left of column centre to column centre as -1
Calculate position of real poi on y-axis and store in predefined matrix	Store distance from poi left of column centre to column centre as -1
Predefine distance from poi left of column centre to column centre as -1	- / -
Predefine distance from poi right of column centre to column centre as -1	- / -
If:	
Poi is on left side of column centre	Calculate distance from poi to centre of column and store in predefined variable
Poi is on right side of column centre	Calculate distance from poi to centre of column and store in predefined variable
- / -	
Change to next poi	

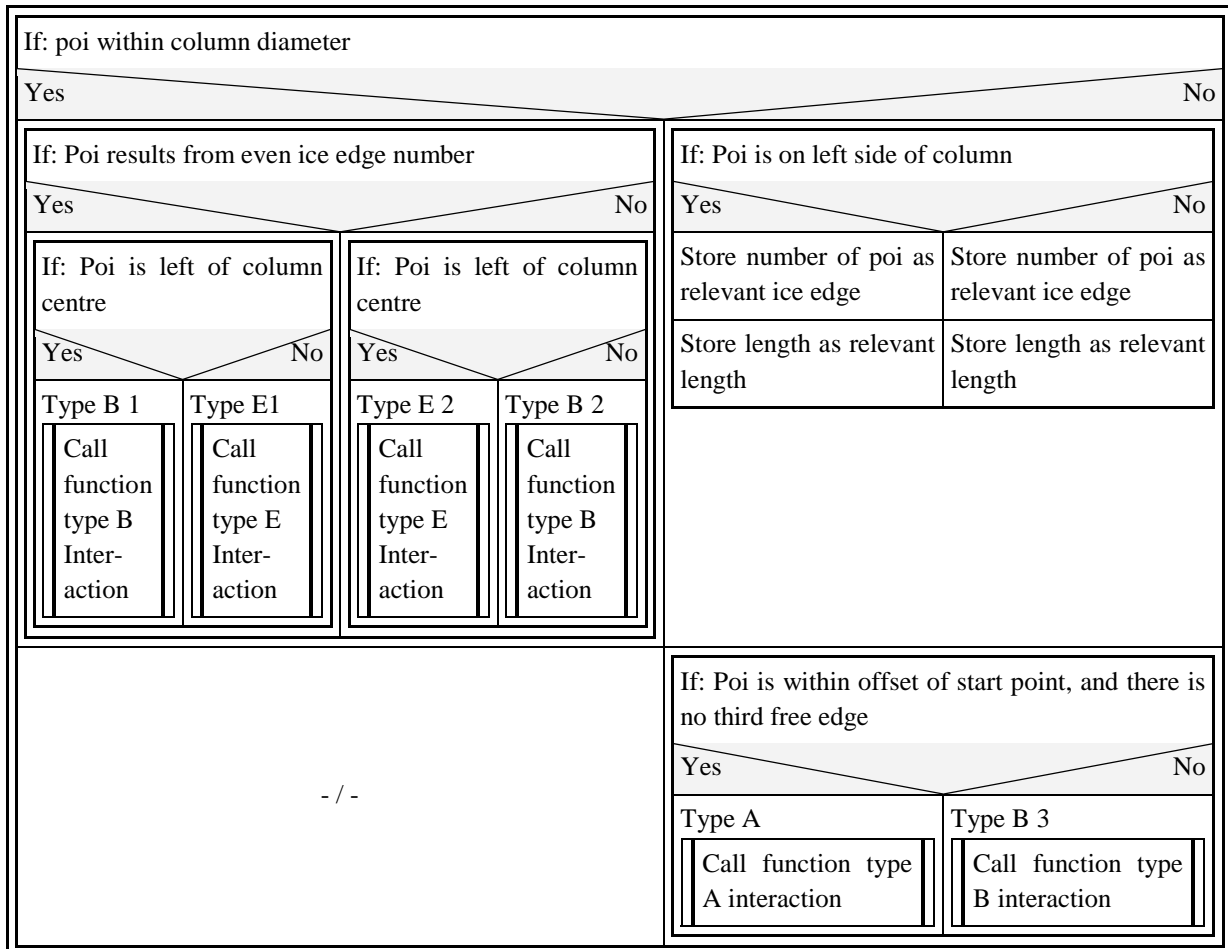
Part B of flowchart to calculate interaction types of structures with four or five columns, respectively three or four legs

If:											
Only one poi from even edge exists on left side and nearest poi is from even edge	Use values for distance to column centre and number of interacting ice edge from poi with even edge										
More than one poi from even edge exists on left side and nearest poi is from even edge	Use values for distance to column centre and number of interacting ice edge from nearest poi										
Only one poi from odd edge exists on left side and nearest poi is from odd edge	Use values for distance to column centre and number of interacting ice edge from poi with odd edge										
More than one poi from odd edge exists on left side, nearest poi is from odd edge and second nearest is not from odd edge	Use values for distance to column centre and number of interacting ice edge from nearest poi										
More than one poi from odd edge and nearest poi is from odd edge	<table border="1"> <tr> <td colspan="2">While: Every poi with odd edge is checked</td> </tr> <tr> <td colspan="2">If: Odd edge are not lying beneath</td> </tr> <tr> <td>Yes</td> <td>No</td> </tr> <tr> <td>Use values of former poi with odd edge for distance to column centre and number of interacting ice edge</td> <td>Change to next odd edge</td> </tr> <tr> <td>Leave loop</td> <td>-/-</td> </tr> </table>	While: Every poi with odd edge is checked		If: Odd edge are not lying beneath		Yes	No	Use values of former poi with odd edge for distance to column centre and number of interacting ice edge	Change to next odd edge	Leave loop	-/-
While: Every poi with odd edge is checked											
If: Odd edge are not lying beneath											
Yes	No										
Use values of former poi with odd edge for distance to column centre and number of interacting ice edge	Change to next odd edge										
Leave loop	-/-										
else	No poi on left side of column centre, set values for relevant poi of left side to -1										

Part C of flowchart to calculate interaction types of structures with four or five columns, respectively three or four legs

If:									
Only one poi from even edge exists on right side and nearest poi is from even edge	Use values for distance to column centre and number of interacting ice edge from poi with even edge								
More than one poi from even edge exists on left side and nearest poi is from even edge	While: Every poi with even edge is checked								
	<table border="1"> <tr> <td colspan="2">If: Even edge are not lying beneath</td> </tr> <tr> <td>Yes</td> <td>No</td> </tr> <tr> <td>Use values of former poi with even edge for distance to column centre and number of interacting ice edge</td> <td>Change to next even edge</td> </tr> <tr> <td>Leave loop</td> <td>- / -</td> </tr> </table>	If: Even edge are not lying beneath		Yes	No	Use values of former poi with even edge for distance to column centre and number of interacting ice edge	Change to next even edge	Leave loop	- / -
	If: Even edge are not lying beneath								
	Yes	No							
Use values of former poi with even edge for distance to column centre and number of interacting ice edge	Change to next even edge								
Leave loop	- / -								
Only one poi from odd edge exists on right side, nearest poi is from odd edge and nearest poi from odd edge is within column diameter	Use values for distance to column centre and number of interacting ice edge from nearest poi with odd edge								
More than one poi from odd edge exists on right side and nearest poi from odd edge is within column diameter	Use values for distance to column centre and number of interacting ice edge from nearest poi with odd edge								
Only one poi from odd edge exists on right side, nearest poi is from odd edge and nearest poi from odd edge is outer column diameter	Use values for distance to column centre and number of interacting ice edge from poi with odd edge								
More than one poi from odd edge exists on right side, nearest poi is from odd edge and nearest poi from odd edge is outer column diameter	Use values for distance to column centre and number of interacting ice edge from nearest poi with odd edge								
More than one poi from odd edge exists on right side, nearest poi is from odd edge	Use values for distance to column centre and number of interacting ice edge from nearest poi with odd edge								
else	No poi on right side of column centre, set values for relevant poi of right side to -1								

Part D of flowchart to calculate interaction types of structures with four or five columns, respectively three or four legs



Part E of flowchart to calculate interaction types of structures with four or five columns, respectively three or four legs

If: Left side poi results from an even ice edge and right side from odd		
Yes		No
If:		Type E 3
Both poi are within column diameter	Type C 1 Call function for type C interaction	Call function for type E interaction
Both poi are out of column diameter	Type C 2 Call function for type C interaction	
Left poi is within column diameter and right poi is out of column diameter	Type C 3 Call function for type C interaction	
Right poi is within column diameter and right poi is out of column diameter	Type C 4 Call function for type C interaction	

Function to calculate type A interaction for vertical surfaces

Start function, input: Characteristic length, column diameter	
If: Ratio of characteristic length to column diameter is between 1 and 5	
Yes	No
Calculate sub factor	Set sub factor to 1
End function, output: Sub factor of column	

Function to calculate type B interaction for vertical surfaces

Start function, input: Characteristic length, column diameter	
If:	
Ratio of characteristic length to column diameter is between 0 and 1	Calculate sub factor
Ratio of characteristic length to column diameter is between 1 and 6	Calculate sub factor
else	Set sub factor to 1
End function, output: Sub factor of column	

Function to calculate type C interaction for vertical surfaces

Start function, input: Characteristic length, leg diameter			
If:			
Length between ice edges is greater than 5 times column diameter	If:		
	Distance on side 1 is smaller one	Set characteristic length to distance on side 1	
		If:	
		Ratio of characteristic length to column diameter is between 0 and 1	Calculate sub factor
		Ratio of characteristic length to column diameter is between 1 and 6	Calculate sub factor
		else	Set sub factor to 1
	else	Set characteristic length to distance on side 2	
		If:	
		Ratio of characteristic length to column diameter is between 0 and 1	Calculate sub factor
		Ratio of characteristic length to column diameter is between 1 and 6	Calculate sub factor
	else	Set sub factor to 1	
	Set uncertainty factor to 0		
Length between ice edges is smaller than 2 times column diameter	Set sub factor to 1 and uncertainty factor to 2		
else	If:		
	Distance on side 1 is smaller one	Set characteristic length to distance on side 1	
		If:	
		Ratio of characteristic length to column diameter is between 0 and 1	Calculate sub factor
		Ratio of characteristic length to column diameter is between 1 and 6	Calculate sub factor
		else	Set sub factor to 1
	else	Set characteristic length to distance on side 2	
		If:	
		Ratio of characteristic length to column diameter is between 0 and 1	Calculate sub factor
		Ratio of characteristic length to column diameter is between 1 and 6	Calculate sub factor
	else	Set sub factor to 1	
	Set uncertainty factor to 1		
End function, output: Sub factor of column, uncertainty factor			

Function to calculate type E interaction for vertical surfaces

Start function, input: -/-
Set sub factor for column to 0.1
End function, output: Sub factor

Function to calculate loads with respect to specific failure mechanism

Start function, input: Ice drift velocity, number of legs, ice thickness, column diameter, calculation parameters, crystal type depending constants for Norton's law, activation energy for Norton's law, universal gas constant, brine volume, elastic modulus, density of ice, gravitational acceleration, brittle compressive strength, leg factor, uncertainty factor

Set compressive strength of columnar and granular ice to equal value

While: Not every ice drift velocity is calculated

While: Not every structure leg is calculated

Calculating Indentation and compatibility factors with respect to Sanderson

Calculate conditions for pure creep

Calculate conditions for buckling

If:

Strain rate fits to pure creep conditions Calculate pure creep conditions, see part F on page A 15

Strain rate fits to buckling conditions Calculate buckling conditions, see part G on page A 16

Strain rate fits to crushing conditions Calculate crushing conditions, see part H on page A 17

Multiplying with specific leg factor

If: Uncertainty factor leads to comparing with buckling load determines use of buckling load due to multiple leg interaction scenario

Yes No

Calculate characteristic length for buckling - / -

Calculate buckling load for specific leg - / -

If: Velocity correction with respect to Korzhavin

Yes No - / -

Multiplying Load with $U^{(-1/3)}$ - / -

If: Temperature correction

Yes No

Differing between layers:

Yes No

Calculate stress in granular layer	Calculating stress by treating all columnar
------------------------------------	---

Call function for temperature correction of granular ice	Call function for temperature correction of columnar ice	- / -
--	--	-------

Calculating stress in columnar layer	Calculate load
--------------------------------------	----------------

Call function for temperature correction of columnar ice	- / -
--	-------

Calculate loads and sum up from each layer	- / -
--	-------

Compare load from specific failure mechanism with buckling load - / -

Is buckling load smaller or uncertainty factor determines buckling action:

Yes No - / -

Use values of buckling load - / -

Change to next column

Sum up loads of single columns

End function, output: Load on structure, identification factor to indicate used failure mechanism

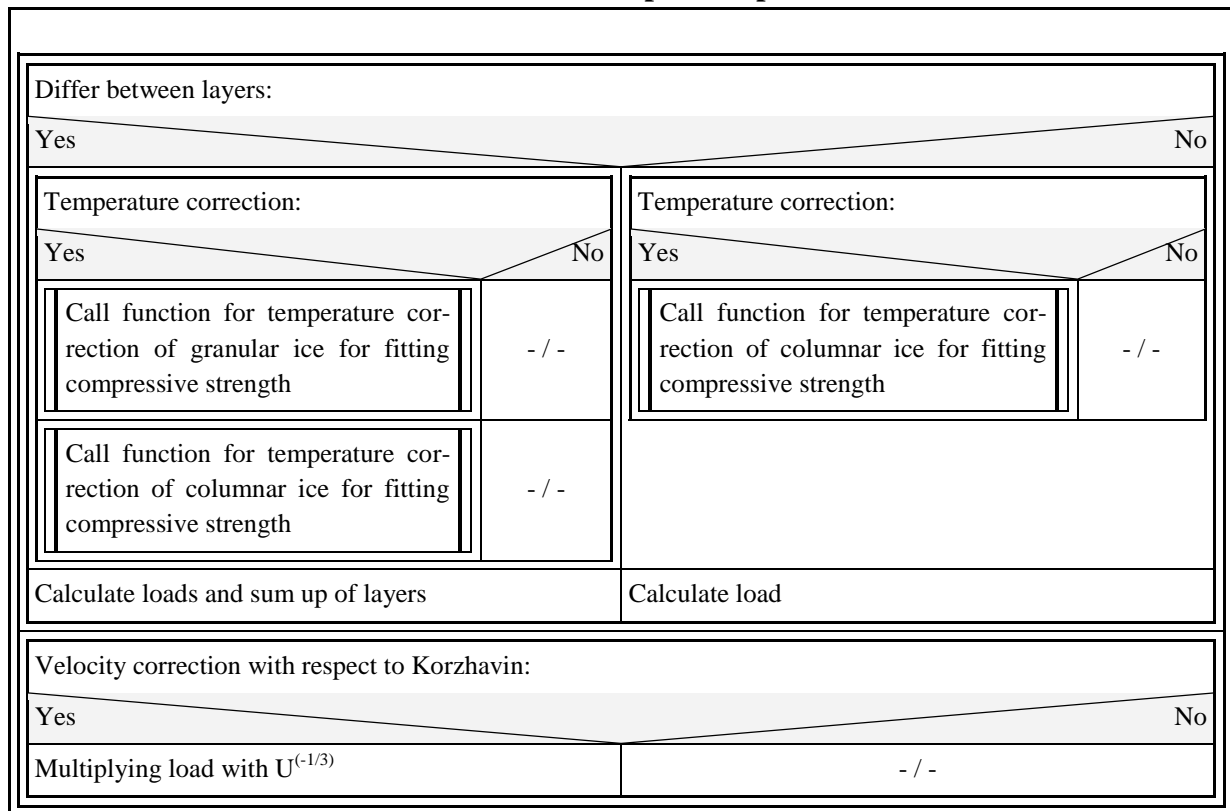
Part F of flowchart to calculate loads with respect to specific failure mechanism

Differing between layers:	
Yes No	
Strain-rate correction with respect to Weingratten:	Strain-rate correction with respect to Weingratten:
Yes No	
Calculate indentation strain rate with respect to Weingratten with aspect ratio of each layer	Calculate indentation strain rate with respect to Sanderson and plastic limit analysis
Calculate indentation strain rate with respect to Weingratten	Calculate indentation strain rate with respect to Sanderson and plastic limit analysis for columnar ice
Use Norton's Law?	Use Norton's Law?
Yes No	
Calculating columnar and granular indentation pressure by Norton's Law	Calculating columnar and granular indentation pressure by Compression test data
Calculating columnar indentation pressure by Norton's Law	Calculating columnar indentation pressure by Compression test data
Temperature correction:	Temperature correction:
Yes No	
Call function for temperature correction of granular ice	- / -
Call function for temperature correction of columnar ice	- / -
Call function for temperature correction of columnar ice	- / -
Calculation and sum up of layer loads	Calculation of load
Velocity correction with respect to Korzhavin:	
Yes No	
Multiplying Load with $V^{(-1/3)}$	- / -

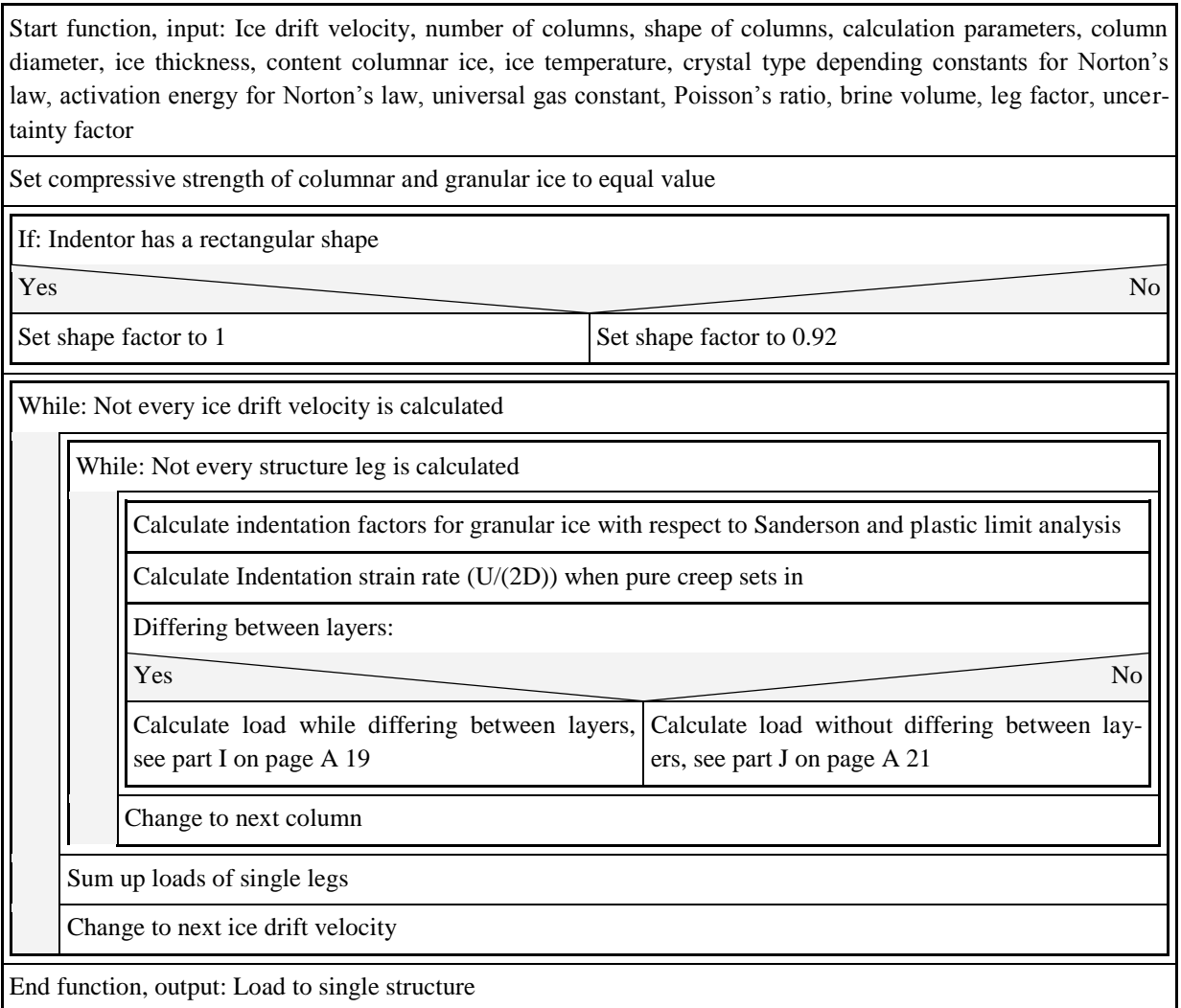
Part G of flowchart to calculate loads with respect to specific failure mechanism

Calculate characteristic length for calculate buckling load	
Calculate buckling load	
Velocity correction with respect to Korzhavin:	
Yes	No
Multiplying Load with $U^{(-1/3)}$	- / -
Temperature correction:	
Yes	No
Differing between layers:	
Yes	No
Calculate stress in columnar layer	Calculating stress by treating all columnar
Call function for temperature correction of columnar ice	Call function for temperature correction of columnar ice
Calculate load due to columnar layer	- / -
Calculating stress in granular layer	- / -
Call function for temperature correction of granular ice	- / -
Calculate load due to granular layer	- / -
Sum up loads from each layer	Calculate load
- / -	

Part H of flowchart to calculate loads with respect to specific failure mechanism



Function to calculate loads with respect to Korzhavin



Part I of flowchart to calculate loads with respect to Korzhavin

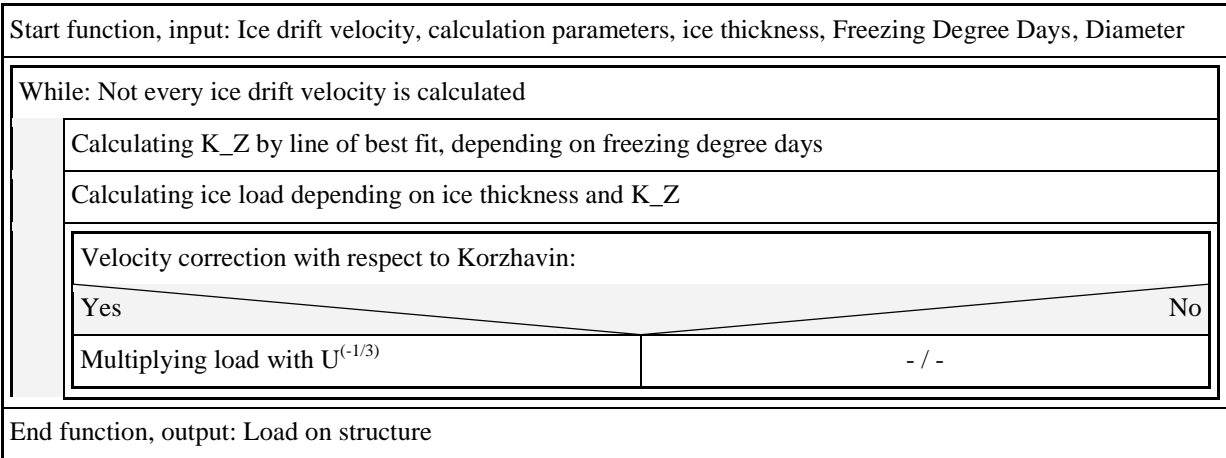
Pure creep conditions with perfect contact:	
Yes No	
Contact factor k equals 1	- / -
Strain rate correction with respect to Weingratten:	
Yes No	
Calculating strain rate of specific aspect ratio for each layer	Calculating strain rate with respect to Sanderson for each layer
If: Calculate contact factor with respect to structure size	
Yes No	
Calculating contact factor	Contact factor k equals 1
Use Norton's Law?	
Yes No	
Calculating stress by Norton's Law	Calculating stress by compression test data
Temperature correction:	
Yes No	
Apply temperature correction for granular layer	- / -
Apply temperature correction for columnar layer	- / -
Temperature correction:	
Yes No	
Fit compressive strength for granular layer	- / -
Fit compressive strength for columnar layer	- / -
Calculate load for single column due to granular layer	Calculate load for single leg due to granular layer
Calculate load for single column due to columnar layer	Calculate load for single leg due to columnar layer
Sum up loads of granular and columnar layer	
Velocity correction with respect to Korzhavin:	
Yes No	
Multiplying load with $U^{(-1/3)}$	- / -
Multiplying with specific leg factor	

If: Uncertainty factor determines comparing with or using of bucking load due to multiple leg interaction scenario		
Yes		No
Calculate characteristic length for buckling load		- / -
Calculate buckling load for specific leg		- / -
If: Velocity correction with respect to Korzhavin		
Yes		No
Multiplying load with $U^{(-1/3)}$		- / -
If: Temperature correction		
Yes		No
Differing between layers:		
Yes		No
Calculate stress in granular layer	Calculating stress by treating all columnar	
Call function for temperature correction of granular ice	Call function for temperature correction of columnar ice	- / -
Calculating stress in columnar layer	Calculate load	
Call function for temperature correction of columnar ice	- / -	
Calculate loads and sum up from each layer	- / -	
Is buckling load smaller or uncertainty factor determines buckling action:		
Yes		No
Take buckling load		- / -

Part J of flowchart to calculate loads with respect to Korzhavin

Pure creep conditions with perfect contact:	
Yes No	
Contact factor k equals 1	- / -
Strain rate correction with respect to Weingratten:	
Yes No	
Calculate stress with respect to strain rate of specific aspect ratio	Calculate stress with respect to strain rate with respect to Sanderson for columnar ice
If: Calculate contact factor with respect to structure size	
Yes No	
Calculating contact factor	Contact factor k equals 1
Use Norton's Law?	
Yes No	
Calculate stress by Norton's Law	Calculate stress by Compression test data
- / -	
Temperature correction:	
Yes No	
Apply columnar temperature correction	- / -
Temperature correction:	
Yes No	
Fit compressive strength for columnar layer	- / -
Calculate load for single leg	Calculate load for single leg
Velocity correction with respect to Korzhavin:	
Yes No	
Multiplying load with $U^{-1/3}$	- / -
Multiplying with specific leg factor	
If: Uncertainty factor determines comparing with or using of buckling load due to multiple leg interaction scenario	
Yes No	
Calculate Buckling load for specific leg	- / -
Is buckling load smaller or uncertainty factor determines buckling action:	
Yes No	
Take buckling load	- / -

Function to calculate loads with respect to Masterson



Function to calculate loads with respect to ISO 19906

Start function, input: Ice drift velocity, number of legs, ice thickness, elastic modulus, ice density, column diameter, gravitation acceleration, Poisson's ratio, specific leg factor, calculation parameters, uncertainty factor, columnar ice content, brine volume

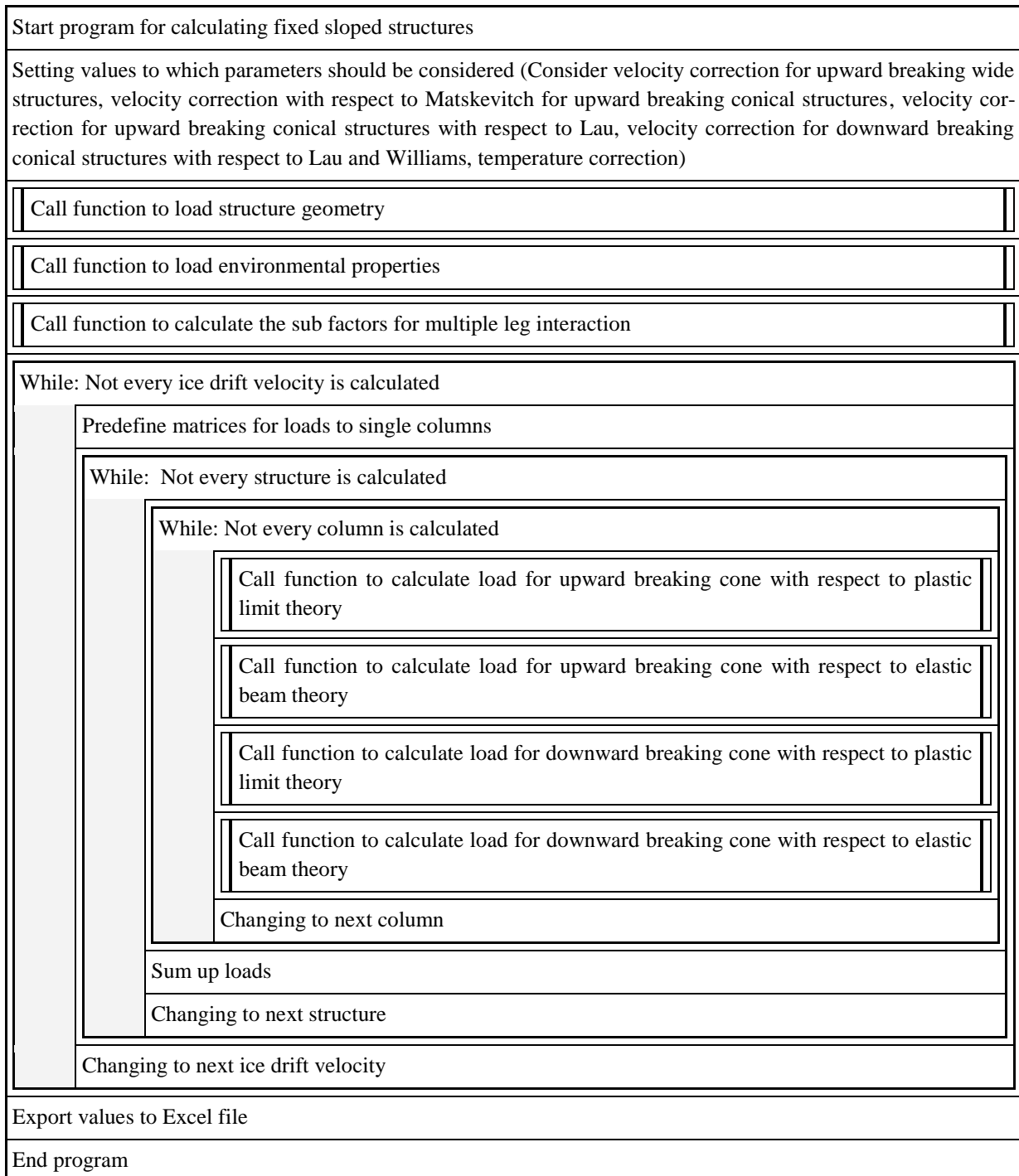
While: Not every ice drift velocity is calculated	
While: Not every structure leg is calculated	
Calculate empirical coefficients	
Calculate ice loads depending on ice thickness, region and coefficients	
Velocity correction with respect to Korzhavin:	
Yes	No
Multiplying load with $U^{(-1/3)}$	- / -
Multiplying with specific leg factor	
If: Uncertainty factor determines comparing with or using of buckling load due to multiple leg interaction scenario	
Yes	No
Calculate characteristic length for buckling load	- / -
Calculate buckling load for specific leg	- / -
If: Velocity correction with respect to Korzhavin	
Yes	No
Multiplying load with $U^{(-1/3)}$	- / -
If: Temperature correction	
Yes	No
If: Differing between layers	
Yes	No
Calculate stress in granular layer	Calculating stress by treating all columnar
Call function for temperature correction of granular ice	Call function for temperature correction of columnar ice
Calculating stress in columnar layer	Calculate load
Call function for temperature correction of columnar ice	- / -
Calculate loads and sum up from each layer	- / -
Is buckling load smaller or uncertainty factor determines buckling action:	
Yes	No
Take buckling load	- / -
Sum up loads from single legs	
End function, output: Load to structure	

Function to calculate temperature and salinity correction for granular or columnar ice

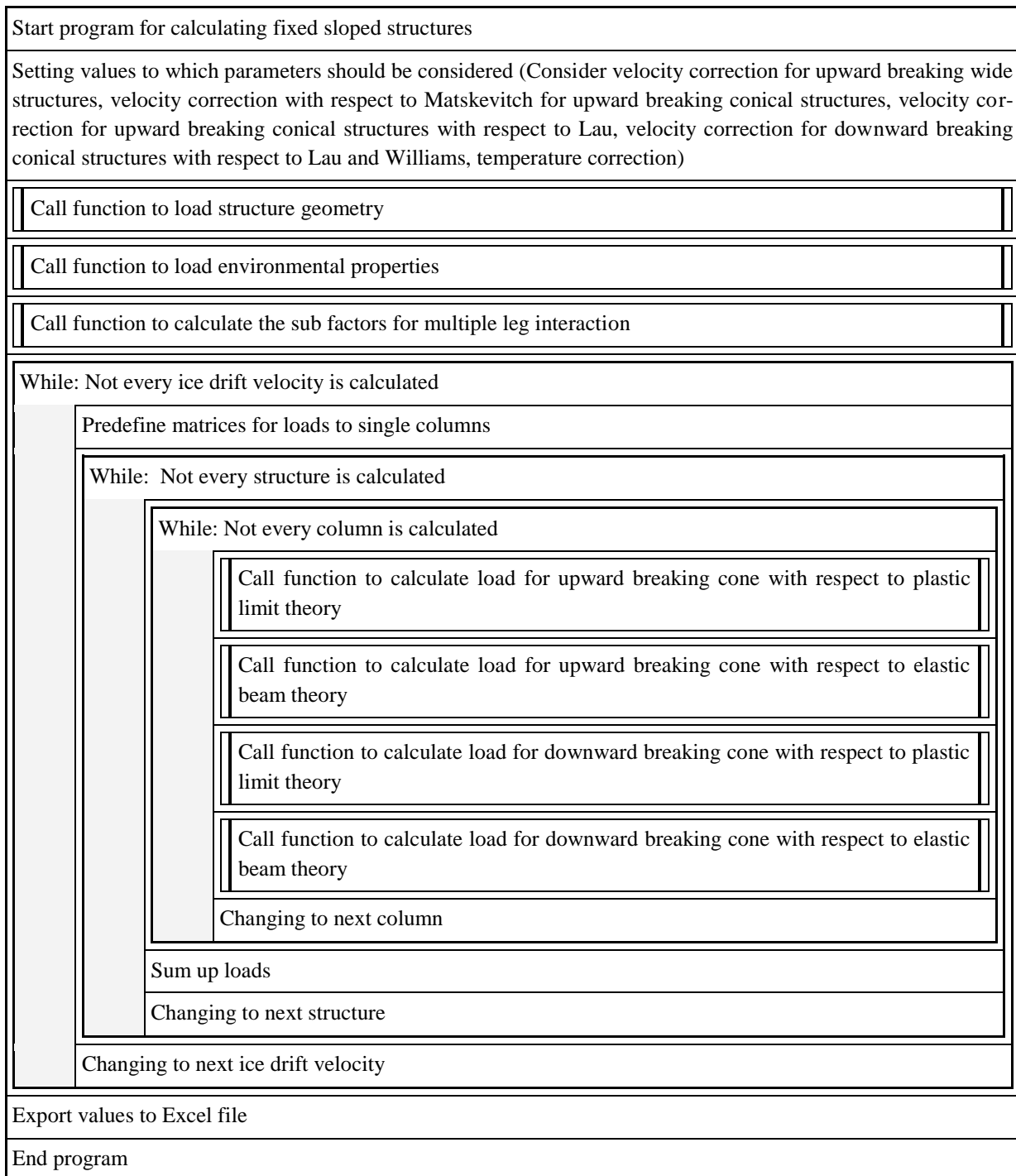
Start function, input: Brine volume, net section stress or strength of uncorrected ice
Calculate reduced strength
End function, output: Corrected stress or strength

Appendix 2: Flow charts for structures with sloped surfaces

Script to calculate fixed sloped structures



Function to load dimensions of fixed sloped structures



Function to load dimensions of fixed sloped structures

Start function to load structure geometry, input: -/-
Set slope angle
Set column diameter at waterline
Set distance between centres of abreast columns
Set distance between centres of consecutive columns
Set column diameter of vertical part
Set number of columns
End function, output: Leg diameter at waterline and vertical part, distance between centres of abreast and consecutive columns, number of columns of each structure, slope angle

Function to load environmental properties for sloped structures

Start function to load environmental properties, input: calculation parameters, slope angle	
Set ice drift speed	
Set intrusion angle	
Set ice mean temperature	
Set thickness of ice cover	
Set salinity of ice cover	
Set ice density	
Set structure material	
Calculate structure-ice friction coefficient	
Calculate ice-ice friction coefficient	
If: Temperature correction	
Yes	No
Calculate brine volume	Set brine volume to 0
Calculate elastic modulus	
Set Poisson's ratio	
Calculate flexural strength	
Set Poisson ratio to 0.33	
Set grain diameter	
Calculate Compressive strength with respect to Sanderson	
If: Temperature correction	
Yes	No
Call function for temperature correction and correct compressive strength	- / -
Set ice ride-up thickness	
Set angle of rubble	
Calculate internal friction angle of rubble	
Calculate cohesion of rubble	
Set porosity of rubble	
Set density of sea water	
Set gravitational acceleration	

Set universal gas constant
End function, output: Ice drift velocity, intrusion angle, temperature, salinity, ice density, brine volume, ice-structure and ice-ice friction, ice thickness, Poisson's ratio, elastic modulus, flexural strength, ride-up thickness, rubble angle, angle of internal friction of rubble, cohesion of rubble, porosity of rubble, density of water, universal gas constant, gravitational acceleration, compressive strength

Function to calculate leg factors of structures with sloped surfaces

Start function, Input: Column diameter at waterline, column diameter at vertical part, distance between abreast columns, distance between consecutive columns, number of legs, intrusion angle theta, flexural strength, ice thickness, density of ice, gravitational acceleration
Set reduction factor to consider non simultaneous failure
Predefining matrix for leg factor
Predefining matrix for interaction type
Call function to calculate leg factors of rectangular structures with five sloped columns
Multiply leg factor with reduction factor
Call function to calculate leg factors of rectangular structures with four sloped columns
Multiply leg factor with reduction factor
Call function to calculate leg factors of triangular structures with four sloped columns
Multiply leg factor with reduction factor
Call function to calculate leg factor of structures with one sloped column
Add leg factors to predefined matrix
Add interaction type factors to predefined matrix
End function, output: Leg factors for single legs and interaction type factors for single legs

Function to calculate interaction types of sloped structures with four or five columns, respectively three or four legs

Start function, input: Leg diameter, distance of centres of abreast columns, distance of centres of consecutive columns, number of legs, predefined matrix for leg factors, predefined matrix for uncertainty factor, predefined matrix for interaction type, intrusion angle

While: Not every structure is calculated		
If: Structure has concerning number of columns		
Yes		No
Set allowed offset for Type A interaction		- / -
If: Intrusion angle is less than 45 °		
Yes		No
Calculate part of offset on x-axis	Set part of offset on x-axis equal to set offset	- / -
Set part of offset on y-axis equal to set offset	Calculate part of offset on y-axis	
Calculate position of centres of columns		- / -
Calculate slope of linear equations of ice edges		- / -
While: Every constant of the linear equations of the ice edges is calculated		
Calculate constant of linear equation of ice edge		- / -
Changing to next ice edge		
While: Not every Column of the structure is calculated		
If: Intrusion angle is equal to 0		
Yes		No
Set type A interaction for first two columns	Calculate parameters of linear equation of line through column centre and orthogonal to ice drift direction	
Set type E interaction for last two columns	Clear variables for following calculations	
Set type BC interaction for centre column	Predefining matrix for coordinates on x-axis of real intersection points from ice edge with line orthogonal to ice drift direction with equal to zero elements	
- / -	Predefining matrix for coordinates on y-axis of real intersection points from ice edge with line orthogonal to ice drift direction with equal to zero elements	
- / -	Loop to find intersection points, part K on page A 31	
If: No real poi exists, resp. matrix with coordinates for real poi contains only elements equal to zero		
Yes		No
No intersection with other column, Type D interaction	Sort distances from left side poi to column centre ascending	
Set sub factor to 1	Chose only real values	- / -
- / -	Store numbers of matching ice edges	
- / -	Differ between even and odd ice edges	
- / -	Find real poi, see part L on page A 32	
- / -	Sort distances from right side poi to column centre ascending	
- / -	Chose only real values	
- / -	Store numbers of matching ice edges	
- / -	Differ between even and odd ice edges	
- / -	Choose relevant poi, see part M on page A 33	
- / -	Clear former variable from finding relevant even and odd edges	
- / -	If: Poi only on one side of column	
Yes		No
Determine interaction type, see part N on page A 34	Determine interaction type, see part O on page A 35	
Change to next column leg		
Plot interaction scenario		
Change to next structure		

End function, output: Leg factor, uncertainty factor to determine Type C interaction and interaction type

Part K of flowchart to calculate interaction types of structures with four or five columns, respectively three or four legs

While: Not every point of intersection (poi) between orthogonal line and different ice edges is calculated	
Calculate coordinate on x-axis of poi with ice edge	
Calculate coordinate on y-axis of poi with ice edge	
If: poi is on already existing ice edge resp. poi is left or in allowed offset of starting point from ice edge and poi belongs not to ice edge of calculated leg	
Yes	No
Store position of real poi on x-axis in predefined matrix	Store distance from poi left of column centre to column centre as -1
Calculate position of real poi on y-axis and store in predefined matrix	Store distance from poi left of column centre to column centre as -1
Predefine distance from poi left of column centre to column centre as -1	- / -
Predefine distance from poi right of column centre to column centre as -1	- / -
If:	
Poi is on left side of column centre	Calculate distance from poi to centre of column and store in predefine variable
Poi is on right side of column centre	Calculate distance from poi to centre of column and store in predefine variable
- / -	
Change to next poi	

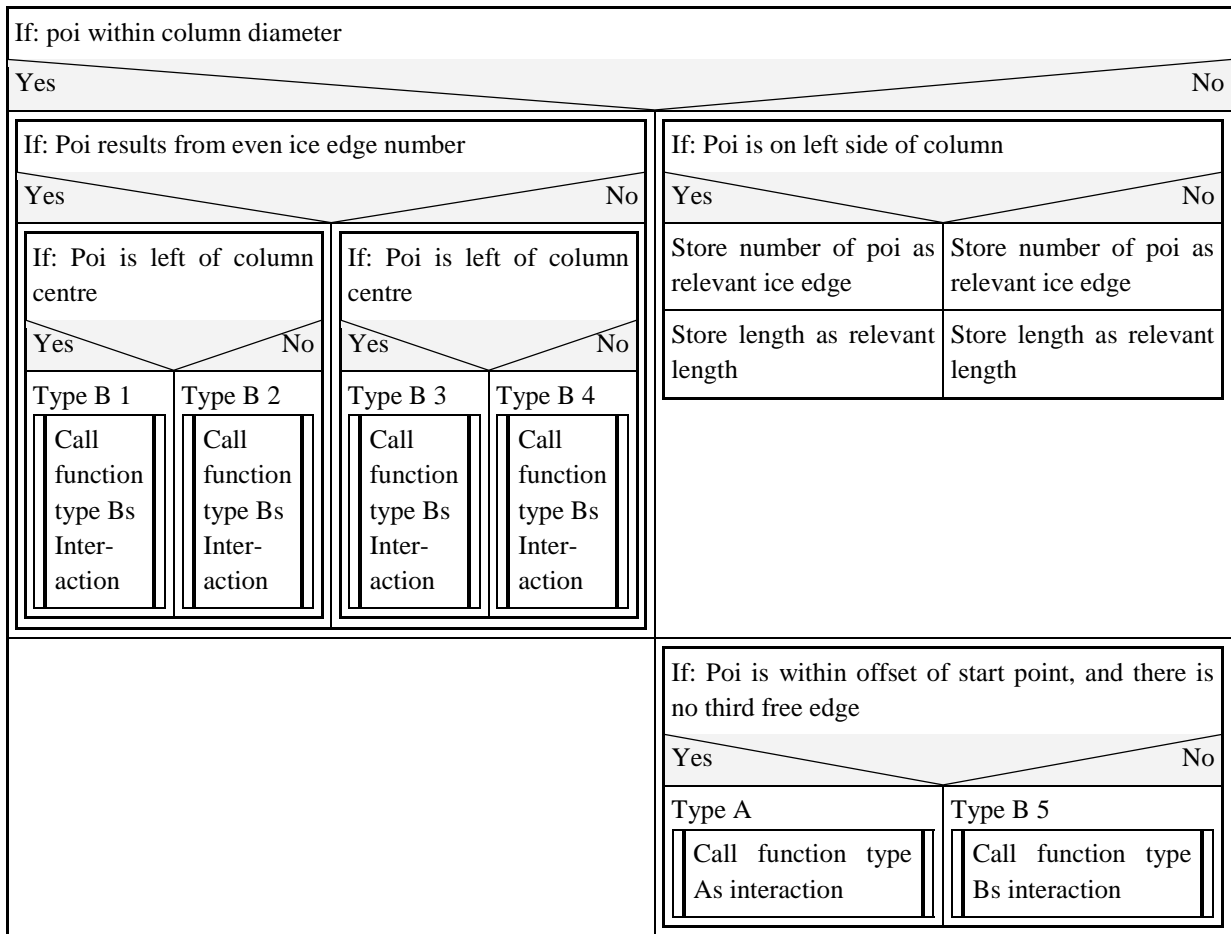
**Part L of flowchart to calculate interaction types of structures with four or five columns,
respectively three or four legs**

If:											
Only one poi from even edge exists on left side and nearest poi is from even edge	Use values for distance to column centre and number of interacting ice edge from poi with even edge										
More than one poi from even edge exists on left side and nearest poi is from even edge	Use values for distance to column centre and number of interacting ice edge from nearest poi										
Only one poi from odd edge exists on left side and nearest poi is from odd edge	Use values for distance to column centre and number of interacting ice edge from poi with odd edge										
More than one poi from odd edge exists on left side, nearest poi is from odd edge and second nearest is not from odd edge	Use values for distance to column centre and number of interacting ice edge from nearest poi										
More than one poi from odd edge and nearest poi is from odd edge	<table border="1"> <tr> <td colspan="2">While: Every poi with odd edge is checked</td> </tr> <tr> <td colspan="2">If: Odd edge are not lying beneath</td> </tr> <tr> <td>Yes</td> <td>No</td> </tr> <tr> <td>Use values of former poi with odd edge for distance to column centre and number of interacting ice edge</td> <td>Change to next odd edge</td> </tr> <tr> <td>Leave loop</td> <td></td> </tr> </table>	While: Every poi with odd edge is checked		If: Odd edge are not lying beneath		Yes	No	Use values of former poi with odd edge for distance to column centre and number of interacting ice edge	Change to next odd edge	Leave loop	
While: Every poi with odd edge is checked											
If: Odd edge are not lying beneath											
Yes	No										
Use values of former poi with odd edge for distance to column centre and number of interacting ice edge	Change to next odd edge										
Leave loop											
else	No poi on left side of column centre, set values for relevant poi of left side to -1										

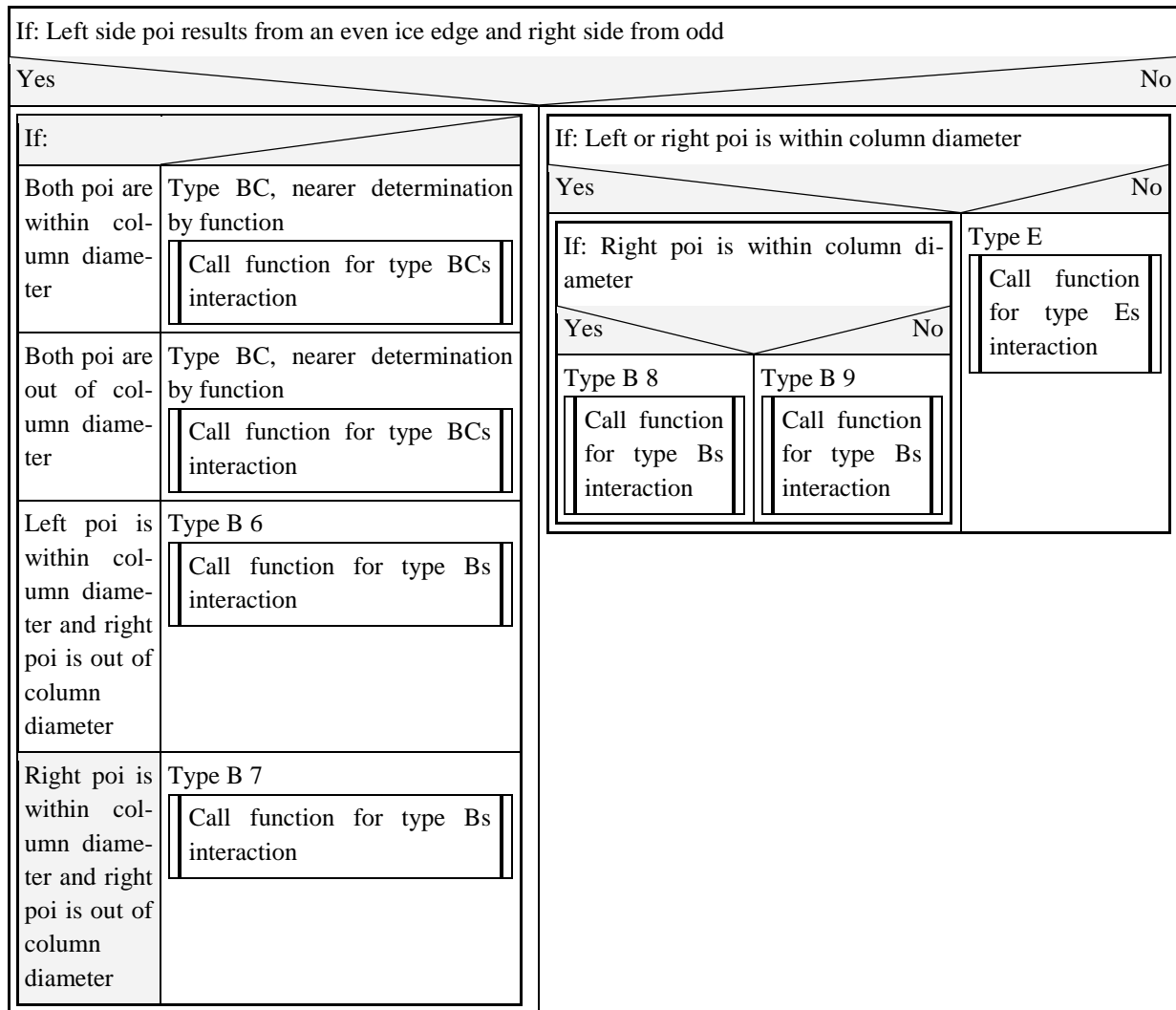
Part M of flowchart to calculate interaction types of structures with four or five columns, respectively three or four legs

If:									
Only one poi from even edge exists on right side and nearest poi is from even edge	Use values for distance to column centre and number of interacting ice edge from poi with even edge								
More than one poi from even edge exists on left side and nearest poi is from even edge	While: Every poi with even edge is checked								
	<table border="1"> <tr> <td colspan="2">If: Even edge are not lying beneath</td> </tr> <tr> <td>Yes</td> <td>No</td> </tr> <tr> <td>Use values of former poi with even edge for distance to column centre and number of interacting ice edge</td> <td>Change to next even edge</td> </tr> <tr> <td>Leave loop</td> <td></td> </tr> </table>	If: Even edge are not lying beneath		Yes	No	Use values of former poi with even edge for distance to column centre and number of interacting ice edge	Change to next even edge	Leave loop	
	If: Even edge are not lying beneath								
	Yes	No							
Use values of former poi with even edge for distance to column centre and number of interacting ice edge	Change to next even edge								
Leave loop									
Only one poi from odd edge exists on right side, nearest poi is from odd edge and nearest poi from odd edge is within column diameter	Use values for distance to column centre and number of interacting ice edge from nearest poi with odd edge								
More than one poi from odd edge exists on right side and nearest poi from odd edge is within column diameter	Use values for distance to column centre and number of interacting ice edge from nearest poi with odd edge								
Only one poi from odd edge exists on right side, nearest poi is from odd edge and nearest poi from odd edge is outer column diameter	Use values for distance to column centre and number of interacting ice edge from poi with odd edge								
More than one poi from odd edge exists on right side, nearest poi is from odd edge and nearest poi from odd edge is outer column diameter	Use values for distance to column centre and number of interacting ice edge from nearest poi with odd edge								
More than one poi from odd edge exists on right side, nearest poi is from odd edge	Use values for distance to column centre and number of interacting ice edge from nearest poi with odd edge								
else	No poi on right side of column centre, set values for relevant poi of right side to -1								

Part N of flowchart to calculate interaction types of structures with four or five columns, respectively three or four legs



Part O of flowchart to calculate interaction types of structures with four or five columns, respectively three or four legs



Function to calculate type A interaction for sloped surfaces

Start function, input: Characteristic length, column diameter at waterline and of vertical part, flexural strength, ice thickness, density of ice, gravitational acceleration	
Calculate constants	
If: Ratio of characteristic length to column diameter is between 1 and 4	
Yes	No
Calculate sub factor	Calculate sub factor
End function, output: Sub factor of column	

Function to calculate type B interaction for sloped surfaces

Start function, input: Characteristic length, column diameter at waterline and of vertical part, flexural strength, ice thickness, density of ice, gravitational acceleration	
If:	
Ratio of characteristic length to column diameter is between -0.5 and 0.5	Calculate sub factor
Ratio of characteristic length to column diameter is between 0.5 and 2	Calculate sub factor
Ratio of characteristic length to column diameter is between 2 and 3	Calculate sub factor
else	Calculate sub factor
End function, output: Sub factor of column	

Function to calculate type BC interaction for sloped surfaces

Start function, input: Characteristic length of each side, leg diameter at waterline and of vertical part, flexural strength, ice thickness, density of ice, gravitational acceleration		
If:		
Length between ice edges is smaller than column diameter	Calculate difference between leg diameter at waterline and ice edge	
- / -	If:	
	Diameter minus difference is greater 0	Decrease waterline diameter and diameter of vertical part
	- / -	Choose smaller value from column centre to ice edge as characteristic length for type Bs interaction
	- / -	Call function for Bs interaction
	- / -	Set value for interaction type
	else	Call function for Es interaction
	- / -	Set value for interaction type
Length between ice edges is greater than column diameter	Choose smaller value from column centre to ice edge as characteristic length for type Bs interaction	
- / -	Call function for Bs interaction	
End function, output: Sub factor of column, interaction type		

Function to calculate type E interaction for sloped surfaces

Start function, input: -/-
Set sub factor for column to 0.1
End function, output: Sub factor

Function to calculate loads with respect to plastic limit theory for downward or upward breaking cones

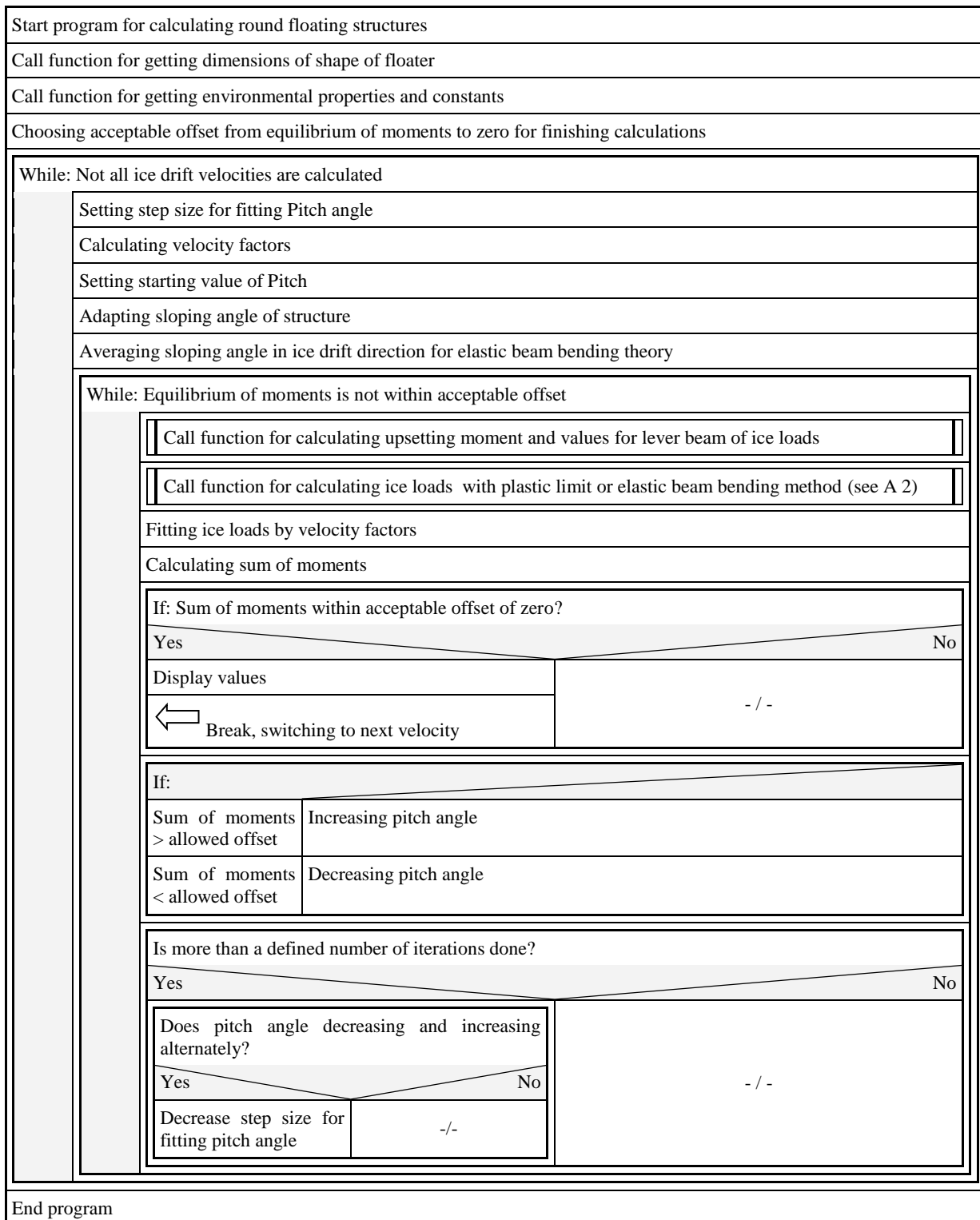
Start function, input: Diameter at waterline and of vertical part, slope angle, calculation parameters, leg factor, ice drift velocity, gravitational acceleration, ice thickness, density of ice, ice-structure friction, flexural strength, compressive strength, ride-up thickness, elastic modulus	
If: Velocity correction with respect to Shkhinek and Uvarova	
Yes	No
Calculate velocity factors for several slope angles	- / -
Calculate load with respect to Shkhinek and Uvarova for several slope angles	- / -
Calculate structures related velocity factor and load by polynomial fitting	- / -
If: Velocity correction with respect to Matskevitch	
Yes	No
If: Ice drift speed is below 0.5 m/s	
Yes	No
Set velocity factor to 1	Calculate velocity factor
	- / -
If: Velocity correction with respect to Lau	
Yes	No
Calculate velocity factor	- / -
Define variable for diameters	
Change slope angle into radian	
Calculate elliptical integral of first and second kind	
Set value for Tresca or Johansen yielding	
Calculate geometric constants	
Calculate horizontal and vertical ride-up action	
Calculate horizontal and vertical breaking action	
Sum up actions	
End function, output: Horizontal and vertical load, load with respect to Shkhinek and Uvarova	

Function to calculate loads with respect to elastic beam theory for downward or upward breaking cones

Start function, input: Diameter at waterline and of vertical part, slope angle, structure number, calculation parameters, leg factor, ice drift velocity, gravitational acceleration, ice thickness, density of ice, ice-structure and ice-ice friction, Poisson's ratio, elastic modulus, rubble angle, internal friction angle of rubble, cohesion of rubble, porosity of rubble, flexural strength, compressive strength, density of water	
If: Velocity correction with respect to Shkhinek and Uvarova	
Yes	No
Calculate velocity factors for several slope angles	- / -
Calculate load with respect to Shkhinek and Uvarova for several slope angles	- / -
Calculate structures related velocity factor and load by polynomial fitting	- / -
If: Velocity correction with respect to Matskevitch	
Yes	No
If: Ice drift speed is below 0.5 m/s	
Yes	No
Set velocity factor to 1	Calculate velocity factor
-	
If: Velocity correction with respect to Lau	
Yes	No
Calculate velocity factor	- / -
Calculate rubble high with respect to high of cone neck	
Calculate relation between vertical and horizontal components	
Calculate characteristic length of ice sheet	
Calculate breaking load	
Calculate load to push ice sheet through rubble	
Calculate load to push ice blocks up the slope through rubble	
Calculate load to turn the ice block at the top of the slope	
Calculate total length of circumferential crack	
Sum up actions for horizontal load	
Calculate vertical load	
End function, output: Horizontal and vertical load	

Appendix 3: Flow charts of floating structures

Script to calculate round floating structures



Function to calculate upsetting moment of round floater

Start function, input: Mass of floater, high cylindrical part, density of water, gravitational acceleration, bottom diameter, slope angle, pitch angle, waterline diameter, draught	
Setting thickness of floater slices	
Setting allowed deviation between displaced volume and volume witch pitch	
Calculating displaced volume without pitch	
While: Displaced volume of floater witch pitch is out of tolerance level	
Calculating number of submerged or partly submerged slices	
While: Not all slices are calculated	
Calculating position of waterline, in coordinate system defined by base line and centre line of floater	
Calculating radius of hull, depending on slice number	
Calculating centre of buoyancy and displaced volume of single slice, in coordinate system defined by base line and centre line of floater	
Changing to next slice	
Calculation and fitting of draught	
Calculation of overall centre of buoyancy for all slices, in coordinate system defined by base line and center line of floater	
Transformation of coordinates from overall centre of buoyancy to coordinate system, parallel to waterline and ordinate through keel of floater	
Calculating upsetting moment	
End function, output: Upsetting moment	

Appendix 4: Source code of velocity correction for wide sloping structures

```

%Calculation of velocity factor
clear i4;
i4=1; %Calculating values for dynamic action for specific ice velocity
%U_max=max(U);
U_kv=U; %[0.05:0.01:U_max];
while i4<=length(U_kv),
    a=((rho_i*E)^0.5*U_kv(i4)/R_C); %Non-dimensional parameter for differ-
ent velocities
    a_qs=((rho_i*E)^0.5*0.05/R_C); %Non-dimensional paramter quasi-static
conditions

    kv(i4,1)=(0.01+0.035*a^0.55)/(0.01+0.035*a_qs^0.55); %Velocity factor
for sloping angle of 30° and velocity U_kv(i4)
    Nh_rdh(i4,1)=(0.01+0.035*a^0.55); %Non-dimensional ice action, divided
by R_C, D and h

    kv(i4,2)=(0.02+0.07*a^0.55)/(0.02+0.07*a_qs^0.55); %Velocity factor
for sloping angle of 40° and velocity U_kv(i4)
    Nh_rdh(i4,2)=(0.02+0.07*a^0.55); %Non-dimensional ice action, divided
by R_C, D and h

    kv(i4,3)=(0.04+0.14*a^0.55)/(0.04+0.14*a_qs^0.55); %Velocity factor
for sloping angle of 50° and velocity U_kv(i4)
    Nh_rdh(i4,3)=0.04+0.14*a^0.55; %Non-dimensional ice action, divided by
R_C, D and h

    %Velocity factor for sloping angle of 60° and velocity U_kv(i4)
    if 0.05<a && a<2,
        kv(i4,4)=(0.08+0.25*a^0.55)/(0.08+0.25*a_qs^0.55);
        Nh_rdh(i4,4)=0.08+0.25*a^0.55; %Non-dimensional ice action, di-
vided by R_C, D and h
    elseif 2<=a && a<=3.4,
        kv(i4,4)=(0.425*a^0.07)/(0.08+0.25*a_qs^0.55);
        Nh_rdh(i4,4)=0.425*a^0.07;
    else
        kv(i4,4)=(0.425*a^0.07)/(0.08+0.25*a_qs^0.55);
        Nh_rdh(i4,4)=0.425*a^0.07;
        display('No value for horizontal force of slope angle equal to 60°,
so N_h is set to the value from lower velocities.')
    end;

    %Velocity factor for sloping angle of 70° and velocity U_kv(i4)
    if 0.05<a && a<1,
        kv(i4,5)=(0.16+0.45*a^0.55)/(0.16+0.45*a_qs^0.55);
        Nh_rdh(i4,5)=0.16+0.45*a^0.55;
    elseif 1<=a && a<=3.4,
        kv(i4,5)=(0.61*a^0.07)/(0.16+0.45*a_qs^0.55);
        Nh_rdh(i4,5)=0.61*a^0.07;
    else
        kv(i4,5)=(0.61*a^0.07)/(0.16+0.45*a_qs^0.55);
        Nh_rdh(i4,5)=0.61*a^0.07;

```

```

        display('No value according to Shkhinek and Uvarova for horizontal
force of slope angle equal to 70°, so N_h is set to the value from lower
velocities.')
    end;

    i4=i4+1;
    end;

%Plotting Velocity factor
figure
hold on;
plot(U_kv,kv(:,1))
plot(U_kv,kv(:,2))
plot(U_kv,kv(:,3))
plot(U_kv,kv(:,4))
plot(U_kv,kv(:,5))
hold off;

i=1;
while i<=length(D1s),           %Loop for each type of structure

    i2=1;
    while i2<=nls(i),         %Loop for each column
        if i2==1,
            D=D1s(i);
        elseif i2==2,
            D=D2s(i);
        elseif i2==3,
            D=D3s(i);
        elseif i2==4,
            D=D4s(i);
        elseif i2==5,
            D=D5s(i);
        end;

        i3=1;
        while i3<=length(U),   %Loop for each ice velocity
            %Calculating specific velocity factors
            x=[30,40,50,60,70];
            p=polyfit(x,kv(i3,:),4);

            kv_poly(i,i2,i3)=p(1)*alpha(i)^4+p(2)*alpha(i)^3+p(3)*alpha(i)^2+p(4)*alpha
            (i)+p(5);
            %Calculating specific ice action
            p2=polyfit(x,Nh_rdh(i3,:),4);

            P_SU(i,i2,i3)=(p2(1)*alpha(i)^4+p2(2)*alpha(i)^3+p2(3)*alpha(i)^2+p2(4)*alp
            ha(i)+p2(5))*R_C*D*h;

            i3=i3+1;
        end;
        i2=i2+1;
    end;
    i=i+1;
end;

```

Appendix 5: Multiple leg interaction scenarios

Group one, structure no. 17

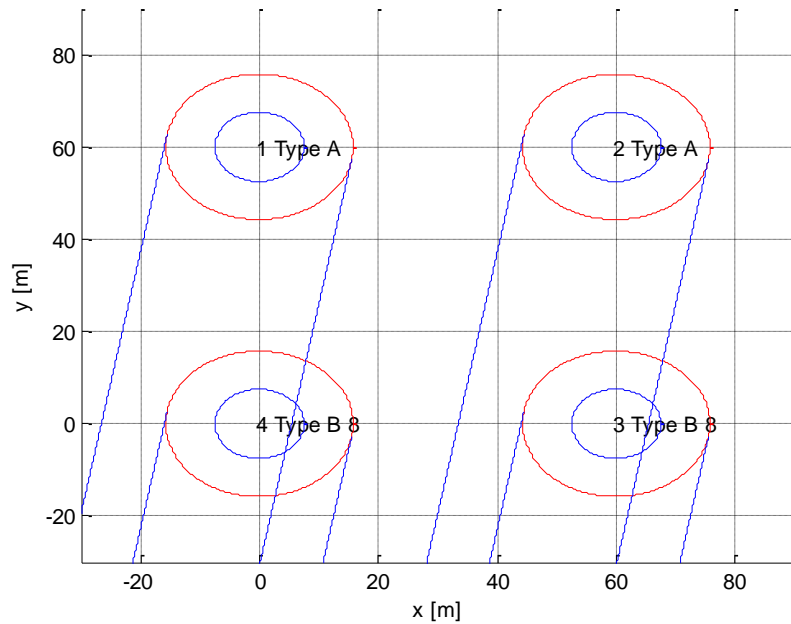


Figure 40: Group one, no. 17, intrusion angle: 10°

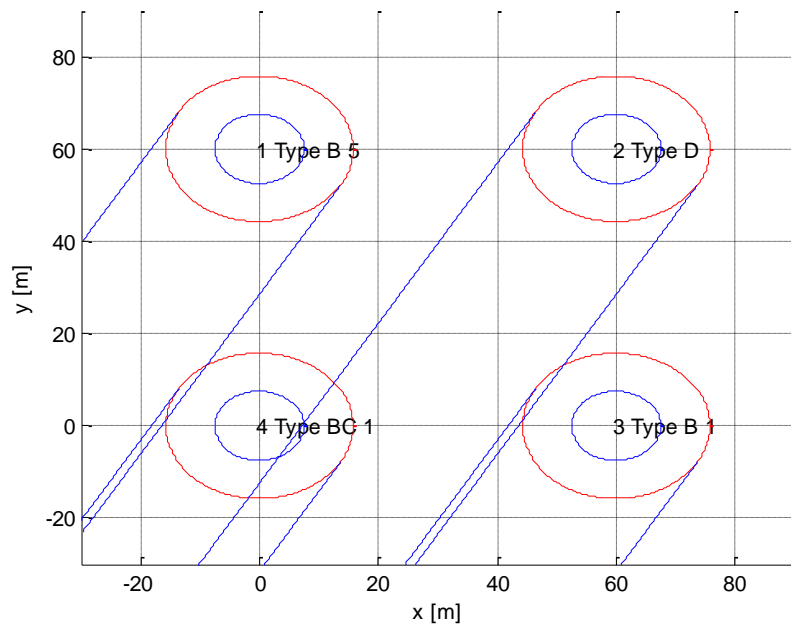


Figure 41: Group one, no. 17, intrusion angle: 30°

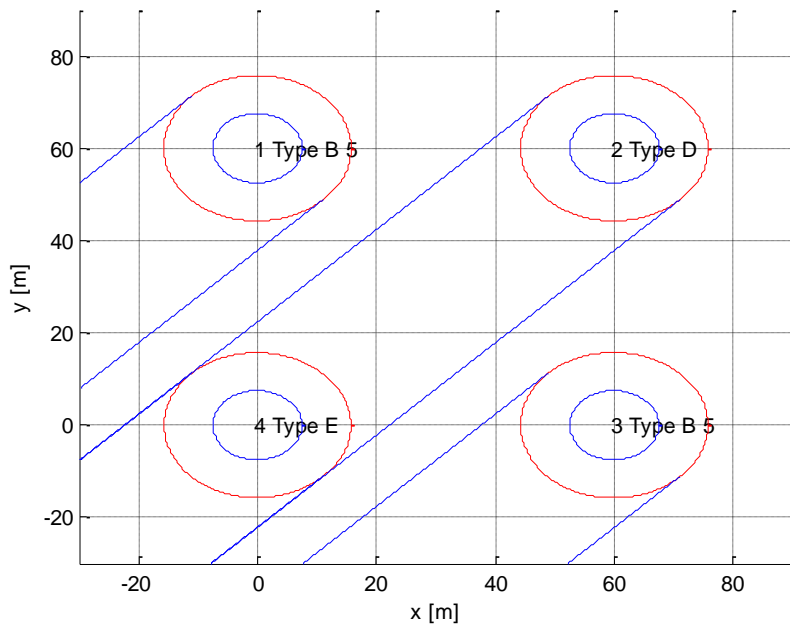


Figure 42: Group one, no. 17, intrusion angle: 45 °

Group two, structure no. 3

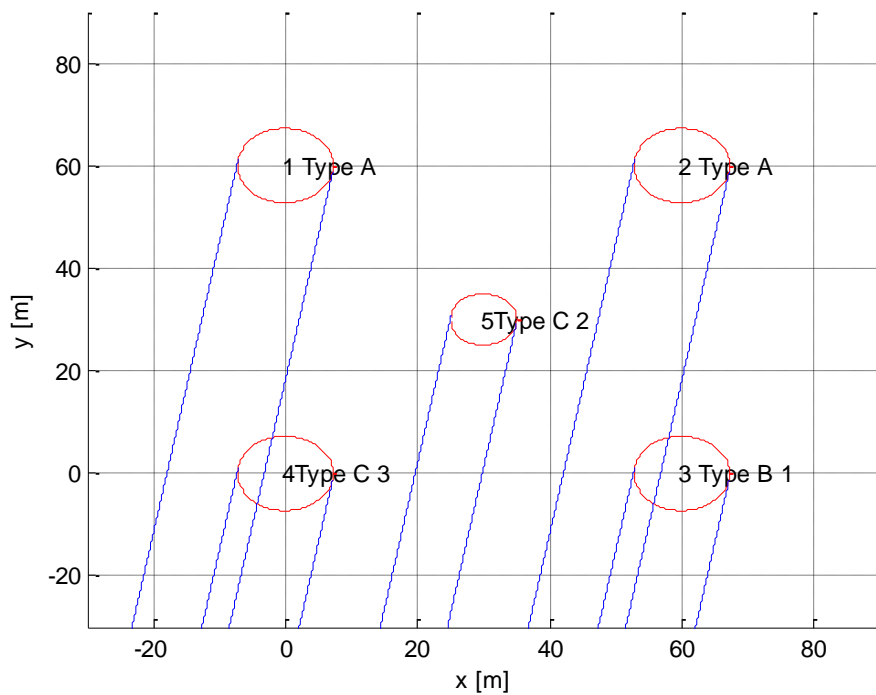


Figure 43: Group two, no. 3, intrusion angle: 10 °

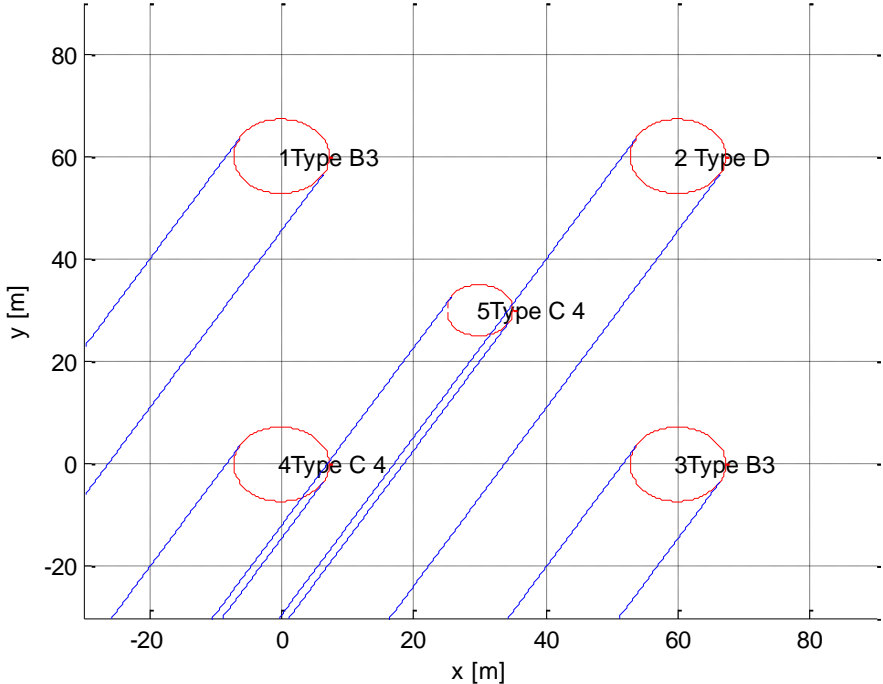


Figure 44: Group two, no. 3, intrusion angle: 30 °

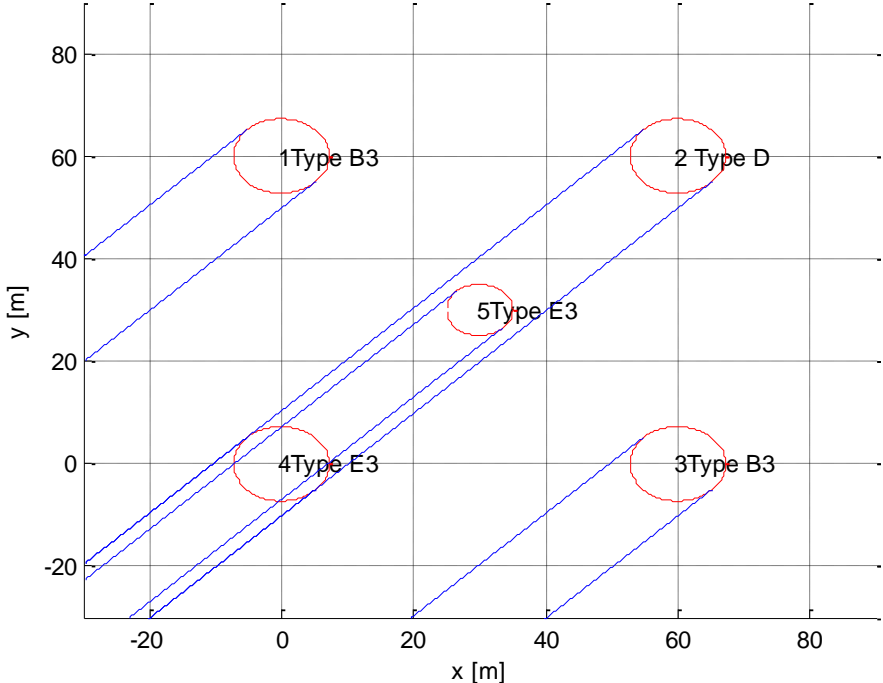
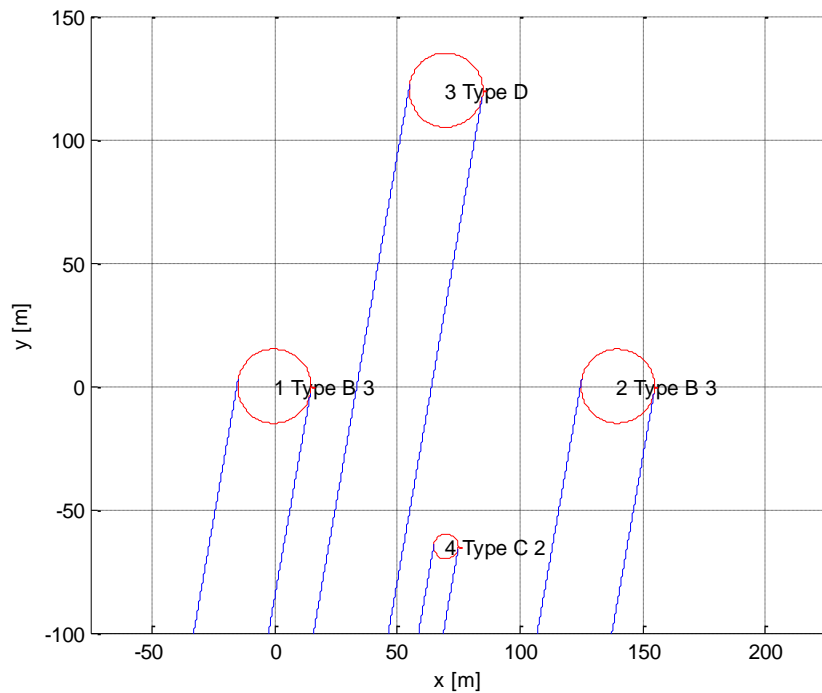
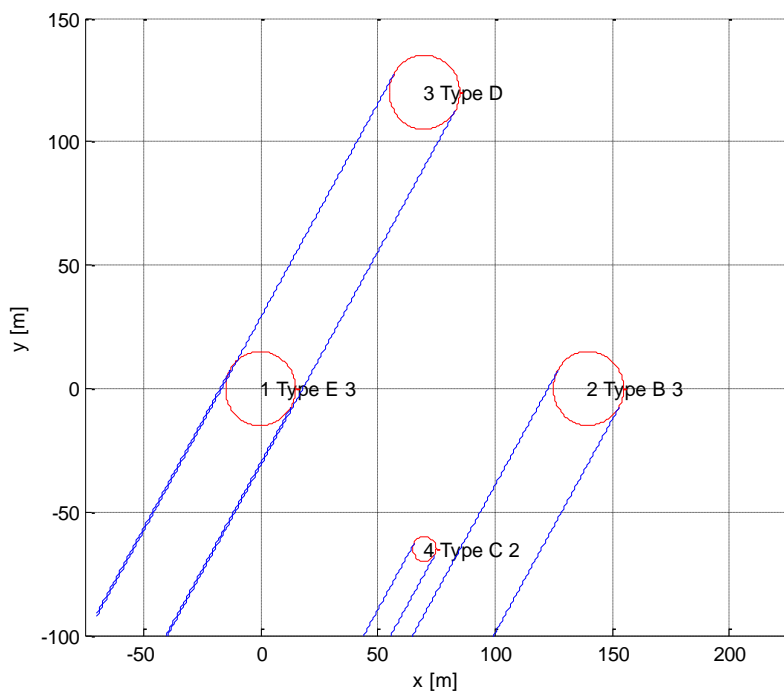


Figure 45: Group two, no. 3, intrusion angle: 45 °

Group two, structure no. 5

Figure 46: Group two, no. 5, intrusion angle: 10° Figure 47: Group two, no. 5, intrusion angle: 30°

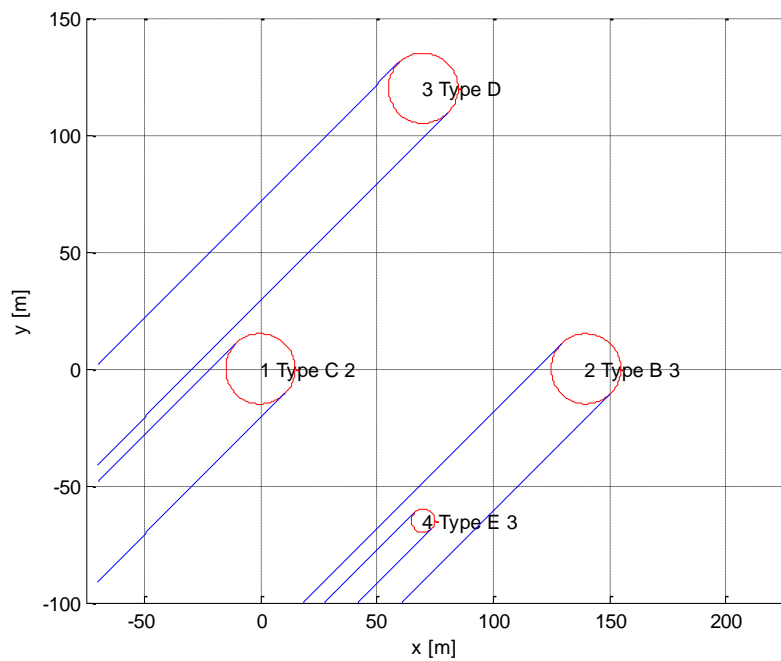


Figure 48: Group two, no. 5, intrusion angle: 45°

Group two, structure no. 18

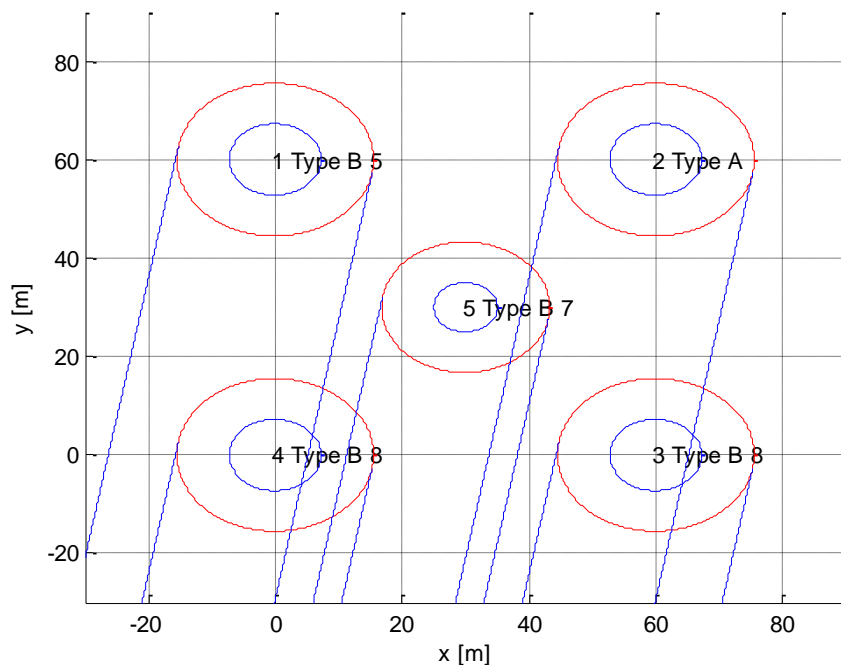


Figure 49: Group two, no. 18, intrusion angle: 10°

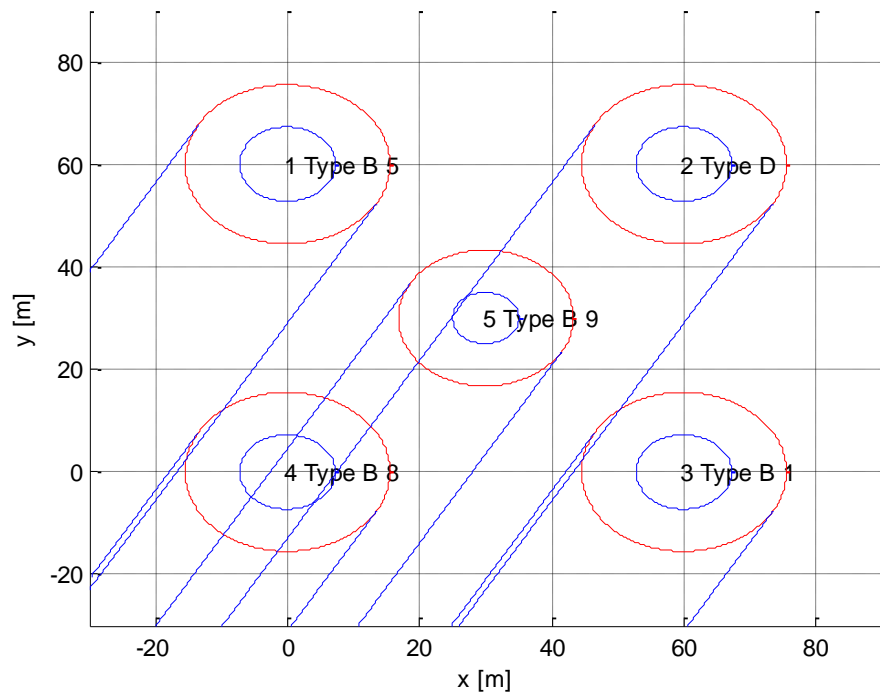


Figure 50: Group two, no. 18, intrusion angle: 30°

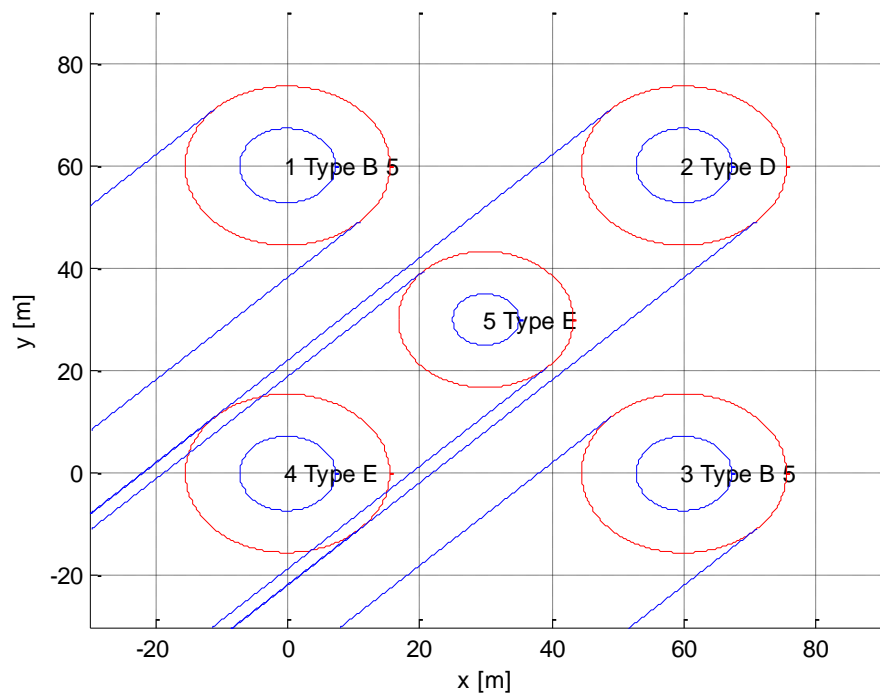
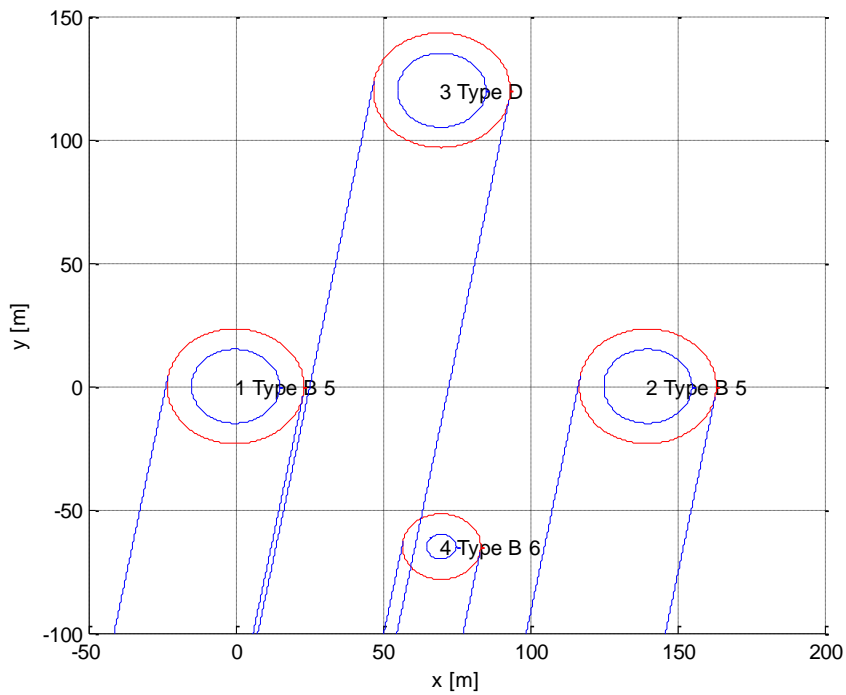
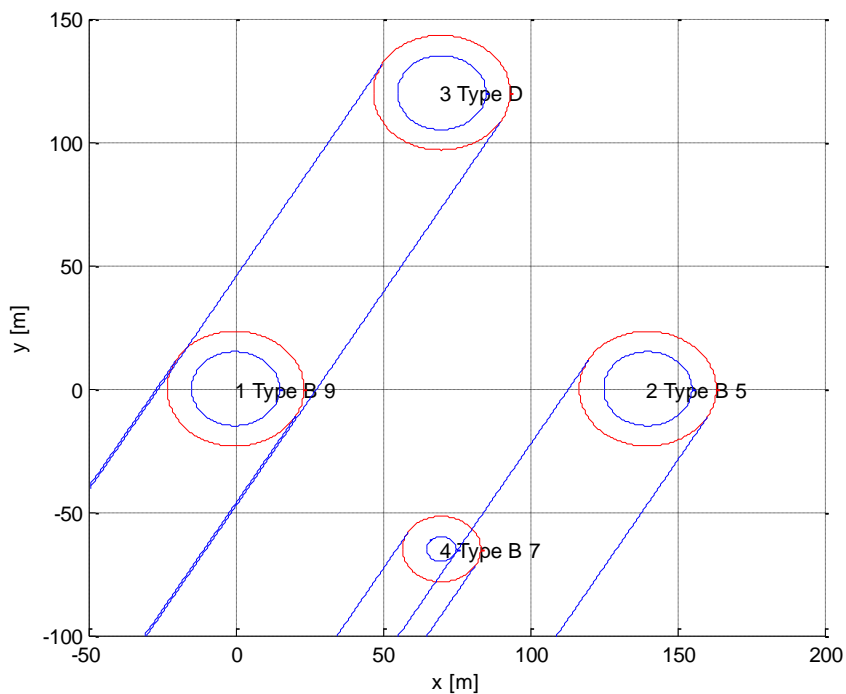


Figure 51: Group two, no. 18, intrusion angle: 45°

Group two, structure no. 28**Figure 52: Group two, no. 28, intrusion angle: 10 °****Figure 53: Group two, no. 28, intrusion angle: 30 °**

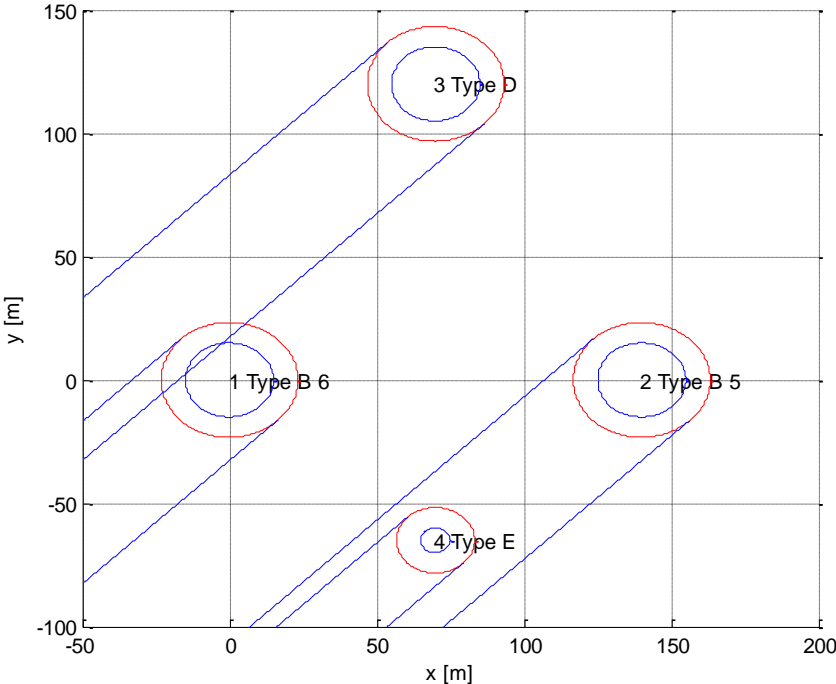


Figure 54: Group two, no. 28, intrusion angle: 45 °

Appendix 6: CD - ROM

Alexander Dummer
MSF LS Ocean Engineering
University of Rostock

Project work
handed in as
“Studienarbeit”

Investigation of Ice Interactions
on Drilling Rigs in
Shallow Water

Appendix 5: Declaration

Hereby I declare that I did this work independently and without using other sources and information as stated. Information obtained from other sources either directly or indirectly has been indicated as such.

Rostock, 28.03.2013

(Alexander Dummer)